In-situ product removal by membrane extraction

Louise Heerema

Cover: The Twelve Apostles, Port Campbell National Park, Great Ocean Road, Victoria, Australia.

In-situ product removal by membrane extraction

Proefschrift

ter verkrijging van de graad van doctor

aan de Technische Universiteit Delft,

op gezag van de Rector Magnificus prof.ir. K.C.A.M. Luyben,

voorzitter van het College voor Promoties,

in het openbaar te verdedigen op maandag 6 februari 2012 om 15.00 uur

door

Louise Danielle HEEREMA

Ingenieur in de Biotechnologie

geboren te ’s Gravenhage.

Dit proefschrift is goedgekeurd door de promotoren:

Prof. dr. ir. L.A.M. van der Wielen

Prof. dr. ir. J.T.F. Keurentjes

Samenstelling promotiecommissie:

Rector Magnificus,	voorzitter
Prof. dr. ir. L.A.M. van der Wielen,	Technische Universiteit Delft, promotor
Prof. dr. ir. J.T.F. Keurentjes,	Technische Universiteit Eindhoven, promotor
Prof. dr. R.M. Boom,	Universiteit Wageningen
Prof. dr. ir. Stankiewicz,	Technische Universiteit Delft
Prof. dr. ir. Heijnen,	Technische Universiteit Delft
Dr. S. Schlosser,	Slovak University Bratislava
Dr. C.P.M. Roelands,	TNO
Prof. dr. G.J. Witkamp,	Technische Universiteit Delft, reservelid

ISBN/EAN: 978-94-6191-122-3

Gedrukt door Ipskamp B.V.

This project is financially supported by the Netherlands Ministry of Economic Affairs and the B-Basic partner organizations (www.b-basic.nl) through B-Basic, a public-private NWO-ACTS programme (ACTS = Advanced Chemical Technologies for Sustainability).

Financial support by the J.E. Jurriaanse Stichting for the publication of this thesis is gratefully acknowledged.

Contents

Summary

In bioproduction processes of chemicals and pharmaceuticals, downstream processing usually is a significant cost factor. The products require a high purity (especially biopharmaceutical products), therefore, the process usually contains a large number of separation steps. Moreover, the high costs in downstream processing are caused by the fact that the products are often produced in a dilute environment. Since high product concentrations can cause inhibition of biological growth and production, the product should be removed from the production medium at relatively low concentrations. The use of in-situ product removal (ISPR) is a useful strategy to overcome this problem. Integration of the first downstream process step with the bioreactor leads to direct removal of product during growth and production reactions, potentially increasing the productivity of the biocatalyst and thus the total yield of product. ISPR potentially decreases waste streams, fermentor volume and the stress on micro-organisms resulting from oxygen limitation and shear stress caused by the cycling of the fermentation broth. In addition, decreasing the number of steps in the downstream processing of the product potentially leads to a decrease in the total process costs and processing time.

The aim of this thesis is to study the potential of integrated membrane extraction as a tool for ISPR for the removal of products from a fermentation broth. Membrane extraction (pertraction) enables a large contacting surface area between fermentation broth (aqueous phase) and solvent without the formation of an emulsion and is therefore a useful technique for ISPR.

The production of phenol by *Pseudomonas putida* S12 was chosen as a model process to illustrate product inhibition and to demonstrate the effects of ISPR by extraction with 1-octanol. Phenol was chosen as a model component and is a typical example of a fine chemical. It serves as a good model for aromatics containing a hydroxyl group. Additionally, due to its toxicity, phenol can well illustrate the effects of product inhibition.

An experimental study to illustrate product inhibition of phenol on the recombinant organism *Pseudomonas putida* S12 is described in chapter 2. It was demonstrated that the implementation of membrane extraction does not influence growth and phenol production. When phenol is removed from the fermentation broth by pertraction, a lower maximum aqueous phenol concentration is achieved, while the total phenol production increases to 132% as compared to the fermentation without pertraction. There are indications that the volumetric productivity increases slightly in the fermentations with in-situ pertraction as compared to the reference experiments.

In chapter 3, detailed calculations on the production of phenol in a conceptual process design illustrate the benefits and disadvantages of ISPR with an implemented membrane extraction unit in a bioreactor as compared to ISPR with a membrane extraction unit outside the reactor. Results show

that running the fermentation process at a lower product concentration results in a more efficient substrate utilization into biomass and phenol. The disadvantage of the integrated process is the need for large distillation columns and a high energy input for solvent regeneration due to the low product concentration in the solvent and the high solvent fluxes. Economic evaluations of the two processes show that to obtain a return of investment of 15%, the product cost price of the integrated process is a factor of three lower as compared to the non-integrated process.

In chapter 4 mass transfer is studied for phenol in fermentation systems and single fiber modules. Additionally, an approach is given for a novel membrane extraction module design for implementation in a large scale bioreactor by combining experimental and theoretical results. Factors that were found to influence the overall mass transfer coefficient are the membrane wall thickness, solvent (partition coefficient), sterilization and fouling (negative effect). Furthermore, bottlenecks and strategies for improvement are discussed. The integration of an extra obstacle into the reactor can give rise to several bottlenecks for both the separation process and the biological growth and production processes, mainly caused by the altered mixing pattern.

In chapters 5 and 6, the use of alternative solvents consisting of polymeric micelles solubilized in water are discussed and an alternative membrane extraction process evaluation is made. The micelles are formed of poly(ethylene oxide)–poly(propylene oxide) (PEO–PPO–PEO) block copolymers, commercially known as Pluronics. Pluronics are water-soluble, nonionic macromolecular surface active agents which are environmentally mild and hardly toxic to micro-organisms. The applicability of aqueous solutions of Pluronics for the removal of phenol in a separation and regeneration process is evaluated. Experimental results show that Pluronic micelles allow extraction of phenol from aqueous solutions at 30 °C (fermentation temperature). The phenol can be released due to the transition of the Pluronic micelles into unimers with a mild temperature switch from 30 to 8 °C. Ultrafiltration membranes provide a barrier between the aqueous Pluronic stripping solution and the aqueous solution in a (bio)reactor containing the desired product. Steady state model analysis and cost estimation show that the process costs are mainly determined by the required membrane area.

In chapter 7 the potential of integrated membrane extraction as an in-situ product recovery tool for the removal of products from a fermentation broth is discussed. Furthermore, improvement of the mass transfer limitation at the reactor side by a discontinuous moving membrane module is discussed. Fouling of micro-organisms and medium components at the aqueous (shell) side of the membrane has a negative effect on the overall mass transfer coefficient by increasing the boundary layer thickness at reactor side at the membrane surface. To improve the shell-side mass transfer, the turbulence at the membrane surface can be increased by the use of alternative membrane modules which cause high surface shear rates along the membrane. The novel membrane module described in this chapter shows interesting possibilities in microfiltration to improve the flux by reducing the fouling at the membrane surface.

Finally, it can be concluded that integrated membrane extraction shows potential as a tool for the removal of products from a fermentation broth. The benefits of an integrated process will pay off even more for very toxic and inhibiting products that do not allow for high concentrations in the (bio)reactor. The alternative process based on Pluronic micelles can be suited for products that allow for a higher critical concentration in the (bio)reactor as compared to phenol. The resulting higher driving force for membrane extraction will result in a decrease of the overall process costs. For products with a lower solubility in water, recovery is easy after regeneration of the micellar solvent.

Samenvatting

De ontwikkeling van nieuwe biologische of groene productieprocessen voor chemicaliën krijgt de laatste jaren veel aandacht. In de biologische productie van chemicaliën en farmaceutica is het zuiveren van de producten vaak een grote kostenpost. Omdat de producten meestal een hoge zuiverheid moeten hebben bevat een zuiveringsproces veel stappen. Ook het feit dat de producten veelal in een verdunde oplossing geproduceerd worden maakt het zuiveren kostbaarder. Een hoge productconcentratie in het medium leidt vaak tot remming van groei van en productie door de gebruikte micro-organismen waardoor het product in lage concentraties al verwijderd moet worden. In-situ productverwijdering (in-situ product removal, ISPR) kan gebruikt worden om dit probleem aan te pakken. Wanneer een scheidingsstap in de bioreactor wordt geïntegreerd kan het product direct verwijderd worden tijdens groei en productie waardoor de productiviteit van de organismen en dus de totale opbrengst van product verhoogd kan worden. Andere voordelen van ISPR zijn verminderde afvalstromen, kleinere reactorvolumes en verminderde stress op de micro-organismen. Tevens zal het verminderen van het aantal scheidingsstappen om een zuiver product te verkrijgen de totale proceskosten aanzienlijk kunnen verlagen en de duur van het totale proces verkorten.

In dit onderzoek is geïntegreerde membraan extractie (pertractie) als ISPR techniek voor het verwijderen van producten uit een bioreactor bestudeerd. Membraan extractie biedt een groot contactoppervlak tussen de fermentatie vloeistof (de waterige oplossing waarin onder andere de organismen en het gewenste product zich bevinden) en het oplosmiddel zonder dat er een emulsie gevormd wordt.

Het modelproces dat gebruikt is voor het onderzoek is de productie van fenol door de genetisch gemodificeerde bacterie *Pseudomonas putida* S12. Fenol is gekozen als model voor aromaten met een hydroxylgroep. Fenol is erg toxisch voor de bacteriën waardoor de effecten van productinhibitie goed aangetoond kunnen worden en de effecten van ISPR door middel van extractie met 1-octanol bestudeerd kunnen worden.

In hoofdstuk 2 wordt een experimentele studie beschreven waarbij is gekeken naar de inhibitie van fenol op *Pseudomonas putida* S12. Het is aangetoond dat de aanwezigheid van een membraan in de reactor geen invloed heeft op de groei van de micro-organismen en de productie van fenol. Wanneer door middel van pertractie fenol wordt verwijderd uit de fermentatievloeistof, verhoogd de totale fenolproductie naar 132% vergeleken met een fermentatie zonder pertractie. De volumetrische productiviteit lijkt toe te nemen in de fermentaties waarbij in-situ pertractie wordt toegepast vergeleken met de referentie-experimenten.

In hoofdstuk 3 wordt het productieproces van fenol door *Pseudomonas putida* S12 beschreven in een procesontwerp en een economische evaluatie. De voor- en nadelen van ISPR met membraan extractie

geïntegreerd in de bioreactor worden beschreven ten opzichte van ISPR met membraan extractie buiten de bioreactor. De resultaten laten zien dat de lage productconcentratie in het fermentatieproces een efficiëntere substraatomzetting in biomassa en product tot gevolg heeft. Nadelen van een geïntegreerd proces zijn grote destillatiekolommen en een groter energieverbruik voor het regenereren van het oplosmiddel. Uit een economische evaluatie van de twee processen blijkt, dat de productkostprijs bij een verhouding tussen inkomsten en investering van 15% (return of investment) een factor drie lager is bij een geïntegreerd proces vergeleken met een niet-geïntegreerd proces.

Hoofdstuk 4 beschrijft de studie naar massatransport van fenol in pertractie in model fermentatiesystemen en enkele-vezel modules. Tevens wordt er een ontwerp beschreven voor een geïntegreerde membraan extractie module voor gebruik in een grootschalige bioreactor. Dit ontwerp is gemaakt door experimentele en theoretische resultaten te combineren. Onderzochte factoren die van invloed zijn op de massatransportcoëfficiënt worden in dit hoofdstuk beschreven: membraantype (wanddikte), oplosmiddel (partitiecoëfficiënt), sterillisatie en het blokkeren of verstoppen van de membraanporiën (fouling). Verder worden mogelijke problemen besproken die kunnen ontstaan door de integratie van een extra obstakel in de reactor zoals het veranderde mengpatroon en het effect op zowel het scheidingsproces als het biologische groei- en productieproces. Als laatste worden oplossingen voor verbetering bediscussieerd.

In hoofdstukken 5 en 6 wordt het gebruik van alternatieve oplosmiddelen van polymere micellen opgelost in water in een nieuw membraan extractie proces besproken. De micellen worden gevormd door poly(ethyleen oxide)–poly(propyleen oxide) (PEO–PPO–PEO) blok copolymeren, commercieel bekend als Pluronics. Pluronics zijn water oplosbare, niet-ionische macromoleculaire oppervlakte actieve componenten die milieuvriendelijk zijn en niet toxisch voor micro-organismen. Het gebruik van waterige oplossingen van Pluronics voor de verwijdering van fenol in een scheidingsproces is geëvalueerd. Experimentele resultaten laten zien dat micellen van Pluronics fenol verwijderen uit waterige oplossingen bij 30°C (fermentatie temperatuur). Wanneer de temperatuur wordt verlaagd naar 8°C komt fenol weer vrij in de oplossing door de (fase) overgang van Pluronic micellen naar Pluronic unimeren. Ultrafiltratie membranen worden gebruikt als barrière tussen het waterige Pluronic oplosmiddel en de waterige oplossing in de bioreactor waar het gewenste product zich in bevindt. Na analyse van steady state modellen en het maken van een kostenschatting blijkt dat de kosten van dit proces voornamelijk worden bepaald door de membraankosten.

In het laatste hoofdstuk, hoofdstuk 7, wordt het potentieel van geïntegreerde membraan extractie als techniek voor product verwijdering uit fermentatievloeistoffen bediscussieerd. Verder wordt een discontinu bewegende membraan module besproken als mogelijkheid om massatransport aan de reactorkant te verbeteren. Door hogere turbulentie die ontstaat door de bewegende module neemt de oppervlaktespanning aan het membraan toe en wordt het blokkeren van de membraan poriën door

micro-organismen en mediumcomponenten aan de grenslaag van het membraan verminderd. Het principe van de nieuwe membraan module wordt beschreven in dit hoofdstuk aan de hand van microfiltratieexperimenten. De flux door het membraan neemt toe bij een discontinu bewegende module in vergelijking met de stilstaande toestand en de module geeft zeker mogelijkheden voor toepassing in membraan extractie.

Er kan worden geconcludeerd dat geïntegreerde membraan extractie potentieel biedt als ISPR techniek voor de verwijdering van producten uit een bioreactor. De voordelen van een geïntegreerd proces zullen nog duidelijker zijn wanneer deze techniek wordt gebruikt voor erg toxische producten die in een lagere concentratie in de bioreactor aanwezig moeten zijn vergeleken met fenol. Het alternatieve proces gebaseerd op Pluronic micellen kan toegepast worden voor producten die een hogere kritische concentratie in de bioreactor kunnen bereiken. De hogere drijvende kracht voor membraanextractie zal de totale proceskosten verlagen. Wanneer de producten een lage oplosbaarheid in water hebben is de zuivering nog gemakkelijker na regeneratie van het op micellen gebaseerde oplosmiddel.

Chapter 1

Introduction

1.1 Bio-based production processes

Over the past decade, the "green" production of chemicals has gained significant public and scientific interest. As a result, many bio-catalytic processes are being developed for the sustainable production of chemicals. There are several reasons why the transition from the use of fossil-based raw materials to renewable bio-based materials in production processes is important. Eventually, commercially available coal and oil reserves will run out. Unlike fossil fuels, renewable sources will not run out. Examples of renewable sources are organic materials and crops such as grass, wood (cellulosic biomass), sugar cane, corn, vegetable oils (soy, coleseed), biogas, animal fats, manure and municipal waste. Various types of agricultural waste can be turned into biofuels or into raw materials for the production of chemical and pharmaceutical products. Another reason for the shift to bio-based processes is that pollution from current industrial processes damages the environment, has adverse health effects and impacts the climate. Bioprocesses will be important in reducing pollution as well as in tackling climate change and public health issues. A growing number of early stage successes across a wide range of bio-based products indicates this sector has tremendous potential. In Table 1 an indication is given for the growth of bio-based chemical products in the coming years.

Table 1. Estimations for the growth of bio-based chemical products.

Chemical sector	**2010 (%)**	**2025 (%)**
Commodity Chemicals	1-2	6-10
Specialty Chemicals	20-25	45-50
Fine Chemicals	20-25	45-50
Polymers	5-10	10-20

Source: USDA, U.S. Biobased Products Market Potential and Projections Through 2025

1.2 Bioproduction of chemicals and the need for ISPR

In bioproduction processes, downstream processing usually is a large cost factor. The products often require a high purity, therefore, the process contains a large number of separation steps. Additionally, the products in bioprocesses are produced in a dilute environment. Since high product concentrations often cause inhibition of biological growth and production, the product should be removed from the production medium at relatively low concentrations. The use of in-situ product removal (ISPR) is a useful strategy to overcome this problem. Integration of the first downstream process step with the bioreactor leads to direct removal of product during growth and production reactions, potentially increasing the productivity of the biocatalyst and thus the total yield of product. ISPR can be applied outside the reactor (referred to as in-stream) or inside the reactor (referred to as in-situ), see also Figure 1. The technique used for ISPR is dependent on the properties of the product to be separated (e.g. volatility, molecular weight, size, solubility, charge and hydrophobicity). Numerous techniques

that can be used for ISPR are described in literature [1-3], including extraction [4, 5], adsorption, extractive capsules [6-8], membrane extraction [9-12], crystallization [13-15], membrane crystallization [16], distillation, gas stripping, filtration [17], centrifugation, size exclusion, pervaporation [18], precipitation [19], ion exchange, electrodialysis or affinity methods. Membrane extraction (pertraction) enables a large contacting surface area between fermentation broth (aqueous phase) and solvent without the formation of an emulsion and is therefore a useful technique for ISPR [20]. In this thesis the potential of integrated membrane extraction as a tool for in-situ product removal is investigated.

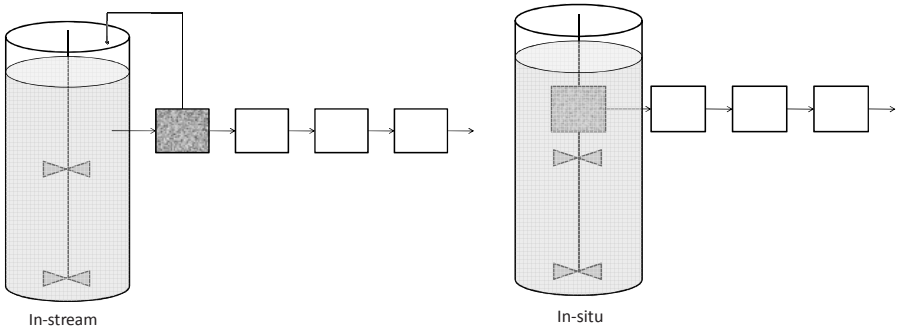

Figure 1. In-stream (left) and in-situ (right) product removal.

1.3 ISPR using membrane extraction

Fermentation processes usually run in batch or fed-batch mode until the inhibiting product concentration is reached where growth and production are haltered. Subsequently, the complete fermentation broth is led through a solid-liquid separation unit, e.g. microfiltration, to separate the biomass from the aqueous phase containing the product of interest, see also Figure 2. Afterwards, the aqueous phase is contacted with the solvent in a (membrane) extraction unit where the product is extracted from the aqueous phase due to the higher affinity of the solvent for the product as compared to water, which is determined by the partition coefficient. Finally, the product is stripped from the solvent phase by for example distillation and the regenerated solvent can be reused in the membrane extraction unit. Disadvantages of this process are the large waste streams (biomass, aqueous phase) and a large fermentor volume required to maintain a certain production rate under inhibiting conditions.

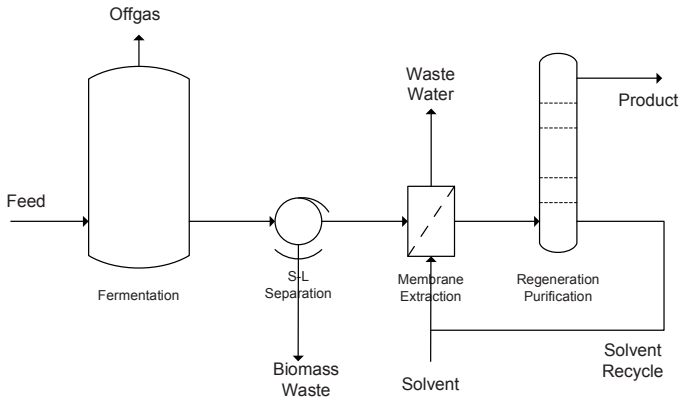

Figure 2. Fed-batch fermentation with batch separation.

To decrease the required fermentor volume, the aqueous concentration of the inhibiting product should be maintained at a low level. This can be achieved by continuous circulation of the fermentation broth over a solid-liquid separation unit, recycling the biomass and aqueous phase back to the fermentor after the inhibiting component is stripped from the aqueous phase in an extraction unit, see also Figure 3. Alternatively, the fermentation broth can be circulated directly through a membrane extraction unit or immobilized biomass, for example in a fibrous bed, can be used[21, 22]. This will reduce the amount of waste produced by the process. Disadvantages of such a system are the difficulties to sterilize the membrane system and clogging of the membrane by biomass. Additional disadvantages of this process are related to stress on the micro-organisms by oxygen limitation and shear stress caused by the continuous circulation of the fermentation broth. Additional stress to the micro-organisms can be caused in production processes of carboxylic or hydrocarboxylic acids, where fermentation pH is not equal to the pKa of the product. In such processes, extraction should run at a lower pH as compared to the fermentation pH[23]. These stress conditions can affect the micro-organisms causing a lower productivity. Other disadvantages are the requirement of a large amount of membrane for the extraction unit and high costs for regeneration and purification due to a lower product concentration in the solvent. External membrane extraction units are commercially available, however, the lack of large modules restrains the use in large scale fermentation production processes.

To avoid stress on the micro-organisms and large circulating streams of fermentation broth, a membrane extraction unit can also be integrated in the fermentor, see Figure 4. The solvent stream is continuously removing the inhibiting product from the reactor during growth and production reactions, maintaining a low product concentration in the reactor [24]. Continuous removal of the toxic product is expected to result in a higher biomass growth rate, productivity and yield of biomass and product on substrate and consequently to a decrease in reactor volume and raw materials costs. On the contrary, the integrated separation process will run at relative low product concentrations which will cause a decrease in driving force for pertraction. Consequently, this leads to an increase in the required

membrane area and a higher energy input for solvent regeneration. Additionally, a membrane extraction module integrated in a reactor can be sensitive to fouling in prolonged operation. Key variables like product concentration in the reactor will influence the substrate requirements, biomass growth rate and production rate which in turn influence the required reactor volume, membrane area, energy input for solvent regeneration and raw materials.

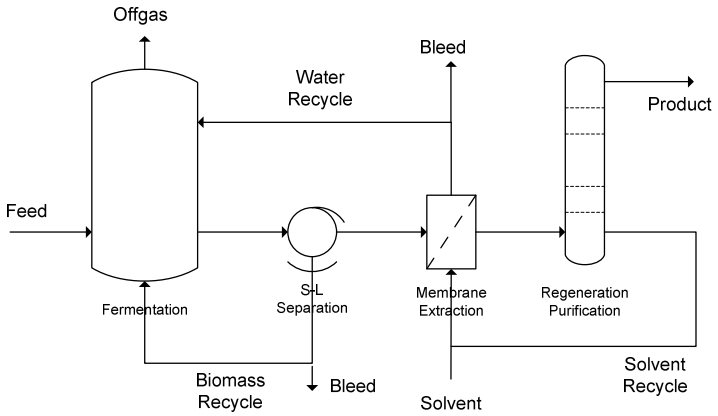

Figure 3. Fed-batch fermentation with continuous separation and recycling aqueous phase and biomass.

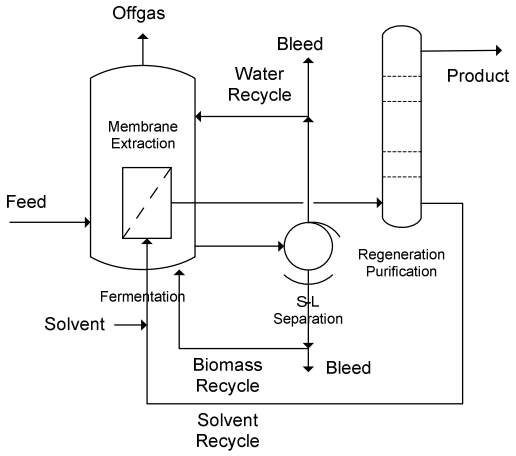

Figure 4. Continuous fermentation with integrated membrane extraction.

1.4 Model system used to study integrated membrane extraction

Pseudomonas putida S12 is a solvent-tolerant bacterium that is used to make recombinants that grow on alternative carbon sources and that produces several aromatics like cinnamic acid [25], phenol [26] and 3-methylcatechol. Moreover, it can be used in direct contact with organic solvents [27]. These aromatics

can have toxic or inhibitory effects on growth and production processes and it is important that their concentration in the production medium remains below a certain level. The solvent-tolerant characteristics of this organism allow for the use of extraction with organic solvents in an ISPR method. In this thesis, the production of phenol by *P. putida* S12 was chosen as a model process to illustrate product inhibition and to demonstrate the effects of ISPR by membrane extraction with 1-octanol.

1.5 Aim and layout of this thesis

The aim of this thesis is to study the potential of integrated membrane extraction (in-situ pertraction) for the removal of inhibiting products from a fermentation broth. The thesis consists of six chapters describing experimental and modeling studies of the separation system and the complete bioprocess.
In chapter 2, in-situ phenol removal from fed-batch fermentations of *P. putida* S12 by continuous pertraction with 1-octanol is described in order to demonstrate the feasibility of in-situ pertraction for this purpose.
In chapter 3, a conceptual process design for the production of phenol by *P. putida* S12 is described. Continuous fermentation with the pertraction unit inside the reactor (integrated process), is compared to fed-batch fermentation with the pertraction unit outside the reactor (non-integrated process). An extended model for fermentation, consisting of biomass growth and phenol production combined with product inhibition, cell removal, pertraction with 1-octanol and regeneration of the solvent by distillation is described with the help of experimental and theoretical data. Additionally, an economic evaluation was made for the two processes to show the benefits of the integrated process.
In chapter 4, a design of a novel membrane extraction module for implementation in a bioreactor is described by combining experimental and theoretical results. The calculations and considerations made in this chapter show interesting possibilities for an integrated membrane extraction process.
In chapters 5 and 6, the use of alternative solvents of polymeric micelles solubilized in water are discussed and an evaluation is made for an alternative membrane-extraction process. The micelles are formed of poly(ethylene oxide)–poly(propylene oxide) (PEO–PPO–PEO) block copolymers, commercially known as Pluronics. Pluronics are water-soluble, nonionic macromolecular surface active agents. They are environmentally mild and hardly toxic to micro-organisms.
Finally, in chapter 7, the main findings of the work described in this thesis are discussed and a novel (microfiltration) membrane module that can reduce the fouling and increase the flux is described. This concept of a discontinuously moving module can possibly be used in the membrane extraction processes described in this thesis.

References

1. Lye, G.J.; Woodley, J.M., Application of in situ product-removal techniques to biocatalytic processes. Trends in Biotechnology 1999, 395-402.
2. Lienqueo, M.E.; Asenjo, J.A., Use of expert systems for the synthesis of downstream protein processes. Computers & Chemical Engineering 2000, 2339-2350.
3. Groot, W.J.; van der Lans, R.G.J.M.; Luyben, K.C.A.M., Technologies for butanol recovery integrated with fermentations. Process Biochemistry 1992, 61-75.
4. Brink, L.E.S.; Tramper, J., Optimization of organic solvent in multiphase biocatalysis. Biotechnology and Bioengineering 1985, 1258-1269.
5. Buhler, B.; Bollhalder, I.; Hauer, B.; Witholt, B.; Schmid, A., Use of the two-liquid phase concept to exploit kinetically controlled multistep biocatalysis. Biotechnology and Bioengineering 2003, 683-694.
6. Berg, C.v.d.; Roelands, C.P.M.; Bussmann, P.; Goetheer, E.L.V.; Verdoes, D.; van der Wielen, L.A.M., Preparation and analysis of high capacity polysulfone capsules. Reactive and Functional Polymers 2009, 766-770.
7. Stark, D.; Kornmann, H.; Münch, T.; Sonnleitner, B.; Marison, I.W.; Stockar, U.v., Novel type of in situ extraction: Use of solvent containing microcapsules for the bioconversion of 2-phenylethanol from L-phenylalanine by Saccharomyces cerevisiae. Biotechnology and Bioengineering 2003, 376-385.
8. Berg, C.v.d.; Wierckx, N.; Vente, J.; Bussmann, P.; Bont, J.d.; Wielen, L.v.d., Solvent-impregnated resins as an in-situ product recovery tool for phenol recovery from *Pseudomonas putida S12TPL* fermentations. Biotechnology and Bioengineering 2008, 466-472.
9. Schlosser, S.; Kertesz, R.; Martak, J., Recovery and separation of organic acids by membrane-based solvent extraction and pertraction: An overview with a case study on recovery of MPCA. Separation and Purification Technology 2005, 237-266.
10. Fernandes, P.; Prazeres, D.M.; Cabral, J.M., Membrane-assisted extractive bioconversions. Advances in biochemical engineering/biotechnology 2003, 115-148.
11. Hüsken, L.E.; Oomes, M.; Schroën, K.; Tramper, J.; de Bont, J.A.M.; Beeftink, R., Membrane-facilitated bioproduction of 3-methylcatechol in an octanol/water two-phase system. Journal of Biotechnology 2002, 281-289.
12. Molinari, F.; Aragozzini, F.; Cabral, J.M.S.; Prazeres, D.M.F., Continuous production of isovaleraldehyde through extractive bioconversion in a hollow-fiber membrane bioreactor. Enzyme and Microbial Technology 1997, 604-611.
13. Urbanus, J.; Laven, J.; Roelands, C.P.M.; ter Horst, J.H.; Verdoes, D.; Jansens, P.J., Template Induced Crystallization: A Relation between Template Properties and Template Performance. Crystal Growth & Design 2009, 2762-2769.
14. Buque-Taboada, E.M.; Straathof, A.J.J.; Heijnen, J.J.; van der Wielen, L.A.M., Microbial reduction and *in situ* product crystallization coupled with biocatalyst cultivation during the synthesis of 6R-dihydrooxoisophorone. Advanced Synthesis and Catalysis 2005, 1147-1154.
15. Urbanus, J.; Roelands, C.P.M.; ter Horst, J.H.; Verdoes, D.; Jansens, P.J., Screening for templates that promote crystallization. Food and Bioproducts Processing 2008, 116-121.
16. Curcio, E.; Di Profio, G.; Drioli, E., Recovery of fumaric acid by membrane crystallization in the production of -malic acid. Separation and Purification Technology 2003, 63-73.
17. Bouchoux, A.; Roux-de Balmann, H.; Lutin, F., Investigation of nanofiltration as a purification step for lactic acid production processes based on conventional and bipolar electrodialysis operations. Separation and Purification Technology 2006, 266-273.
18. Groot, W.J.; den Reyer, M.C.H.; Baart de la Faille, T.; van der Lans, R.G.J.M.; Luyben, K.C.A.M., Integration of pervaporation and continuous butanol fermentation with immobilized cells I: Experimental results. The Chemical Engineering Journal 1991, B1-B10.
19. Hirata, D.B.; Oliveira, J.H.H.L.; Leão, K.V.; Rodrigues, M.I.; Ferreira, A.G.; Giulietti, M.; Barboza, M.; Hokka, C.O., Precipitation of clavulanic acid from fermentation broth with potassium 2-ethyl hexanoate salt. Separation and Purification Technology 2009, 598-605.
20. Klaassen R.; Feron P. H. M.; Jansen A. E., Membrane contractors in industial applications. Chemical Engineering Research and Design 2005, 234-246.
21. Wu, Z.T.; Yang, S.T., Extractive fermentation for butyric acid production from glucose by Clostridium tyrobutyricum. Biotechnology and Bioengineering 2003, 93-102.

22. Jiang, L.; Wang, J.F.; Liang, S.Z.; Wang, X.N.; Cen, P.L.; Xu, Z.N., Butyric acid fermentation in a fibrous bed bioreactor with immobilized Clostridium tyrobutyricum from cane molasses. Bioresource Technology 2009, 3403-3409.
23. Blahušiak, M.; Schlosser, Š.; Marták, J., Simulation of Hybrid Fermentation-Separation Process for Production of Butyric Acid. Chemical Papers 2010, 213–222.
24. Heerema, L.; Wierckx, N.; Roelands, M.; Hanemaaijer, J.H.; Goetheer, E.; Verdoes, D.; Keurentjes, J., In situ phenol removal from fed-batch fermentations of solvent tolerant Pseudomonas putida S12 by pertraction. Biochemical Engineering Journal 2011, 245-252.
25. Nijkamp, K.; van Luijk, N.; de Bont, J.; Wery, J., The solvent-tolerant Pseudomonas putida S12 as host for the production of cinnamic acid from glucose. Applied Microbiology and Biotechnology 2005, 170-177.
26. Wierckx, N.J.P.; Ballerstedt, H.; De Bont, J.A.M.; Wery, J., Engineering of solvent-tolerant *Pseudomonas putida* S12 for bioproduction of phenol from glucose. Applied and environmental microbiology 2005, 8221-8227.
27. Husken, L.E.; Dalm, M.C.F.; Tramper, J.; Wery, J.; de Bont, J.A.M.; Beeftink, R., Integrated bioproduction and extraction of 3-methylcatechol. Journal of Biotechnology 2001, 11-19.

Chapter 2

In-situ phenol removal from fed-batch fermentations of solvent tolerant *Pseudomonas putida* S12 by pertraction

This chapter was published as:
Heerema, L.; Wierckx, N.; Roelands, M.; Hanemaaijer, J. H.; Goetheer, E.; Verdoes, D.; Keurentjes, J., In situ phenol removal from fed-batch fermentations of solvent tolerant Pseudomonas putida S12 by pertraction. Biochem. Eng. J. 2011, 245-252.

Chapter 2 **-** In-situ phenol removal from fed-batch fermentations of solvent tolerant *Pseudomonas putida* S12 by pertraction

Abstract

In-situ phenol pertraction with 1-octanol has been experimentally studied to improve the production of the model component phenol by a recombinant strain of *Pseudomonas putida* S12. When the phenol concentration in the reactor reaches 2 mM, the cells in fermentations without phenol removal are inhibited in growth and phenol production. Growth and phenol production stop after approximately 80 hours at a phenol concentration in the reactor of 3.8 mM. When phenol is removed from the fermentation broth by pertraction, a lower maximum aqueous phenol concentration of 2.6 mM is achieved, while the total phenol production increases to 132%, as compared to the fermentation without pertraction. There are indications that the volumetric productivity ($mmol.L^{-1}.h^{-1}$) increases slightly in the fermentations with in-situ pertraction compared to the reference experiments. As expected, the amount of phenol produced per gram biomass (the specific productivity, $mmol.g^{-1}.L^{-1}$) remains constant in time for all fermentations. The use of pertraction for in-situ phenol removal is compared to in-situ second phase extraction, in-situ solvent impregnated resins and in-stream pertraction. Although the system shows promising results, further modifications such as using a solvent with a higher partition coefficient can improve the overall performance.

2.1 Introduction

Downstream processing usually is a large cost factor in bioproduction processes of fine or bulk chemicals and pharmaceuticals. The products require a high purity (especially biopharmaceutical products), therefore, the process contains a large number of separation steps. Another reason for the high costs in down stream processing is the fact that the products in bioprocesses are produced in a dilute environment. Since high product concentrations can cause inhibition of biological growth and production, the product should be removed from the production medium at relatively low concentrations. The use of in-situ product removal (ISPR) is a useful strategy to overcome this problem. Integration of the first downstream process step with the bioreactor leads to direct removal of product during growth and production reactions, potentially increasing the productivity of the biocatalyst and thus the total yield of product. ISPR can be applied outside the reactor (referred to as in-stream) or inside the reactor (referred to as in-situ) and the technique used is dependent on the properties of the product to be separated (e.g. volatility, molecular weight, size, solubility, charge and hydrophobicity). Numerous techniques that can be used for ISPR are described in literature [1-3], including extraction [4, 5], adsorption, extractive capsules [6-8], membrane extraction [9-12], crystallization [13-15], membrane crystallization [16], distillation, gas stripping, filtration [17], centrifugation, size exclusion, pervaporation [18], precipitation [19], ion exchange, electrodialysis or affinity methods.

Pseudomonas putida S12 is a solvent tolerant bacterium that is used to make recombinants that grow on alternative carbon sources and that produces several aromatics like cinnamic acid [20], p-coumarate [21] and phenol [22]. These aromatics can have toxic or inhibitory effects on growth and production processes and it is important that their concentration in the production medium remain below a certain level. Moreover, the fact that this organism is solvent tolerant allows for the use of extraction with (organic) solvents in an ISPR method.

The toxicity of products or solvents to microorganisms can be illustrated with the logP-value. The logP-value is defined as the logarithm of a solvent's partition coefficient in a standard octanol-water mixture and can be used as a quantitative index of solvent polarity. The limiting logP-value for *P. putida* species is 3.1 [23]. Phenol is a toxic component for microorganisms due to its low logP-value (1.5). The phenol concentration in the reactor should be maintained at a very low level to avoid product inhibition. Therefore, the production of phenol by *P. putida* S12 was chosen as model process to illustrate product inhibition and to demonstrate the effects of ISPR by extraction with 1-octanol.

In the past, several methods were evaluated to extract phenol from the fermentation medium, see Figure 1a, 1b and 1c. The first method is liquid-liquid extraction (Figure 1a) [22]. Direct contact of the solvent and the micro-organisms can lead to toxic effects. Additionally, the presence of a solvent can

result in emulsion formation in the reactor which can not easily be broken into separate phases. Consequently, a two phase extraction system can not be used as a continuous ISPR method.

Another method used for the extraction of phenol from fermentation broth is the use of porous particles that are impregnated with a solvent (Solvent Impregnated Resins or SIRs), see Figure 1b [8]. SIRs offer a large surface area for extraction while the solvent and the fermentation broth are separated to decrease or prevent solvent toxicity and emulsion formation. One of the disadvantages of the use of SIRs is the fact that they can not easily be used in a continuous extraction and regeneration process.

A continuous method that can be used for phenol extraction is in-stream pertraction (Figure 1c). The use of a membrane decreases the contact between the solvent and the micro-organisms and prevents emulsification [24]. Using in-stream pertraction, the toxic effects of both phenol and the solvent are expected to decrease. The experimental results, however, show poor biomass growth that was probably caused by lack of oxygen in the membrane loop [25].

In this work, a continuous integrated membrane extraction process is used to optimize phenol extraction from fermentation broth: in-situ pertraction (Figure 1d). Compared to in-stream pertraction, the integration of a hollow fiber membrane extraction unit in a bioreactor eliminates the circulation of fermentation broth, containing the micro-organisms, and therefore no oxygen limitation occurs. In previous work [26], in-situ pertraction in a cell-free model system showed good potential for the use in a bioreactor system. In this study, the stepwise implementation of the pertraction unit in a bioreactor is evaluated in the fermentation process. The model solvent chosen for this study is 1-octanol to allow for a comparison of the performance of this system with second phase extraction described earlier [22].

2.2 Materials and methods

Bacterial strain

The bacterial strain that was used in this study was *P. putida* S12 TPL3 [22]. This strain was constructed by introduction of the gene encoding for the enzyme tyrosine phenol lyase (TPL). The strain was further optimized to establish an increased carbon flux to the central metabolite tyrosine which is converted into phenol by TPL and excreted into the medium.

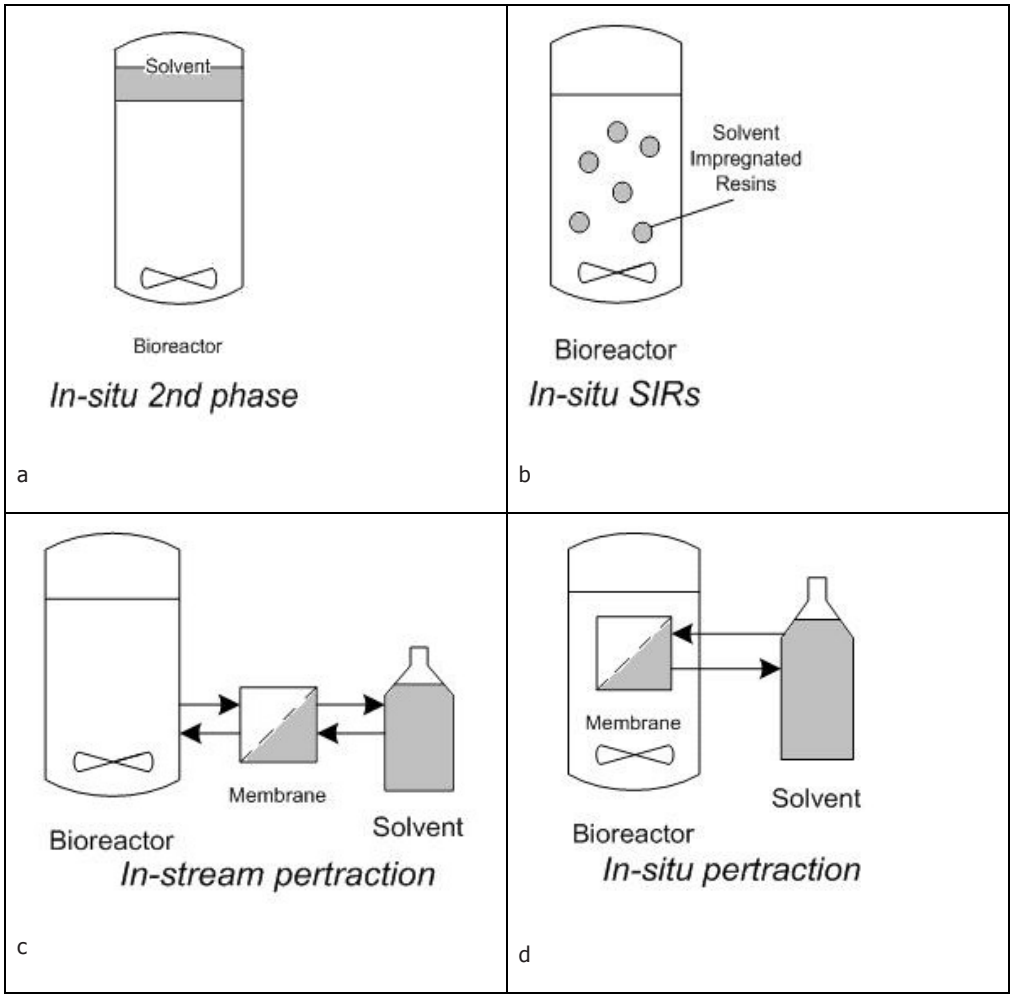

Figure 1. In-situ liquid-liquid (second phase) extraction (a), in-situ extraction using Solvent Impregnated Resins (SIRs) (b), in-stream pertraction (c) and in-situ phenol pertraction (d).

Culture conditions

Precultures of *P. putida* S12 TPL3 were grown in 250 mL shake flasks containing 75 mL mineral salts medium with pH7 [27], see Table 1. Sodium salicylate was added as inducer of the *tpl* gene.
Fed-batch cultivation was performed in a BioFlo 3000 fermentor (New Brunswick Scientific), with a maximum working volume of 2.5 L. The batch medium used in fermentation was comparable to the mineral medium except for the $(NH_4)_2SO_4$ and glycerol concentration, see Table 1. The start volume of the batch phase was approximately 1.75 L.

The pH in the reactor was controlled at 7.0 by addition of 1 M NaOH. Dissolved oxygen was maintained at 15% saturation by headspace aeration with air, mixed with pure oxygen if needed, and by adjusting the stirrer speed between 100 and 500 rpm. The standard stirrer in the reactor consists of two rushton stirring blades. To increase mixing efficiency after membrane implementation, the lower stirring blade was replaced by a propeller. All fermentations were executed with this stirrer configuration. From our measurements, it was demonstrated that the oxygen transfer rate in the reactor did not change with this altered stirrer configuration in the presence of a membrane compared to the standard configuration with two rushton stirring blades in the absence of a membrane.

The batch phase of the fermentation started with the addition of 150 mL cells from the preculture (washed and resuspended in buffer) to obtain an initial biomass concentration in the reactor of approximately 0.1 $g.L^{-1}$. The initial biomass concentration in the reactor was determined by sampling after inoculation. The feed phase was started when the ammonium concentration measured in the broth was zero. During the feed phase, the micro-organisms were grown in a nitrogen-limited environment. The contents of the feed medium are given in Table 1.

The feed rate was determined by the (linear) decrease of nitrogen concentration in the batch phase in time ($mg.L^{-1}.h^{-1}$). In the feed phase, the nitrogen concentration was maintained at zero by continuous measurements and adjustment of the feed rate. The glycerol content in the fermentation broth was monitored to be surplus during the complete fermentation process. Samples were taken at regular intervals from the fermentation broth and phenol, ammonium, biomass (cell growth) and glycerol concentrations were measured.

All fermentation experiments were executed at least twice to show the reproducibility. Only the experiment in which a membrane was placed in a bioreactor was executed once because it was expected that the results are comparable to the reference fermentations.

2.3 Pertraction

Pertraction was carried out with Accurel PP V8/HF polypropylene hollow fiber microfiltration membranes (Membrana). The membrane fibers have a pore size of 0.2 µm, outer diameter (d_{out}) of 8.6 mm and inner diameter (d_{in}) of 5.5 mm. The area available for pertraction in all experiments was approximately 0.014 m^2 (~7 $m^2.m^{-3}$). The porosity (ε) and tortuosity (τ) of the membrane are 0.8 and 2.25, respectively (data obtained from Membrana).

1-Octanol and phenol (analytical grade) were purchased from Sigma-Aldrich and used as delivered. The 1-octanol was circulated with volumetric flow rates between 50 and 70 $mL.min^{-1}$ through the

membrane lumen and the solvent volume used was approximately 0.6 L. The membrane was integrated in the reactor and sterilized in the presence of demineralized water at 120°C. For all pertraction experiments, samples were taken in time from the aqueous and the 1-octanol phase to determine the phenol concentration.

Table 1. Concentration of the different components in the three media used for growth and phenol production.

Component	**Amount per L in mineral salts medium**	**Amount per L in bach medium**	**Amount per L in feed medium**
K_2HPO_4	3.88 g	3.88 g	-
$NaH_2PO_4.2H_2O$	2.13 g	2.13 g	-
$(NH_4)_2SO_4$	4 g	1 g	15 g
$MgCl_2.6H_2O$	200 mg	200 mg	300 mg
EDTA	20 mg	20 mg	30 mg
$ZnSO_4.7H_2O$	4 mg	4 mg	6 mg
$CaCl_2.2H_2O$	2 mg	2 mg	3 mg
$FeSO_4.7H_2O$	10 mg	10 mg	15 mg
$Na_2MoO_4.2H_2O$	0.4 mg	0.4 mg	0.6 mg
$CuSO_4.5H_2O$	0.4 mg	0.4 mg	0.6 mg
$CoCl_2.6H_2O$	0.8 mg	0.8 mg	1.2 mg
$MnCl_2.6H_2O$	2 mg	2 mg	3 mg
Glycerol	10 g	9 g	138 g
Gentamicin	10 mg	10 mg	10 mg
Sodium salicylate	16 mg	16 mg	16 mg

2.4 Analytical methods

Cell density in the fermentation broth was measured at 600 nm with a Biowave Cell Density Meter (WPA Ltd.). After measuring the cell density, the samples were centrifuged for 2 minutes at 9000 rpm at room temperature (Eppendorf centrifuge, 5415R). The supernatant samples were used for phenol analysis by high-performance liquid chromatography HPLC (Agilent 1100 system) using a Zorbax SB-C18 column. The phenol was analyzed with a Chromopak UV detector (detection at 268 nm). Samples (20 µL) were injected in a mobile phase consisting of 20 mM KH2PO4 (pH 2,0)+ 1% acetonitril at a flow rate of 1.5 $mL.min^{-1}$.

To determine the amount of phenol in the 1-octanol phase, 1 M NaOH was added to the samples at a volume ratio 1-octanol:NaOH of 1:2 and equilibrated overnight. After phase separation, the NaOH phase of the samples was neutralized with an equal amount of 1 M HCl and measured as described for the supernatant samples.

The total (hypothetical) phenol concentration ($c_{ph,total}$, mM) was calculated according to Equation 1, where $c_{ph,b}$ and $c_{ph,s}$ are the concentration of phenol in the bulk (aqueous) and stripping (1-octanol) phase (mM), respectively. V_{aq} and V_{oct} are the volumes of the aqueous and octanol phase (L), respectively.

$$c_{ph,total} = \frac{c_{ph,b} \cdot V_{aq} + c_{ph,s} \cdot V_{oct}}{V_{aq}} \quad (1)$$

Glycerol was analyzed from the centrifuged samples using a Dionex ICS-3000 with an IonPac ICE-ASI column and a mobile phase of 0.1 M methanesulfonic acid (MSA) at 1.2 mL.min^{-1} and 30°C. Ammonium concentrations were determined from the centrifuged samples by cation exchange chromatography (Dionex) using an IonPac CS17 column and a mobile phase of 20 mM MSA at 0.4 mL.min^{-1} and 30°C. Additionally, for quick determination of ammonium concentrations during fermentation, a lab-testkit (LCK303 sample cuvette) was used after 15 minutes incubation using a sensor array photometer (LASA 20, Hach Lange).

2.5 Determination of the overall mass transfer coefficient

Mass transfer experiments were carried out in duplo with the reactor as used in the fermentation experiments and with an aqueous reactor volume of 2 L. A feed containing phenol was added at a feed rate corresponding to the average production rate in a reference fed-batch fermentation process. Additionally, mass transfer coefficients were determined in experiments with a sterilized membrane, in fermentation medium without cells and with a phenol feed rate of a factor three higher than the average production rate. The temperature in the reactor for the mass transfer experiments was maintained at 30°C, the stirrer speed at 250 rpm with an airflow rate of 1 L.min^{-1} (headspace aeration) and 1-octanol was circulated at a flow rate of 50 mL.min^{-1}. Samples were taken in time from the aqueous- and the 1-octanol phase and the phenol concentration in the samples was determined.
The phenol concentration in the aqueous and 1-octanol phase was determined in time. From these concentrations, combined with the feed rate of phenol, the amount of phenol removed from the aqueous (reactor) phase in time (mM.h^{-1}) could be determined. The overall mass transfer coefficient can be determined by a simple model, see Equation 2:

$$\frac{dc_{ph,b}}{dt} = \frac{k_{ov} \cdot A \cdot \left(c_{ph,b} - c_{ph,eq}\right)}{V_{aq}} \quad (2)$$

Where $dc_{ph,b}.dt^{-1}$ is the amount of phenol removed from the bulk (aqueous phase) in time ($mM.h^{-1}$), k_{ov} the overall mass transfer coefficient ($m.s^{-1}$), A the outer membrane area (m^2), V_{aq} the water volume (m^3), $c_{ph,b}$ the phenol concentration in de bulk at time t (mM) and $c_{ph,eq}$ the phenol concentration in the water phase at equilibrium (mM).

The overall mass transfer coefficient can be divided into three separate mass transfer coefficients, according to the resistance-in-series model: shell side (reactor or bulk side) mass transfer (k_b), membrane mass transfer (k_m) and mass transfer in the lumen (stripping side) (k_s). The solute diffuses first through the boundary layer in the reactor phase, then through the membrane and finally through the boundary layer in the stripping phase.

A relation for overall mass transfer coefficient (k_{ov}) and the separate mass transfer coefficients was derived:

$$\frac{1}{k_{ov}} = \frac{1}{k_b} + \frac{d_{out}}{d_{LM}} \frac{1}{P} \frac{1}{k_m} + \frac{d_{out}}{d_{in}} \frac{1}{P} \frac{1}{k_s} \quad (3)$$

Where d_{in} is the inner diameter of the membrane (m), d_{out} the outer diameter of the membrane (m), d_{LM} the logarithmic mean of the membrane inner and outer diameter (m) and P the partition coefficient of phenol in 1-octanol, which is 30 $mM_{org}.mM_{aq}^{-1}$ [28].

The mass transfer coefficient for the membrane was calculated using Equation 4:

$$k_m = D_{ps} \frac{\varepsilon}{\left(d_{out} - d_{in}\right)/2 \, \tau} \quad (4)$$

Where ε and τ are the membrane porosity and tortuosity respectively and D_{ps} the diffusion coefficient of phenol in solvent ($m^2.s^{-1}$) at 30 °C, determined by the Wilke Change method.

The mass transfer coefficient in the stripping phase (in the lumen of the membrane) (k_s) was given as a function of Reynolds (Re) and Schmidt (Sc) numbers. For laminar flows and Graetz (Gz) number greater than 4, Gabelman [29] states that the mass transfer coefficient in the tube can be calculated using:

$$Sh = \frac{k_s \cdot d_{in}}{D_{ps}} = 1.62 \cdot Gz^{\frac{1}{3}} \quad (5)$$

$$Gz = \frac{d_{in}}{L} \cdot \mathrm{Re} \cdot Sc \quad (6)$$

Where Sh is the Sherwood number and L the length of the membrane (m).

The prediction of the shell-side mass transfer coefficient in the bulk, k_b, is not as straightforward compared to the mass transfer coefficient for the membrane and in the lumen, because it is depending on the geometry of the system used. Several relations used for the determination of the Sherwood number are proposed by different authors. An overview was presented by Fernandes [10] and Gabelman [29]. The equations used for the prediction of the k_b are usually in the following form:

$$k_b = \frac{Sh \cdot D_{pw}}{\Delta z} \quad (7)$$

And:

$$Sh = a \cdot \mathrm{Re}^x \cdot Sc^y \quad (8)$$

With Δz the thickness of the boundary layer (m). The factor a is a function of geometry. The coefficients x and y vary for different setups described by different authors, but are always smaller than unity.

2.6 Results and discussion

Product inhibition in fed-batch fermentation

Fed-batch fermentations were performed to study the growth of the recombinant *P. putida* S12 strain and the phenol production in a reactor. In Figure 2, the biomass growth and phenol production in a typical fed-batch fermentation is illustrated. The biomass concentration and the amount of phenol produced increased in time. The growth and the phenol production is significantly reduced at a phenol concentration of approximately 4 mM. The cells were affected by the high phenol concentration in the growth medium and stopped growing. Since phenol production is coupled to biomass growth, the cells also stopped producing phenol. The same behavior of the phenol producing recombinant *P. putida* S12 was reported by other authors [22], [8]. These results show that the need for removal of phenol from the fermentation medium to keep the concentration below the inhibiting value is essential to reach a high total production.

The amount of phenol produced in time, the volumetric productivity ($mM.h^{-1}$) and the amount of phenol produced per gram biomass per liter, the specific phenol productivity ($mmol.g^{-1}.L^{-1}$) in the feed phase was determined. To determine the volumetric productivity, the slope of the line corresponding to the phenol concentration in time in the feed phase was determined. The volumetric productivity

determined from two separate fed-batch fermentations was 0.05 ± 0.004 $mM.h^{-1}$. This value is somewhat lower than the volumetric productivity determined from the data for a reference experiment reported by reference [8] (0.07 $mM.h^{-1}$). The specific phenol productivity was calculated by determination of the phenol/biomass concentration ratio (mM).$(g.L^{-1})^{-1}$ divided by the reactor volume at a specific time point. The specific phenol productivity was determined for all data points and for two separate fed-batch fermentations. The average productivity in fed-batch fermentations remained constant in time and was determined to be 0.35 ± 0.04 $mmol.g^{-1}.L^{-1}$. This value was comparable to the average productivity estimated from reference [8] (0.35 $mmol.g^{-1}.L^{-1}$).

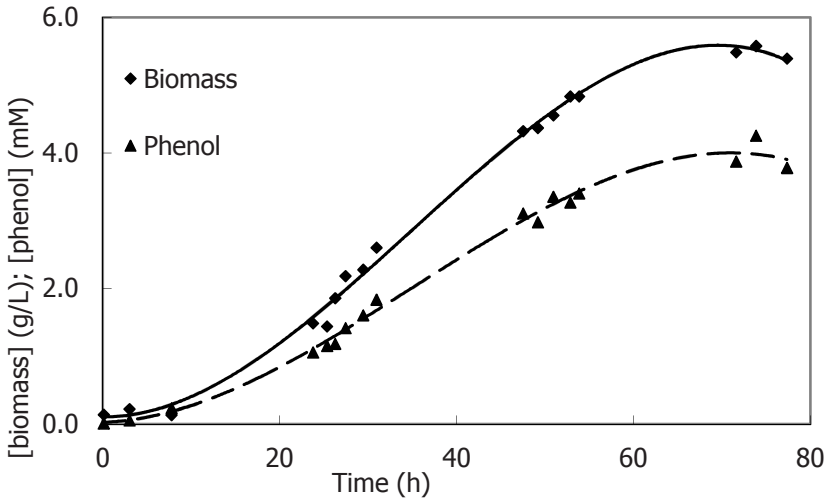

Figure 2. Phenol (mM) and biomass ($g.L^{-1}$) concentration in the fermentation broth in time for a fed-batch fermentation without *in-situ* pertraction. The feed phase started at t=27h.

Mass transfer in in-situ pertraction in aqueous model solutions

Experiments were executed to evaluate the overall mass transfer coefficient of phenol from the reactor through the membrane to the 1-octanol phase. The phenol feed rate applied in experiments 1 and 2 (0.058 $mM.h^{-1}$) was slightly higher than the phenol production rate determined from experimental data from fed-batch fermentations (0.05 $mM.h^{-1}$). In mass transfer experiment 3 a phenol feed of 0.17 $mM.h^{-1}$ was applied. The feed was applied during the first 50 hours of the experiments. The membrane used in experiment 1 was not sterilized and the membrane used in experiment 2 was sterilized at 120°C in the presence of demineralized water. The membrane in

experiment 3 was not sterilized and the experiment was executed in the presence of fermentation medium without cells. In Figure 3 and Table 2 the results of the mass transfer experiments are illustrated.

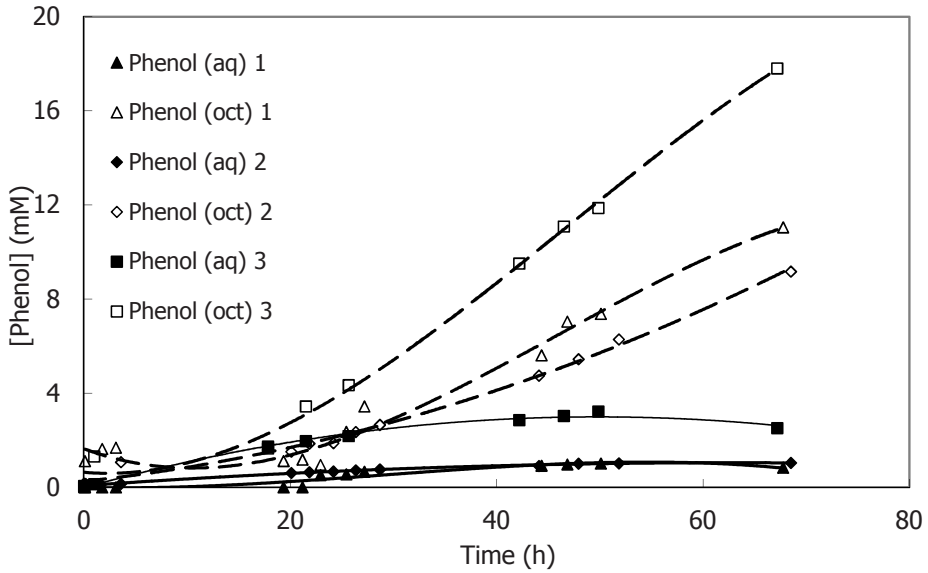

Figure 3. In-situ phenol pertraction with 1-octanol in a fermentor with aqueous phenol solutions at phenol production rate (r_p) 0.058 mmol.L^{-1}.h^{-1} (1 and 2) and 0.17 mmol.L^{-1}.h^{-1} (3), for a non-sterilized membrane (1 and 3), for a sterilized membrane (2) and for a non-sterilized membrane in the presence of medium components (3).

The results showed that the sterilization of the membrane had a noticeable effect on the rate of phenol removal from the aqueous phase and on the overall mass transfer coefficient. The overall mass transfer coefficients found in the experiments were comparable with those found in literature, between 10^{-7} - 10^{-5} m.s^{-1}. These values are reported for membrane extraction of phenol with various solvents and membranes and for similar process conditions as used here [30-33]. In experiment 1, the phenol removal rate was equal to the phenol feed rate. In experiment 2 the phenol removal rate was slightly lower. The heating of the membrane probably caused the pores to become smaller and the overall mass transfer coefficient to decrease. This can be expected because the melting temperature (T_m) of polypropylene is approximately 160°C. At a temperature of 120°C, the temperature of the membrane material approaches the melting temperature. The required force to obtain a given deformation for a given polymer (the tensile modulus E in N.m^{-2}) decreases with temperature [34] and in

our case the membrane material is most likely in transition to a solid phase. The membranes used for experiments 1 and 2 were further evaluated to proof this statement. Both membranes were immersed in water and one end of the tube was sealed. The other end of the membrane tube was connected to a pressurized air tube (1.2-1.3 bar) and the size of the resulting air bubbles in the water phase was observed. The results showed a decrease in bubble size when the membrane of experiment 2 was connected to the pressurized air tube. This is an indication that the membrane material changed after sterilization. This fact has to be taken into account when performing fermentations with a sterilized polypropylene (PP) membrane.

Table 2. Phenol removal rate and the overall mass transfer coefficients (k_{ov}) in the fermentor with aqueous phenol solutions at phenol production rate (r_p) 0.058 mmol.L^{-1}.h^{-1} (1 and 2) and 0.17 mmol.L^{-1}.h^{-1} (3), for a non-sterilized membrane (1), for a sterilized membrane (2) and for a non-sterilized membrane in the presence of medium components (3).

	r_p (mmol.L^{-1}.h^{-1})	**Phenol removal rate (aq) (mmol.L^{-1}.h^{-1})**	**k_{ov} (m.s^{-1})**
1	0.058	0.056	$4.4*10^{-6}$
2	0.058	0.050	$2.9*10^{-6}$
3	0.17	0.094	$2.6*10^{-6}$

The overall mass transfer coefficient determined with aqueous phenol solutions in a fermentor using fermentation medium (experiment 3) was $2.6*10^{-6}$ m.s^{-1}, see also Table 1. This membrane was not sterilized and it was expected that the overall mass transfer coefficient would be comparable to the one of experiment 1. The results indicate that the medium components present in the reactor have an effect on the overall mass transfer.

The mass transfer coefficient for transport through the membrane (k_m) and in the lumen (stripping phase) (k_s) are equal for experiments 1 and 3 because these experiments were performed at equal experimental conditions (aqueous and solvent volume, temperature, airflow rate, stirrer speed, solvent circulation rate and membrane area). The membrane in experiment 2 was sterilized at 120°C. The membrane structure and/or properties like wall thickness, porosity and tortuosity might be altered after sterilization. Therefore, it is not possible to determine a k_m or k_s. The calculated k_m for a non-sterilized membrane was $1.8*10^{-6}$ m.s^{-1} and the k_s was determined to be $3.4*10^{-6}$ m.s^{-1}. It should be noted that the Greatz number was determined to be approximately 2, which can lead to an overestimation of the k_s according to Gabelman et al. [29]. Using Equation 2, the mass transfer coefficient in the reactor (bulk) (k_b) for experiments 1 and 3 were determined to be $5.4*10^{-6}$ and $2.9*10^{-6}$ m.s^{-1}. The calculations showed that the limitation appeared to be in the membrane with the currently used experimental conditions.

Fed-batch fermentation with in-situ pertraction

A membrane was integrated in a bioreactor and a fed-batch fermentation was performed in the absence of solvent to study the effect of the membrane on the performance of the micro-organisms. The biomass growth and the phenol production of the recombinant *P. putida* S12 strain in presence of a membrane show the same trend as the reference experiments. After approximately 55 hours of fermentation, the biomass and phenol concentration were 4.8 $g.L^{-1}$ and 3.1 mM respectively. For the reference experiment the biomass and phenol concentration after 55 hours was 4.8 $g.L^{-1}$ and 3.3 mM respectively. The membrane did not influence the growth and the phenol production. This illustrates that no oxygen limitation occurs.

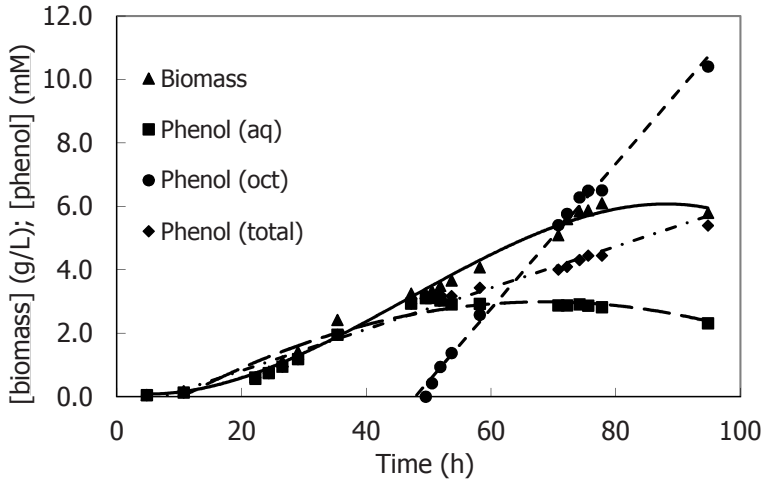

Figure 4. Phenol and biomass concentration in the fermentation broth in time for a fed-batch fermentation with in-situ pertraction. Additionally, the phenol concentration in the 1-octanol and the total phenol concentration are given. The feed phase started at t=29h, pertraction started at t=50h.

The effect of integrated membrane extraction (pertraction) on growth and the phenol production by the recombinant *P. putida* S12 strain was investigated. In Figure 4, the biomass growth and phenol production in a fed-batch fermentation with integrated membrane extraction is illustrated. No emulsion formation was observed in the pertraction experiments, which indicated a good separation between the solvent and the fermentation broth. It can be assumed that the maximum amount of 1-octanol dissolved in the fermentation broth is equal to the solubility of 1-octanol in water, approximately 0.5 $g.L^{-1}$. The (toxic) influence of the solvent on the performance of the micro-

organisms was assumed to be minimal. This can be concluded from Figure 4: the biomass growth increased with the same rate after pertraction was started (after 50 hours) as compared to the growth rate before the start of pertraction.

The micro-organisms started growing and producing phenol directly upon starting the experiment and after the start of in-situ pertraction, the phenol concentration in the reactor showed a modest decrease, see Figure 4. The biomass concentration appeared to reach a plateau before the pertraction was started; at that point the phenol concentration in the aqueous phase reached the value of approximately 3 mM. After the start of pertraction, the biomass concentration increased again and reached a plateau around 80 hours. Although the phenol concentration in the fermentation broth was lower than in the reference experiments, the total phenol production increased from 3.8 ± 0.1 mM to 5.0 ± 0.4 mM after approximately 100 hours. The phenol concentration in the 1-octanol phase increases linearly in time after the pertraction was started. The solvent was not saturated at the end of the fermentation, indicated by the fact that the phenol concentration in the solvent did not reach a plateau. As a consequence, no partition coefficient could be determined for this particular (dynamic) system. It is expected that with an increase of the phenol concentration in the solvent phase together with a decrease of the phenol concentration in the aqueous phase, considering Equation 1 and the partition coefficient of phenol between water and 1-octanol, the total phenol concentration can be further increased. However, the partition coefficient of phenol between 1-octanol and fermentation medium might be different as compared to the partition coefficient of phenol between 1-octanol and water due to the components present in the medium like salt and micro-organisms. From Figure 4 it follows that the phenol increase in the 1-octanol phase was equal to 0.2 $mM.h^{-1}$. With a solvent volume of 600 mL, this corresponds to a phenol uptake rate of 0.12 $mmol.h^{-1}$. The phenol concentration in the reactor remains constant, therefore it can be assumed that the phenol production rate is comparable to this value. Additionally, results from a fed-batch pertraction fermentation where pertraction was already started at a phenol concentration below inhibiting values (below 2 mM) shows a relatively low phenol removal rate and consequently an increase in the phenol concentration in the aqueous phase after the start of pertraction. This results in phenol inhibition and eventually to the end of growth and phenol production. The results described above indicate mass transfer limitations in the pertraction system.

The volumetric productivity of phenol ($mM.h^{-1}$) and the specific phenol productivity ($mmol.g^{-1}.L^{-1}$) in the feed phase for the fed-batch fermentation with membrane (one single experiment, n=1) and for the pertraction fermentations (performed in threefold, n=3) were determined, see Table 3. The volumetric productivity of the fed-batch fermentation with the membrane was determined to be 0.064 $mM.h^{-1}$ and for the pertraction fermentations the volumetric productivity was determined to be 0.072

± 0.012 mM.h^{-1}. As expected, the specific productivity remained constant in time and was comparable to the reference experiments (0.4 mmol.g^{-1}.L^{-1}) for all fermentations.

Table 3. Max. phenol concentration in the reactor ([phenol]$a_{aq,max}$, mM), total phenol concentration ([phenol]$_{tot}$, mM), max. biomass concentration ([biomass], g.L^{-1}), volumetric productivity in the feed phase (Vol. Prod., mM.h^{-1}) and specific phenol productivity in the feed phase (Spec. Prod., mmol.g^{-1}.L^{-1}). Results shown from our experiments compared to the values estimated from van den Berg et al, 2008.

Fermentation type[a]	**[phenol]$_{aq,max}$**	**[phenol]$_{tot}$**	**[biomass]**	**Vol. Prod.**	**Spec. Prod.**
Fed-batch (n=2)	3.8 ± 0.1	3.8 ± 0.1	5.4 ± 0.03	0.05 ± 0.004	0.4 ± 0.04
Fed-batch-membrane (n=1)	3.1	3.1	4.6	0.06	0.4
Fed-batch-pertraction (n=3)	2.6 ± 0.4	5.0 ± 0.4	6.5 ± 1.2	0.07 ± 0.01	0.4 ± 0.1
Fed-batch (ref.)	3.5	3.5	5	0.07	0.4
Fed-batch XAD-4 (ref.)	2	6.5	7	0.09	0.5
Fed-batch SIRs (ref.)	0.5	9.5	10.5	0.14	0.5

[a] n represents the number of experiments executed

For comparison, the volumetric productivities, specific phenol productivity, maximum phenol- and biomass concentration in the aqueous phase for the fermentation experiments performed in this work and those found by reference [8] are given in Table 3. The *P. putida* strain used in [8] is the same strain that was used in this study. The results in Table 3 show that the maximum phenol concentration in the reactor reached in the experiment described by [8] with XAD-4 particles (adsorption) is 2 mM. This resulted in a higher total phenol production. Using solvent impregnated resins (SIRs), the phenol concentration in the reactor was maintained below 1 mM and the total phenol production reached 9.5 mM. Also the volumetric productivity and specific productivity were higher in the experiments with XAD-4 and SIRs. The particles have a relatively high surface area in contact with the fermentation broth compared to the membrane unit. Therefore, the phenol removal rate by the particles is higher and the phenol concentration in the aqueous phase can be maintained below the inhibiting value.

Additionally, the use of a solvent with a high partition coefficient in the SIRs particles [6] compared to 1-octanol, leads to faster kinetics.

Wierckx et al [22] showed an increase in total phenol concentration by second-phase extraction with 1-octanol in fermentations with the phenol producing recombinant *P. putida* S12. The fed-batch fermentations without extraction led to product inhibition at phenol concentrations of approximately 2.4 mM. The biphasic fed-batch fermentations reached a total phenol concentration of 9.2 mM. The phenol concentration in the water phase during these fermentations was limited to 1.7 mM.

The results described above indicate that the phenol concentration in the reactor should be decreased to below 2 mM to avoid product inhibition. The experiments described in this paper reached aqueous phenol concentrations in the reactor above 2 mM, therefore the overall phenol production was not increased to a large extent.

2.7 Optimization of in-situ pertraction

It was demonstrated that the sterilization of the polypropylene (PP) membrane probably causes the membrane material to change and this had an effect on the rate of phenol removal and the overall mass transfer coefficient. For future optimization of this process, an alternative membrane type can be chosen, for example a ceramic membrane. Ceramic membranes could have a high chemical and thermal stability. Although the purchase costs are higher than for organic membranes such as the PP membrane used in this study, the lifetime is longer. Another alternative hydrophobic membrane material that can be used instead of PP is polytetrafuoroethylene (PTFE). This material is highly crystalline and exhibits excellent thermal stability. Additionally, this material shows high chemical resistance. Poly(vinylidene fluoride) (PVDF) also shows good thermal and chemical resistance although not quite as good as PTFE [34]. In addition, the PP membranes used can be sterilized by using alternative methods such as using chemical agents and physical methods as ionising radiation and dry heat sterilization [35].

The membrane mass transfer coefficient (k_m) can be improved for by example using a membrane with a smaller wall thickness, for example the type Accurel PP S6/2 (Membrana). With a diameter of $2.7*10^{-3}$ m and a wall thickness of $0.45*10^{-3}$ m, the k_m is calculated to be $1.4*10^{-5}$ $m.s^{-1}$. This is approximately a factor 10 higher as compared to the k_m determined with the membrane used in our experiments ($1.8*10^{-6}$ $m.s^{-1}$). Other options for improving the (membrane) mass transfer coefficient are for example to use another solvent with a higher partition coefficient like methyl isobutyl ketone (MIBK, partition coefficient for phenol ~120) as described by reference [36] or n-butanol [37]. The pores of the hydrophobic membrane are filled with solvent and based on Equation 3, a solvent with a high

partition coefficient for phenol will result in a reduced membrane- and stripping resistance and will make the aqueous resistance the most important resistance for mass transfer. The diffusion coefficient of the product in the solvent will change when using another solvent, although in the case of MIBK, the D_{ps} is similar to the one of 1-octanol due to similar properties like molecular weight and dynamic viscosity. On the other hand, a solvent with a high partition coefficient usually dissolves well in water and vice versa. MIBK, for example, has a solubility in water of 19 $g.L^{-1}$, while 1-octanol dissolves in water at a maximum concentration of 0.5 $g.L^{-1}$[38]. This potentially leads to additional solvent toxicity effects, especially when taking into account the logP-value. In addition, experiments were executed with tributylphosphate (TBP), a solvent with a partition coefficient for phenol around 400. This value is comparable with the value reported by Burghoff et al: a partition coefficient for phenol in TBP of 450 [39]. The overall mass transfer coefficient determined in single-fiber modules with TBP and the membrane type used in this study increased with a factor 5 as compared to the overall mass transfer coefficient determined with 1-octanol. Additionally, in experiments using membrane type Accurel PP S6/2 (Membrana), the overall mass transfer coefficient increased with a factor 2.2. These combined results show that, when using TBP and membrane type S6/2, the overall mass transfer coefficient can be improved with a factor 11.

The second important resistance to improve is the mass transfer coefficient in the lumen (k_s), which is dependent on the membrane diameter, the solvent flow rate and the diffusion coefficient of phenol in the solvent. The k_s can be improved by a higher superficial solvent flow rate ($m.s^{-1}$) in the membrane tube by either decreasing the inner diameter of the membrane or increasing the volume flow rate of the solvent through the lumen. As described above, the choice of an alternative solvent can result in an increase in the D_{ps} and consequently in the k_s.

As described in Equations 7 and 8, the mass transfer coefficient in the bulk (k_b) is a function of Reynolds number (Re), Schmidt number (Sc) and geometry (a). Additionally, the diffusion coefficient of the product in the reactor phase and the thickness of the boundary layer is of importance. The Schmidt number is influenced by the properties of the product and the solvent (viscosity, density and diffusivity of the product). The Schmidt number cannot contribute to improvement of the bulk mass transfer coefficient because the liquid composition in the reactor cannot be altered. The mass transfer coefficient in the bulk is more difficult to improve by changing the reactor geometry because of the limited degrees of freedom. The membrane was mounted in the laboratory reactor in a certain configuration to avoid contact with for example the electrodes and the stirring blades. Therefore, the available volume for a membrane unit in the lab fermenter is small. The liquid flow pattern in the bulk is influenced by the presence of the membrane module and the flow rate at the membrane surface changes for different locations along the surface. It can, however, be assumed that the flow in the reactor is turbulent considering the applied stirrer speed (100 – 500 rpm).

The fouling at the membrane surface and/or in the pores by medium components will increase the boundary layer thickness at the surface (see Figure 2) and, in addition, it may decrease the available contact area between the solvent and the fermentation broth. To decrease the thickness of this boundary layer, several strategies can be followed. One way to improve the shell side mass transfer is to increase the turbulence at the membrane surface. However, in a bioreactor, this is not a preferred option because the process conditions in the reactor are fixed. The liquid flow rate in the reactor is determined by the stirrer speed, which in turn is automated to control the dissolved oxygen level in the reactor. It is impossible to increase the stirrer speed to a very high value because the micro-organisms will be damaged by the high shear forces. Another option to decrease the thickness of the boundary layer is to design the configuration of the integrated membrane unit such that the water flow rate across the membrane surface becomes more turbulent.

Other authors describe, for example, rotating [40] or vibrating [41, 42] membrane modules, the addition of external forces such as ultrasound [43] or membrane surface modification [44-47] to reduce fouling at the membrane surface and to improve the flux in (pressure driven) (micro)filtration processes. Although the driving force for the membrane process described in this paper is a concentration difference instead of pressure, and thus different causes of fouling will decrease the flux of certain components through the membrane, it is interesting to investigate the above mentioned concepts in a fermentation process. However, the mixing efficiency of the reactor and thus oxygen transfer will probably decrease and the growth and phenol production process can be negatively influenced. Additionally, the shear forces in the reactor might reach critical values which can affect and destroy the micro-organisms.

2.8 Conclusions

In this paper, in-situ phenol removal from fermentation broth with membrane extraction (pertraction) was experimentally studied as model process. In fed-batch fermentations of a phenol producing recombinant strain of *P. putida* S12, it was observed that biomass growth and phenol production are already inhibited from phenol concentrations in the reactor medium of 2 mM and that growth and production stop at a phenol concentration of 3.8 mM. In-situ pertraction is successfully implemented in fermentations with this micro-organism. Upon careful arrangement, the presence of a membrane unit does not affect the growth and phenol production in the fermentations compared with reference experiments. In-situ pertraction results in a lower maximum aqueous phenol concentration of 2.6 ± 0.44 mM. With in-situ pertraction, the total phenol production increases from 3.8 to 5.0 mM and the volumetric productivity appears to slightly increase from 0.05 to 0.07 $mM.h^{-1}$ while the specific productivity of phenol remains constant in time and in all fermentations at 0.4 mmol phenol per gram biomass per liter as expected. However, the phenol concentration in the reactor phase in the

pertraction fermentations exceeds the inhibiting concentration. This indicates that the removal rate of phenol from the reactor is not high enough to maintain the phenol concentration level below limiting values. The removal rate of phenol from the reactor is determined by the available membrane area, by the driving force and by the overall mass transfer coefficient (k_{ov}). To increase the removal rate of phenol, a larger membrane area can be used and/or the driving force can be increased by for example choosing a solvent with a higher partition coefficient such as tributylphosphate. Two possible causes for decrease in k_{ov} were identified in this paper to be the fouling of medium components and the change of the membrane material by sterilization. To improve the k_{ov}, the separate mass transfer coefficients (k_b, k_m and k_s) can be optimized.

References

[1] G.J. Lye, J.M. Woodley, Application of in situ product-removal techniques to biocatalytic processes, Trends Biotechnol., 17 (1999) 395-402.

[2] M.E. Lienqueo, J.A. Asenjo, Use of expert systems for the synthesis of downstream protein processes, Comput. Chem. Eng., 24 (2000) 2339-2350.

[3] W.J. Groot, R.G.J.M. van der Lans, K.C.A.M. Luyben, Technologies for butanol recovery integrated with fermentations, Process Biochem., 27 (1992) 61-75.

[4] L.E.S. Brink, J. Tramper, Optimization of organic solvent in multiphase biocatalysis, Biotechnol. Bioeng., 27 (1985) 1258-1269.

[5] B. Buhler, I. Bollhalder, B. Hauer, B. Witholt, A. Schmid, Use of the two-liquid phase concept to exploit kinetically controlled multistep biocatalysis, Biotechnol. Bioeng., 81 (2003) 683-694.

[6] C. van den Berg, C.P.M. Roelands, P. Bussmann, E.L.V. Goetheer, D. Verdoes, L.A.M. van der Wielen, Preparation and analysis of high capacity polysulfone capsules, React. Funct. Polym., 69 (2009) 766-770.

[7] D. Stark, H. Kornmann, T. Münch, B. Sonnleitner, I.W. Marison, U.v. Stockar, Novel type of in situ extraction: Use of solvent containing microcapsules for the bioconversion of 2-phenylethanol from L-phenylalanine by Saccharomyces cerevisiae, Biotechnol. Bioeng., 83 (2003) 376-385.

[8] C.v.d. Berg, N. Wierckx, J. Vente, P. Bussmann, J.d. Bont, L.v.d. Wielen, Solvent-impregnated resins as an in-situ product recovery tool for phenol recovery from *Pseudomonas putida S12TPL* fermentations, Biotechnol. Bioeng., 100 (2008) 466-472.

[9] S. Schlosser, R. Kertesz, J. Martak, Recovery and separation of organic acids by membrane-based solvent extraction and pertraction: An overview with a case study on recovery of MPCA, Sep. Purif. Technol., 41 (2005) 237-266.

[10] P. Fernandes, D.M. Prazeres, J.M. Cabral, Membrane-assisted extractive bioconversions, Adv. Biochem. Eng./Biotechnol., 80 (2003) 115-148.

[11] L.E. Hüsken, M. Oomes, K. Schroën, J. Tramper, J.A.M. de Bont, R. Beeftink, Membrane-facilitated bioproduction of 3-methylcatechol in an octanol/water two-phase system, J. Biotechnol., 96 (2002) 281-289.

[12] F. Molinari, F. Aragozzini, J.M.S. Cabral, D.M.F. Prazeres, Continuous production of isovaleraldehyde through extractive bioconversion in a hollow-fiber membrane bioreactor, Enzyme Microb. Technol., 20 (1997) 604-611.

[13] J. Urbanus, J. Laven, C.P.M. Roelands, J.H. ter Horst, D. Verdoes, P.J. Jansens, Template Induced Crystallization: A Relation between Template Properties and Template Performance, Cryst. Growth Des., 9 (2009) 2762-2769.

[14] E.M. Buque-Taboada, A.J.J. Straathof, J.J. Heijnen, L.A.M. van der Wielen, Microbial reduction and *in situ* product crystallization coupled with biocatalyst cultivation during the synthesis of 6R-dihydrooxoisophorone, Adv. Synth. Catal., 347 (2005) 1147-1154.

[15] J. Urbanus, C.P.M. Roelands, J.H. ter Horst, D. Verdoes, P.J. Jansens, Screening for templates that promote crystallization, Food Bioprod. Process., 86 (2008) 116-121.

[16] E. Curcio, G. Di Profio, E. Drioli, Recovery of fumaric acid by membrane crystallization in the production of -malic acid, Sep. Purif. Technol., 33 (2003) 63-73.

[17] A. Bouchoux, H. Roux-de Balmann, F. Lutin, Investigation of nanofiltration as a purification step for lactic acid production processes based on conventional and bipolar electrodialysis operations, Sep. Purif. Technol., 52 (2006) 266-273.

[18] W.J. Groot, M.C.H. den Reyer, T. Baart de la Faille, R.G.J.M. van der Lans, K.C.A.M. Luyben, Integration of pervaporation and continuous butanol fermentation with immobilized cells I: Experimental results, Chem. Eng. J., 46 (1991) B1-B10.

[19] D.B. Hirata, J.H.H.L. Oliveira, K.V. Leão, M.I. Rodrigues, A.G. Ferreira, M. Giulietti, M. Barboza, C.O. Hokka, Precipitation of clavulanic acid from fermentation broth with potassium 2-ethyl hexanoate salt, Sep. Purif. Technol., 66 (2009) 598-605.

[20] K. Nijkamp, N. van Luijk, J. de Bont, J. Wery, The solvent-tolerant Pseudomonas putida S12 as host for the production of cinnamic acid from glucose, Appl. Microbiol. Biotechnol., 69 (2005) 170-177.

[21] K. Nijkamp, R.G.M. Westerhof, H. Ballerstedt, J.A.M. de Bont, J. Wery, Optimization of the solvent-tolerant Pseudomonas putida S12 as host for the production of p-coumarate from glucose, Appl. Microbiol. Biotechnol., 74 (2007) 617-624.

[22] N.J.P. Wierckx, H. Ballerstedt, J.A.M. De Bont, J. Wery, Engineering of solvent-tolerant *Pseudomonas putida* S12 for bioproduction of phenol from glucose, Appl. Environ. Microbiol., 71 (2005) 8221-8227.

[23] Klaassen R., Feron P. H. M., Jansen A. E., Membrane contractors in industial applications, Chemical Engineering Research and Design, 83 (2005) 234-246.

[24] N. Wierckx, Personal communication: experimental data file Excel, in, Delft, 2007.

[25] L. Heerema, M. Roelands, J.H. Hanemaaijer, J. de Bont, D. Verdoes, In-situ phenol removal from fermentation broth by pertraction, Desalination, 200 (2006) 485-487.

[26] S. Hartmans, J.A.M. de Bont, W. Harder, Microbial metabolism of short-chain unsaturated hydrocarbons, FEMS Microbiol. Lett., 63 (1989) 235-264.

[27] V. Makovskaya, J.R. Dean, W.R. Tomlinson, M. Comber, Octanol-water partition coefficients of substituted phenols and their correlation with molecular descriptors, Anal. Chim. Acta, 315 (1995) 193-200.

[28] A. Gabelman, S.-T. Hwang, Hollow fiber membrane contactors, J. Membr. Sci., 159 (1999) 61-106.

[29] M.J. Gonzalez-Munoz, S. Luque, J.R. Alvarez, J. Coca, Recovery of phenol from aqueous solutions using hollow fibre contactors, J. Membr. Sci., 213 (2003) 181-193.

[30] M. Xiao, J. Zhou, Y. Tan, A. Zhang, Y. Xia, L. Ji, Treatment of highly-concentrated phenol wastewater with an extractive membrane reactor using silicone rubber, Desalination, 195 (2006) 281-293.

[31] S. Han, F.C. Ferreira, A. Livingston, Membrane aromatic recovery system (MARS) -- a new membrane process for the recovery of phenols from wastewaters, J. Membr. Sci., 188 (2001) 219-233.

[32] M.J. Gonzalez-Munoz, S. Luque, J. Alvarez, J. Coca, Simulation of integrated extraction and stripping processes using membrane contactors, Desalination, 163 (2004) 1-12.

[33] M. Mulder, Basic principles of membrane technology, Kluwer Academic Publishers, 1991.

[34] M. Berovic, M.R. El-Gewely, Sterilisation in biotechnology, in: Biotechnology Annual Review, Elsevier, 2005, pp. 257-279.

[35] K.K.S. R. Prasad, Dispersion-free solvent extraction with microporous hollow-fiber modules, AlChE J., 34 (1988) 177-188.

[36] J. Ruhl, A. Schmid, L.M. Blank, Selected Pseudomonas putida Strains Able To Grow in the Presence of High Butanol Concentrations, Appl. Environ. Microbiol., 75 (2009) 4653-4656.

[37] C.v.d. Berg, Personal communication in, Delft, 2009, pp. Table of solvents with their properties.

[38] B. Burghoff, E.L.V. Goetheer, A.B. de Haant, COSMO-RS-based extractant screening for phenol extraction as model system, Ind. Eng. Chem. Res., 47 (2008) 4263-4269.

[39] R. Bouzerar, L. Ding, M.Y. Jaffrin, Local permeate flux-shear-pressure relationships in a rotating disk microfiltration module: implications for global performance, J. Membr. Sci., 170 (2000) 127-141.

[40] S.P. Beier, G. Jonsson, Separation of enzymes and yeast cells with a vibrating hollow fiber membrane module, Sep. Purif. Technol., 53 (2007) 111-118.

[41] M. Frappart, M.Y. Jaffrin, L.H. Ding, V. Espina, Effect of vibration frequency and membrane shear rate on nanofiltration of diluted milk, using a vibratory dynamic filtration system, Sep. Purif. Technol., 62 (2008) 212-221.

[42] H.M. Kyllönen, P. Pirkonen, M. Nyström, Membrane filtration enhanced by ultrasound: a review, Desalination, 181 (2005) 319-335.

[43] N. Hilal, V. Kochkodan, L. Al-Khatib, T. Levadna, Surface modified polymeric membranes to reduce (bio)fouling: a microbiological study using E. coli, Desalination, 167 (2004) 293-300.

[44] N. Hilal, L. Al-Khatib, B.P. Atkin, V. Kochkodan, N. Potapchenko, Photochemical modification of membrane surfaces for (bio)fouling reduction: a nano-scale study using AFM, Desalination, 158 (2003) 65-72.

[45] H.-Y. Yu, M.-X. Hu, Z.-K. Xu, J.-L. Wang, S.-Y. Wang, Surface modification of polypropylene microporous membranes to improve their antifouling property in MBR: NH3 plasma treatment, Sep. Purif. Technol., 45 (2005) 8-15.

[46] M. Taniguchi, J.E. Kilduff, G. Belfort, Low fouling synthetic membranes by UV-assisted graft polymerization: monomer selection to mitigate fouling by natural organic matter, J. Membr. Sci., 222 (2003) 59-70.

Chapter 3

In-situ product removal from fermentations by membrane extraction: conceptual process design and economics

This chapter was published as:
Heerema, L.; Roelands, M.; Goetheer, E.; Verdoes, D.; Keurentjes, J., In-Situ Product Removal from Fermentations by Membrane Extraction: Conceptual Process Design and Economics. Industrial & Engineering Chemistry Research 2011, 9197-9208.

Chapter 3 - In-situ product removal from fermentations by membrane extraction: conceptual process design and economics

Abstract

This paper describes a conceptual process design for the production of the model component phenol by a recombinant strain of the micro-organism *Pseudomonas putida* S12. The (bio)production of the inhibiting component phenol in a bioreactor is combined with direct product removal by membrane extraction (pertraction). Continuous fermentation with the pertraction unit inside the reactor (integrated process), is compared to fed-batch fermentation with the pertraction unit outside the reactor (non-integrated process). In the non-integrated process, the bioprocess is completely separated from the pertraction process. An extended model for fermentation, consisting of biomass growth and phenol production combined with product inhibition, cell removal, pertraction with 1-octanol and regeneration of the solvent by distillation is described with help of experimental and theoretical data.

Running the fermentation process at a lower product concentration results in a more efficient substrate utilization into biomass and phenol. The disadvantage of the integrated process is the need for large distillation columns and a high energy input for solvent regeneration due to the low product concentration in the solvent and the high solvent fluxes.

Economic evaluation of the two processes show that to obtain a return of investment of 15%, the product cost price of the integrated process is a factor three lower as compared to the non-integrated process.

The benefits of an integrated process will pay off even more for very toxic and inhibiting products that do not allow for a high concentration in the (bio)reactor as compared to phenol.

3.1 Introduction

Pseudomonas putida S12 is a solvent tolerant bacterium that is used to make recombinants that grow on alternative carbon sources and that produces several aromatics like cinnamic acid [1], p-coumarate [2] and phenol [3]. These aromatics can have toxic or inhibitory effects on the growth and production processes. Therefore, it is important that the concentration of these products in the production medium remain below a certain level. The use of in-situ product removal (ISPR) is a useful strategy to overcome this problem. Several techniques of ISPR can be explored to increase the total production of aromatics by *P. putida* S12. ISPR can be applied outside the reactor (non-integrated) or inside the reactor (integrated) and the technique used is dependent on the properties of the product to be separated (e.g. volatility, molecular weight, size, solubility, charge and hydrophobicity). Numerous techniques that can be used for ISPR are described in literature [4-6], including extraction [7, 8], adsorption, extractive capsules [9-11], membrane extraction [12-15], crystallization [16-19], membrane crystallization [20], distillation, gas stripping, filtration [21], centrifugation, size exclusion, pervaporation [22], precipitation [23], ion exchange, electrodialysis or affinity methods.

The production of phenol by *P. putida* S12 was chosen as model process to illustrate product inhibition and to demonstrate the effects of ISPR by extraction with 1-octanol. Phenol was chosen as a model component and a typical example of a fine chemical. It serves as a good model for aromatics containing a hydroxylgroup. Additionally, due to its toxicity, phenol can well illustrate the effects of product inhibition. Only little effort was made so far to describe the (bio)production process of inhibiting components like phenol in detail using experimental data in combination with extended model calculations, especially combined with ISPR and product recovery.

In earlier work[24], the (bio)production of the model compound phenol by a genetically modified strain of *P. putida* S12 in combination with integrated membrane extraction (pertraction) was studied. Compared to a process with the membrane extraction unit outside the reactor, the integration of a hollow fiber membrane extraction unit in the fermentor eliminates the need for circulating the fermentation broth, containing the micro-organisms, avoiding oxygen limitation. The integration of the membrane extraction unit in the bioreactor using the solvent 1-octanol led to continuous phenol removal from the fermentation broth, increasing the total phenol production. Experimental studies showed that when phenol was removed from the fermentation broth by pertraction, a lower maximum aqueous phenol concentration was achieved, while the total phenol production increased to 132%, as compared to the fermentation without pertraction. There were indications that the volumetric productivity increased slightly in the fermentations with in-situ pertraction compared to the reference experiments. As expected, the amount of phenol produced per gram biomass (the specific productivity) remained constant in time for all fermentations.

In this work, the phenol production process with non-integrated and integrated phenol removal by pertraction is evaluated and compared using extended model simulations. Additionally, process cost analysis are made to determine the final product cost price. Continuous removal of the toxic product will result in a higher biomass growth rate, productivity and yield of biomass and product on substrate and consequently to a decrease in reactor volume and raw materials costs. However, the integrated separation process will run at relative low product concentrations which will cause a decrease in driving force for pertraction and consequently an increase in the required membrane area and a higher energy input for solvent regeneration and product purification. In this work, the influence of the two processes on key variables that determine total process costs are evaluated. Key variables like phenol concentration in the reactor will influence for example the substrate requirements, biomass growth rate and phenol production rate which in turn influence the required reactor volume, the required membrane area, the energy input for solvent regeneration and product purification and the flux of raw materials. The purpose is to evaluate the advantages and disadvantages of both processes and to determine whether the integrated process results in a lower product cost price as compared to the non-integrated process.

3.2 Basis of Design

The basis of design for this study is a plant capacity of 10 kton of phenol per year. The required purity of the product stream is set to 99% and the overall phenol recovery 90%. The selected location is The Netherlands. Local regulations and social determinations such as labour cost will be assumed according to European standards. Chemical storage facilities, buildings, auxiliaries and laboratories need to be installed. The design of the plant has been considered "brownfield", therefore waste treatment facilities and utilities are available on site and no equipment investments were necessary for these type of facilities. The operational time is set to 8000 hours per year, with approximately 9% of the annual hours devoted to maintenance operations. The plant life for economic estimations has been assumed to be 10 years. The plant is in production at the design capacity for all the 10 years, starting from 2010.

3.3 Process description

The benefits and limitations of ISPR by membrane extraction is evaluated based on the comparison between 1) a non-integrated process where fermentation and product recovery are separated and performed in a non-integrated fashion and 2) an integrated process with a pertraction system inside the bioreactor, see also Figure 1. For both processes, the most optimal process configuration is chosen according to microbial kinetics by using a metabolic network model according to Heijnen [25]. The non-integrated process consists of the production of phenol in a fed-batch fermentation, at a growth rate that determines the maximum yield of phenol on substrate. This operation is followed by a biomass removal step and product recovery by pertraction, using the solvent 1-octanol. The

integrated process consists of a continuous fermentation with simultaneous product recovery by pertraction to promote the productivity of phenol. Part of the biomass leaving the fermentor is separated from the liquid stream and recycled to the fermentor. For both processes, the solvent is recycled back to the pertraction unit after regeneration by distillation and, finally, the product is further purified using distillation. Additionally, it is assumed that no by-products from the fermentation broth are co-extracted by 1-octanol. The processes are evaluated based on conceptual design, with the dimensioning of all the major pieces of equipment.

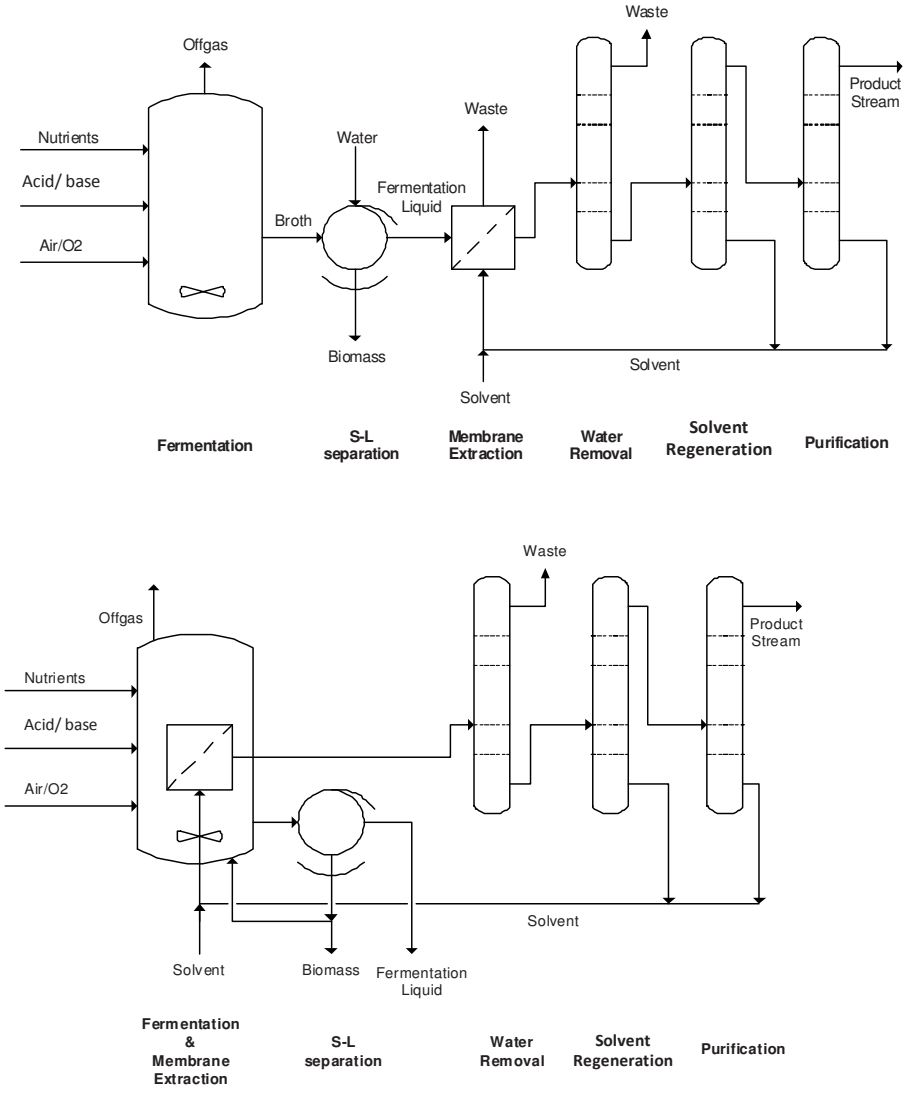

Figure 1. Process flow sheet of the non-integrated (top) and integrated (bottom) processes for phenol production

The technical battery limit defines all the equipment and facilities to be designed. The economic battery limit defines which items will be considered for the cost estimations. The feedstock glucose, other raw materials and utilities are assumed available outside battery limits (OSBL). All the processing steps for production of phenol are inside battery limits (ISBL). Utilities and waste treatment units will not be designed, but consumed utilities and wastes produced will be assigned costs. An overview of the battery limits and the most important in and outgoing streams of the phenol production plants are given in the supplementary data, Table 1 and Figure 1.

3.4 Process simulation

The fermentation, cell separation and pertraction units are modeled in Matlab, solvent regeneration and product recovery by distillation are modeled in Aspen. The equations, parameters and constants used for the calculations can be found in the supplementary data, Tables 2 - 13. Overall mass and energy balances are setup for both processes using model simulations and equipment sizing is performed.

Fermentation

The growth and production of phenol with *P. putida* S12 in a stirred tank reactor is well described by several authors [3, 11, 24, 26]. A metabolic network model is prepared, describing the conversion of the nutrients through the internal metabolism to obtain biomass growth and phenol production under carbon-limitation. The carbon source for both processes is glucose and the nitrogen source is an ammonium salt. The equations and constants used for the fermentation section are given in Tables 2 - 6 in the supplementary data.

The phenol concentration in the reactor influences most of the important kinetic parameters: microbial growthrate (μ, h^{-1}), phenol production rate (q_p, mol phenol per C-mol biomass per hour) and glucose consumption rate (q_s, mol substrate per C-mol biomass per hour). The phenol concentration in the reactor is determined for both the fed-batch non-integrated and continuous integrated process. From this working point, the reactor volume and the substrate requirements are determined. The initial fermentor volume is assumed to be 400 m^3, the height to diameter ratio (H/D) for a fermentor is assumed to be 3 and the fermentation temperature is 30°C. The dimensioning of the stainless steel (SS316) fermentor is performed using the H/D ratio and the final fermentor volume (V_{ferm}). The power input for the fermentor is assumed to be mainly determined by the gasflow power input (P_g, W), which is influenced by the gas (in)flowrate ($F_{g,in}$, $m^3.s^{-1}$), the temperature of the gas (T_g, K) and the pressure at the bottom and top of the fermentor (P_b and P_t, atm).

Additionally, the fermentor requires cooling with chilled water of 5°C (F_{ch}, $kg.h^{-1}$) to compensate for the heat produced during the bioreaction. The total heat generated during the bioreaction (r_{ht}, W) is the sum of the heat generated by metabolic activity as a function of the oxygen uptake rate (OUR) (r_{hm}), the heat generated by the gas flowing through (r_{hg}), the heat dissipated by the stirrer (r_{hs}), the heat loss from vaporization (r_{hv}), the heat loss through the fermentor walls (r_{hw}) and the heat generated by all other sources (r_{hh}) [27]. For this process evaluation, only the following parameters: r_{hg}, r_{hm} and r_{hh} are taken into account, see also Table 2. The r_{hh} in this process is determined by the heat of the feeding streams (r_{hf}). The three feeding streams that determine the r_{hf} are substrate (r_{hS}), nitrogen (r_{hN}) and hydrochloric acid (r_{hHCl}). They can be determined in the same manner as compared to the r_{hg}, using the specific heat capacities and the mass flow rate ($kg.h^{-1}$) of the feeding streams.

Biomass removal

The cell separation equipment used for the removal of the biomass from the fermentation liquid is a stainless steel (SS316) rotary drum filter. The equations and constants used for the biomass removal section are given in Tables 7 and 8 in the supplementary data. For the non-integrated process, the biomass rejection is assumed to be 1 kg biomass slurry per kg biomass feed and the concentration factor, CF, to be 20. Therefore, the biomass concentration after the biomass removal section is a factor twenty higher as compared to the biomass concentration in the bioreactor, the inlet stream of the biomass removal section. The CF in the integrated process is assumed to be 2. The required wash water volume is 2 m^3 wash water per m^3 solids and the moist coefficient is 0.20 kg solution per kg solids in the slurry. For the integrated process, it is assumed that the volumetric recycle flow from the S-L separation unit (ϕ_{rec}, $m^3.s^{-1}$) is equal to the volumetric feed flow (φ_{in}, $m^3.s^{-1}$) multiplied with the recycle ratio (RR_{SL}). The filtrate mass flow ($kg.h^{-1}$) follows from the overall mass balances around the filter. Using the filtrate mass flow and the filtrate density (ρ_f, $kg.m^{-3}$), the volumetric flow rate of the filtrate (φ_{SL}, $m^3.h^{-1}$) is determined. The membrane area (A_{SL}, m^2) and the filtration flux (F_{SL} $m^3.m^{-2}.s^{-1}$) are determined according to the equation given in Table 7 in the supplementary data. The dimensioning of the cell separation equipment is mainly determined by the required membrane area. The power input for filtration ($P_{SL,}$ W) is determined by the volumetric flow rate of the filtrate, the pressure drop ($\Delta p_{SL,}$ assumed to be 0.5 bar) and the pump efficiency ($0.5<n_{SL}<0.8$).

Pertraction

The pertraction model corresponds to the differential steady-state phenol balance in the solvent (1-octanol) phase. In Figure 2 a section of a tubular membrane fiber is represented. Solvent flows inside the membrane lumen and phenol is extracted from the aqueous phase to the solvent phase. The flow is not influenced by entrance effects and the velocity profile does not vary along the axis of flow in the x direction. The control volume is a cylinder with diameter d_i (m), and thickness Δx (m).

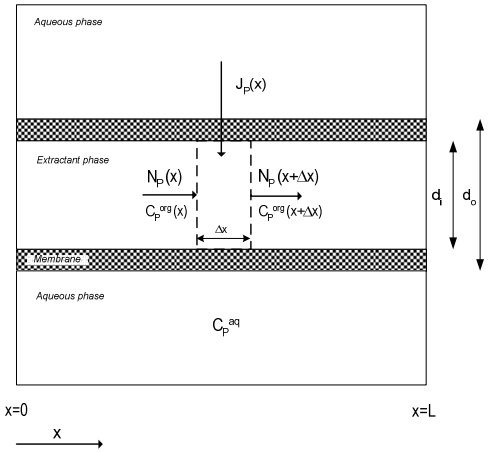

Figure 2. Section of a tubular membrane fiber.

At steady state the phenol conservation balance is as follows: 0 (no accumulation) = rate of transport into the volume – rate of transport out + rate of transfer from the aqueous phase:

$$0 = \left(\pi \cdot \frac{d_i^2}{4}\right) \cdot \left(N_p(x) - N_p(x+\Delta x)\right) + \left(\Delta x \cdot \pi \cdot d_{lm}\right) \cdot J_p(x) \tag{1}$$

With d_{lm} the logarithmic mean diameter (m), N_P the phenol transport flux in the x direction (inside the tube) (kg.m^{-2}.s^{-1}) and J_P is the phenol phase transfer flux (kg.m^{-2}.s^{-1}), with direction normal to transport:

$$N_p = C_P^{org} \cdot v_s \tag{2}$$

with v_s the average linear solvent velocity in the tubes (m.s^{-1}) and:

$$J_p = K^{aq} \cdot \left(C_P^{aq} - \frac{C_P^{org}}{m_P^{w/org}}\right) \tag{3}$$

with K^{aq} the overall mass transfer coefficient relative to the aqueous phase (m.s^{-1}) and $m_P^{w/org}$ the phenol partition coefficient between the aqueous and the solvent phase (28.8). If the aqueous phase is well mixed, C_P^{aq} is independent of the spatial coordinate. Replacing the equations above and letting $\Delta x \rightarrow 0$, the phenol concentration in the solvent phase (kg.m^{-3}) can be described by:

$$\frac{dC_P^{org}}{dx} = A \cdot K^{aq} \cdot \left(C_P^{aq} - \frac{C_P^{org}(x)}{m_p^{w/org}} \right) \quad (4)$$

With A the membrane area available for pertraction (m^2).

The overall mass transfer resistance (R^{total}) is determined by three separate mass transfer resistances: the resistance at the shell side of the membrane (R^{shell}), the resistance of the membrane (R^{memb}) and the resistance inside the membrane lumen (R^{lumen}). The determination of the separate resistances with transport equations is described in the supplementary data, Table 9. The overall mass transfer coefficients have been determined for Accurel PP hydrophobic capillary membrane types V8/HF, S6/2 and Q3/2, Membrana (see Table 12 and Figure 2 in the supplementary data). For the model calculations described in this paper, membrane Q3/2 has been used with a K^{aq} of $2*10^{-5}$ $m.s^{-1}$. This membrane type has an internal diameter of 0.6 mm and a wall thickness of 0.2 mm. The (maximum) specific membrane area (a_{sp}) determined for this membrane is between 524 – 1428 $m^2.m^{-3}$. The maximum allowable pressure drop over the membrane (0.3 bar) results in a maximum superficial solvent flow rate through the tube (v_s) of 0.39 $m.s^{-1}$. After theoretical analysis of the K^{aq} at varying v_s, a superficial solvent flow rate through the tube of 0.01 $m.s^{-1}$ has been chosen. This flow rate allows for a high K^{aq} and a high phenol concentration in the solvent. For a consistent comparison, the non-integrated and the integrated pertraction processes both run at 30°C, although the non-integrated process can run at elevated temperatures due to the fact that this process is not dependent on the temperature of the bioprocess.

To evaluate both processes, the required extraction rate (*E*, $kg.h^{-1}$) is determined. This value follows from the fermentation section, *E* should be at least equal to the phenol production rate in fermentation. From the extraction rate, the number of required membrane fibers (N_{fibers}) and the required membrane area (A_{memb}, m^2) are calculated, see also Table 10 in the supplementary data. The length of the membrane module (L) is assumed considering the saturation of phenol in the solvent along the tube length to be 1.4 m for the non-integrated case and 2.1 m for the integrated case.
Finally, the specific membrane area is determined. This value should be below the given boundary limits previously determined.

The power input for the pertraction unit was determined for one module ($P_{ME,mod}$, W) according to the volumetric flow rate at the tube side (φ_{tube}, $m^3.s^{-1}$) and the pressure drop (Δp_{ME}, Pa) multiplied with the number of modules (N_{mod}) and divided by the pump efficiency (n_{ME}, assumed to be 0.6) to obtain the total power input (P_{ME}, W).

Transport equations, additional equations and constants used for the pertraction unit are given in the supplementary data, Tables 9 - 13.

Distillation

With the software package Aspen Plus, a distillation sequence was designed and optimized to process the solvent stream from the membrane extraction unit. This model involves three steps: water removal, solvent regeneration and purification (see also Figure 1). The distillation model used for the simulations is RADFRAC with the thermodynamic properties database NRTL. The specification for optimization of the distillation process is a final product stream with a mass flow rate of 1250 $kg.h^{-1}$, a purity of phenol of 99% and a phenol recovery of 90%. The optimization is performed by manipulation of the distillate to feed ratio (D:F) and/or the reflux ratio (RR).

The Aspen simulations results in the following parameters: operational temperature and pressure (T_{dest}, °C and p_{dest}, atm), number of stages (N_{stages}), (molar) reflux ratio (RR), distillate to feed ratio (D:F), feed stage (FS), packing (Pall Rings) height (H_{pack}, m), column height (H_{column}, m), column diameter (D_{column}, m) and energy input for heating and cooling (Q_{heat} and Q_{cool}, MW) of the process streams. The parameters obtained from the Aspen simulations have been used to determine the column wall thickness (tw, m) and the total volume of stainless steel (SS316) required and the resulting pressure vessel weight (W_{column}, kg).

3.5 Results process simulation

The process models for the non-integrated and integrated processes were evaluated and optimized. Extended tables with mass balances for both processes are given in the supplementary data, Tables 14 and 15. A schematic presentation of the different stream numbers is given in Figure 3 in the supplementary data. The most important differences, advantages and disadvantages of the two processes are discussed below.

Fermentation

For the fermentation section, the influence of the phenol concentration in the reactor on the most important kinetic parameters have been investigated: microbial growthrate (μ), phenol production rate (q_p) and glucose consumption rate (q_s). In Figure 3 these parameters are given as function of phenol concentration. Figure 3 was derived by determining growth rate, production rate and substrate consumption rate at a certain phenol concentration using the equations given in Table 2 in the supplementary data.

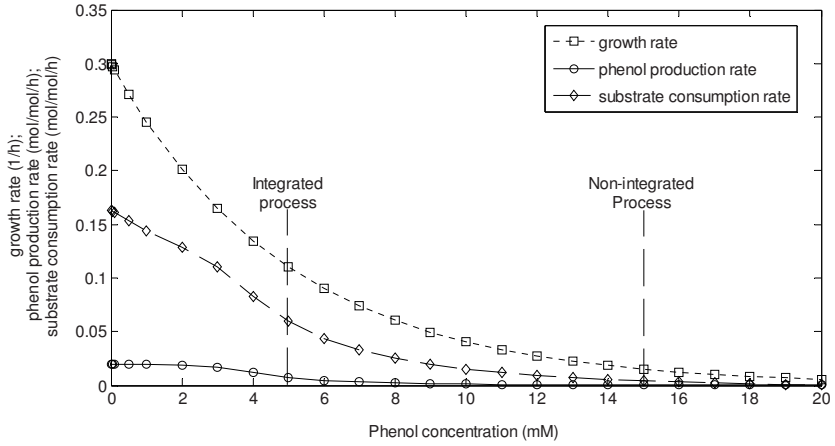

Figure 3. Microbial growth rate, phenol production rate and substrate consumption rate as a function of phenol concentration

From Figure 3, as expected, it is clear that at higher phenol concentrations the biomass growth rate, the phenol production rate and the substrate consumption rate decrease. In the non-integrated process, a fed-batch fermentation where a high phenol concentration in the reactor is reached, a decrease in abovementioned parameters causes less efficient utilization of raw materials to biomass and product. In the integrated process, a continuous fermentation with continuous phenol removal, the phenol concentration in the reactor is lower compared to the non-integrated process. This results in less product inhibition and thus a more efficient growth and production can be reached.

The phenol production rate is approximately constant for phenol concentrations lower than 3 – 4 mM, at higher concentrations a decrease is observed. The sharpness of this decrease and the critical phenol concentration at which it occurs depends on the operating growth rate. At higher growth rates a sharper decrease is observed. At a defined operating growth rate, the productivity of the integrated system approaches that of the non-integrated system for high phenol concentrations.

The non-integrated process runs until a high phenol concentration in the reactor of 15 mM to illustrate the effect of product inhibition. The integrated process runs at a lower phenol concentration in the reactor of 5 mM. At this concentration there is already a negative effect on the growth and phenol production, however if the phenol concentration is chosen too low the driving force for pertraction is very small. These limits are determined by simulation and include parameters estimated from experimental work. However, the chosen working points are different as compared to the limits given in reference [24] from fermentation experiments. In future work, this discrepancy should be addressed.

The phenol production rate for the integrated process is a factor 37 higher as compared to the phenol production rate for the non-integrated process at the final phenol concentration. However, at lower phenol concentrations the production rate for the non-integrated process is higher as compared to the final production rate at a high phenol concentration. The phenol concentration will increase at a slower rate in time due to the accumulating phenol in the reactor. Additionally, the biomass concentration will follow the same trend. However, the amount of phenol produced per gram biomass (the specific productivity) will remain constant in time.

For the fermentation section of the integrated process, it has been determined that 6 reactors are needed (this includes one spare reactor), each with a vessel volume of 507 m^3 and a liquid volume of 456 m^3, see also Table 1. The number of reactors needed for the non-integrated process has been determined to be 45 (this includes one spare reactor), each with a vessel volume of 520 m^3 and a liquid volume of 440 m^3. The total fermentation liquid volume (V_{total}) is thus 2280 m^3 for the integrated process and 19360 m^3 for the non-integrated process, a difference of a factor 8.5.

For both fermentation processes, the annual runtime is assumed to be 8000 $h.yr^{-1}$ with a maintenance time of 760 $h.yr^{-1}$. This indicates a fed-batch time for the non-integrated process of 13 h with 4 h down time, which results in approximately 470 batches per year for the required annual phenol production. In practice, a fermentation process with genetically modified micro organisms cannot run continuously for a long period of time without mutation of the organism. Considering an average run time of a continuous fermentation of one week (168 h) with a down time of 4 h per fermentation results in a total of 47 fermentations of 172 h with a total down time of 186 h, 2% of the annual runtime of 8000 h. This can be considered negligible and thus, for simplicity, it is assumed that the continuous fermentations in the integrated process run continuously for 8000 hours.

The large volume of fermentation liquid is required for the non-integrated process due to the lower phenol productivity to obtain a final phenol mass flow of 1250 $kg.h^{-1}$ (10 $kton.yr^{-1}$). Additionally, a higher phenol concentration in the reactor causes a lower yield of phenol on substrate, which causes a higher requirement of glucose.

The gas flow power input per fermentor for the non-integrated process is $8.6*10^3$ W and $1.2*10^3$ W for the integrated process, a difference of a factor 7. Additionally, the flow rate of chilled water (F_{ch}) to compensate for the total heat produced during the bioreaction (r_{ht}, $6.6*10^6$ W in the integrated process and $2.2*10^7$ W in the non-integrated process) is approximately a factor 3.4 higher for the non-integrated process. This can be explained by the higher gas flow through ($F_{g,in}$), the larger volume of feed streams and thus the heat generated by adding these streams and possible increased oxygen uptake rate to cope with a product inhibiting environment in the non-integrated process as compared to the integrated process, see also Table 6.

The heat generated by the stirrer has not been taken into account for these calculations, however, it should be mentioned that for commercial fermentations the r_{hs} is generally in de order of 0.5 – 5 $kW.m^{-3}$ [27]. This corresponds to an additional (minimum) heat generation of approximately $2.5*10^5$ W for both processes.

Table 1. Simulation results for the fermentation unit for the integrated and non-integrated process

Parameter	**Symbol**	**Integrated process**	**Non-integrated process**	**Unit**
Fermentor liquid height	H_{liq}	17.4	18.1	m
Fermentor diameter	D	5.8	6.0	m
Fermentation vessel volume	V_{ferm}	507	520	m^3
Number of fermentors	N_{ferm}	6 (5+1 spare)	45 (44+1 spare)	-
Total fermentation volume	V_{total}	2280	19360	m^3
Gas power input per fermentor	P_g	$1.2*10^3$	$8.6*10^3$	W
Total heat generated	r_{ht}	$6.6*10^6$	$2.2*10^7$	W
Flow of chilled water	F_{ch}	$1.0*10^5$	$3.4*10^5$	$kg.h^{-1}$

Biomass removal

The cell separation unit in the non-integrated process has been determined to contain a membrane area of 1217 m^2, while this unit in the integrated process contains only 22 m^2, see also Table 2. This large difference is caused by the large broth and wash water fluxes in the non-integrated process compared to the small bleed of broth in the integrated process, see also mass balances in the supplementary data, Table 14, stream 10 – 13 (non-integrated) and Table and 15, stream 6 – 10 (integrated). The volume flux through the membrane (the filtrate flux) has been determined to be 341 $L.m^{-2}.h^{-1}$ in the integrated process versus 868 $L.m^{-2}.h^{-1}$ in the non-integrated process. Furthermore, the non-integrated process will cause a large amount of biomass waste, which causes additional costs for waste treatment. Finally, due to the large fluxes in the filtration unit for the non-integrated process, the power input is very high: a factor 141 higher as compared to the integrated process.

Table 2. Simulation results for the biomass removal unit for the integrated and non-integrated process

Parameter	**Symbol**	**Integrated process**	**Non-integrated process**	**Unit**
Volumetric recycle flow	Φ_{rec}	0.149	-	$m^3.h^{-1}$
Volumetric flow rate filtrate	Φ_{SL}	7	1056	$m^3.h^{-1}$
Required filtration area S-L separation	A_{SL}	22	1217	m^2
Filtration flux S-L separation unit	F_{SL}	341	868	$L.m^{-2}.h^{-1}$
Power input S-L separation unit	P_{SL}	$1.7*10^2$	$2.4*10^4$	W

Pertraction

The phenol removal rate by the solvent (*E*) has been determined to be 1117 $kg.h^{-1}$ for the non-integrated process and 1389 $kg.h^{-1}$ for the integrated process, see also Table 3 and Table 14 (stream 16) and Table 15 (stream 12) in the supplementary data.

The membrane area required per reactor has been determined to be $1.4*10^4$ m^2 for the integrated process (38 $m^2.m^{-3}$ fermentation volume) and $1.1*10^3$ m^2 for the non-integrated process (2.6 $m^2.m^{-3}$ fermentation volume). Both values are below the maximum specific membrane area (max 524 – 1428 $m^2.m^{-3}$).

The phenol concentration in the solvent in the integrated process is lower as compared to that in the non-integrated process. This difference is caused by the lower phenol concentration in the reactor in the integrated process: 5 mM as compared to 15 mM in the non-integrated process. Although the higher phenol concentration in the reactor in the non-integrated process decreases the productivity of the micro-organisms, the driving force for pertraction is higher and the amount of phenol in the solvent is higher. Tables 14 and 15 in the supplementary data illustrate a phenol concentration of 0.031 kg phenol per kg solvent for the non-integrated process (stream 16) as compared to 0.013 kg phenol per kg solvent in the integrated process (stream 12). This corresponds to a phenol concentration in the solvent of 24 $kg.m^{-3}$ (250 mM) for the non-integrated process and 10 $kg.m^{-3}$ (111 mM) for the integrated process. Using the extraction rate and the phenol concentration in the solvent, the solvent flux (Φ_{tube}) in a membrane module has been determined. In the non-integrated process the solvent flux is determined to be $1.3*10^{-2}$ $m^3.s^{-1}$ and in the integrated process the solvent flux is $3.7*10^{-2}$ $m^3.s^{-1}$. With a pressure drop per module of 0.1 bar and 0.24 bar, the resulting power input per module ($P_{ME,mod}$) is $6.2*10^2$ W for the integrated process and $5.2*10^2$ W for the non-integrated

process, respectively. The total power input for pertraction per fermentor (P_{ME}) is calculated to be $7.8*10^5$ W for the integrated process and $1.6*10^5$ W for the non-integrated process.

The power input for the pertraction unit is dependent on the volumetric flow rate at the tube side and the pressure drop. Since the volumetric flow rate in the integrated process is higher as compared to the non-integrated process, the power input is higher.

Table 3. Simulation results for the pertraction unit for the integrated and non-integrated process

Parameter	**Symbol**	**Integrated process**	**Non-integrated process**	**Unit**
Phenol removal rate	E	1389	1117	$kg.h^{-1}$
Number of fibers per fermentor	N_{fibers}	$1.3*10^6$	$3.2*10^5$	-
Required membrane area per fermentor	A_{per}	$1.4*10^4$	$1.1*10^3$	m^2
Specific membrane area	a_{sp}	38	2.6	$m^2.m^{-3}$
Solvent flux tube side	φ_{tube}	$3.7*10^{-2}$	$1.3*10^{-2}$	$m^3.s^{-1}$
Pressure drop per module	Δp_{ME}	0.1	0.24	bar
Power input pertraction unit per fermentor	P_{ME}	$7.8*10^5$	$1.6*10^5$	W
Total membrane area	A_{tot}	$7.2*10^4$	$4.5*10^4$	m^2

Distillation

The mass balances given in Table 14 (stream 17) and Table 15 (stream 12) in the supplementary data illustrate the solvent stream fed to the first distillation column. A solvent feed stream of $1.1*10^5$ $kg.h^{-1}$ containing 1389 $kg.h^{-1}$ phenol has been calculated for the integrated process and for the non-integrated process a solvent feed stream of $3.8*10^4$ $kg.h^{-1}$ containing 1276 $kg.h^{-1}$ phenol. The phenol concentration in the solvent is 3.4 wt% in the non-integrated process as compared to 1.2 wt% in the integrated process. The lower phenol concentration in the solvent and the larger solvent volume flux in the integrated process lead to heavier columns (mainly due to the larger column diameter) and a higher heating and cooling energy requirement for distillation compared to the non-integrated process, see also Table 16 in the supplementary data. The composition of the final product stream is given in Table 14 in the supplementary data (stream 23) for the non-integrated process: 1163 $kg.h^{-1}$ phenol, a purity of 98.8% and a phenol recovery of 84%. The composition of the final product stream for the integrated process is given in Table 15 in the supplementary data (stream 18): 1252 $kg.h^{-1}$ phenol, a purity of 99.0% and a phenol recovery of 90% was obtained. The differences in the final results are due to the models used and separate model optimization. Therefore, it is not possible to

have equal results. The higher recovery in the integrated process might be explained by the fact that the implementation of the pertraction unit into the fermentor reduces the number of separation steps and therefore improves the overall recovery.

3.6 Process economics

Equipment costs and CAPEX

The purchased equipment costs (PEC) are determined by the costs for reactors, storage tanks and vessels, distillation columns, solid-liquid separation equipment, heat exchangers, membrane contactors and pumps and electrical motors. The estimation of the equipment costs has been performed using reference [28]. In Table 4 the results from the bare equipment cost calculations are given. The total costs for the bare equipment is a factor 2.4 higher for the non-integrated process as compared to the integrated process. For the calculation of the PEC, a 10% extra costs in material to compensate for non calculated materials is considered.

The cost of the reactor is determined by the total required reactor volume. The reactor costs were multiplied with the number of reactors for both processes. The reactor costs for the integrated process result in 18% of the total equipment costs as compared to the non-integrated case where the reactor costs are as high as 63% of the total equipment costs.

The costs of the storage tanks and vessels are determined by the total vessel weight and by the required internal pressure. The different tanks used are: glucose preparation and supply tank, ammonia preparation and supply tank, hydrochloric acid tank, fresh water supply tank, solvents supply and recycle tank and buffer tanks. The total costs for the storage tanks and vessels are comparable for both processes: 2% of the total equipment costs.

The costs for pressure vessels and towers for distillation are higher for the integrated process (12% of the total equipment costs) as compared to the non-integrated process (2% of the total equipment costs). This was expected due to the lower phenol concentration in the solvent fed to the distillation columns in the integrated process.

The cost of the solid-liquid separation equipment is determined by the total membrane area required. The total membrane area required for the non-integrated process is higher as compared to the integrated process (see also Table 2), therefore the equipment costs are higher. The solid-liquid equipment costs are 15% of the total equipment costs for the non-integrated process against 2% for the integrated process.

The costs of the heat exchangers are determined by the required area for heat exchange and by the required internal pressure. The heat exchangers are more expensive for the integrated process due to the higher energy requirements for solvent recovery and phenol purification (see also Table 16 in the supplementary data).

The costs for the membrane extraction unit is determined by total membrane area required. Since the total membrane area required for the integrated process is higher as compared to that of the non-integrated process (see also Table 3), the costs are higher. Additionally, the costs for the membrane extraction unit as a percentage of the total equipment costs is higher for the integrated process: 63% against 16% for the non-integrated process. The costs for the membrane extraction unit for the non-integrated process can be lowered by working at a higher temperature. Increasing the extraction temperature results is a higher overall mass transfer coefficient and thus a lower amount of membrane required. However, the heating of the solvent stream will increase the energy requirements of the process.

The costs for the pumps and electrical motors are determined by the required flow rate. These costs are comparable for both processes and negligible compared to the costs of the other equipment.
The total capital investment (TCI) can be calculated as a function of the PEC, see Table 5 [29]. From Table 5 it becomes clear that the total capital investment (CAPEX or TCI) for the non-integrated process is higher as compared to the integrated process.

Table 4. Summary bare equipment costs

	Integrated		**Non-integrated**	
Equipment description	Bare Equipment Cost (kEUR)	%	Bare Equipment Cost (kEUR)	%
Reactors and Fermenters	6.0E+03	18	5.1E+04	63
Storage Tanks and Vessels	4.9E+02	2	2.0E+03	2
Pressure Vessels and Towers for Distillation	3.8E+03	12	1.3E+03	2
Solid-Liquid Separation Equipment	7.9E+02	2	1.2E+04	15
Heat Exchangers	8.9E+02	3	3.1E+02	0
Membrane Contactors	2.1E+04	63	1.3E+04	16
Pumps and Electrical Motors	2.9E+02	1	3.2E+02	0
Total	3.3E+04	100	8.0E+04	100

Table 5. Total capital investment, CAPEX

	Cost		**Integrated**	**Non-integrated**
Item			Cost (kEUR)	Cost (kEUR)
Purchased equipment costs (delivered) (PEC)	1	PEC	3.7E+04	8.8E+04
Equipment installation	0.4	PEC	1.5E+04	3.5E+04
Instrumentation	0.2	PEC	7.3E+03	1.8E+04
Piping	0.7	PEC	2.6E+04	6.2E+04
Electrical	0.1	PEC	3.7E+03	8.8E+03
Buildings and storages	0.45	PEC	1.6E+04	4.0E+04
Site development	0.05	PEC	1.8E+03	4.4E+03
Direct plant costs (DPC)	2.9	PEC	1.1E+05	2.6E+05
Design and engineering	0.3	DPC	3.2E+04	7.7E+04
Contractors' fee	0.05	DPC	5.3E+03	1.3E+04
Contingency	0.1	DPC	1.1E+04	2.6E+04
Indirect plant costs (IPC)	0.45	DPC	4.8E+04	1.2E+05
Fixed capital investment (FCI)	4.2	PEC	1.5E+05	3.7E+05
Working capital	0.1	FCI	1.5E+04	3.7E+04
Start up	0.08	FCI	1.2E+04	3.0E+04
TOTAL CAPITAL INVESTMENT (TCI)	4.96	PEC	1.8E+05	4.4E+05

Variable costs and OPEX

The variable costs (VC) are determined by the costs for feedstocks (glucose, ammonia, hydrochloric acid, process water, inoculum (biomass) and 1-octanol), utilities (low pressure (LP) steam, medium pressure (MP) steam, cooling water, chilled water, electricity and pressurized air) and waste treatment (biomass and waste water).

In Table 6 the variable costs are illustrated for both processes. As described before, in practice, a fermentation process with genetically modified micro organisms cannot run continuously for a long period of time without mutation of the organism. The flow of biomass (inoculum) needed for the integrated process was determined by taking into account the amount of fermentations run in one year, the total fermentation broth volume and the initial biomass concentration (15 $g.L^{-1}$). The total variable costs are mainly determined by the costs for feedstocks: 70% and 78% of the total costs for the non-integrated and integrated process, respectively. In both cases the determining cost factor is the cost of glucose.

Additionally, as expected, the costs for utilities in the integrated process is higher as compared to the non-integrated process (solvent regeneration and phenol purification step). It should be noted again that due to the complexity of estimating the stirrer power input for both cases, especially for the integrated process, it was neglected for the calculations. Stirring rate is constantly changing to maintain a certain dissolved oxygen level in the fermentation broth. When assuming for example an equal stirrer power input as given in the text of a minimum of 0.5 $kW.m^{-3}$ and the total reactor volume as given in Table 1, the calculated total stirrer power input for the non-integrated process will be a factor 9 higher as compared to the integrated process. This would result in an increase of the costs for electricity to approximately $2*10^3$ and $8*10^3$ keuro/yr instead of $1.6*10^3$ and $3.4*10^3$ keuro/yr for the integrated and non-integrated process respectively (see also Table 6). Compared to the % of the total variable costs compared to for example the costs of feedstocks this change is negligible.

Furthermore, the cost for waste treatment is higher in the non-integrated process as compared to the integrated process (waste stream from biomass separation step). Overall, the variable costs in the non-integrated process are a factor 5 higher as compared to the integrated process.

The total manufacturing cost (TMC) can be calculated as the sum of the VC and the fixed costs. The fixed costs are estimated as fractions of the fixed capital investment (FCI), see also Table 5. The annual total production costs (OPEX or TPC), illustrated in Table 7, are a factor 3.5 higher for the non-integrated process.

Table 6. Summary variable costs

	Integrated		**Non-integrated**	
Description	Annual Cost (kEUR.yr^{-1})	%	Annual Cost (kEUR.yr^{-1})	%
Feedstocks				
Glucose	3.4E+04	72	1.5E+05	61
Ammonia	2.6E+02	1	4.4E+03	2
Hydroclric acid	6.1E-06	0	1.5E+02	0
Process Water	8.6E+01	0	7.8E+03	3
Inocullum (biomass)	2.7E+03	6	4.4E+03	2
1-Octanol	2.4E+01	0	5.6E+03	2
Total	*3.7E+04*	*78*	*1.7E+05*	*70*
Utilities				
LP steam	0.0E+00	0	5.9E+02	0.2
MP steam	5.2E+03	11	8.9E+02	0.4
Cooling water	1.5E+03	3	4.8E+02	0.2
Chilled water	2.7E+02	1	8.8E+02	0.4
Electricity	1.6E+03	3	3.4E+03	1.4
Pressurized air	5.6E+02	1	1.4E+03	0.6
Total	*9.1E+03*	*19*	*7.6E+03*	*3.1*
Waste treatment				
Biomass waste treatment	1.2E+03	2.5	5.8E+04	24
Waste water treatment	1.0E+02	0.2	8.6E+03	4
Total	*1.3E+03*	*3*	*6.6E+04*	*27*
Total	4.8E+04	100	2.4E+05	100

Table 7. Annual total production costs, OPEX

			Integrated	**Non-integrated**
Item	Cost		Cost (kEUR.yr^{-1})	Cost (kEUR.yr^{-1})
Variable costs (Raw materails & Utilities) (VC)	calculated		4.8E+04	2.4E+05
Maintenance	0.05	FCI	9.1E+03	2.2E+04
Operating labour (OL)	0.1	FCI	1.8E+04	4.4E+04
Laboratory costs	0.2	OL	3.6E+03	8.8E+03
Supervision	0.2	OL	3.6E+03	8.8E+03
Patents and royalties	0.01	FCI	1.5E+03	3.7E+03
Direct production costs			8.4E+04	3.3E+05
Local taxes	0.02	FCI	3.1E+03	7.4E+03
Insurance	0.01	FCI	1.5E+03	3.7E+03
Capital charges	0.15	FCI	2.3E+04	5.6E+04
Fixed costs			2.8E+04	6.7E+04
Plant overheads	0.5	OL	9.1E+03	2.2E+04
TOTAL MANUFACTURING COST (TMC)	Sum		1.2E+05	4.2E+05
General expenses (GE)	0.25	x sum previous items	3.0E+04	1.0E+05
TOTAL PRODUCTION COST (TPC)	Sum		1.5E+05	5.2E+05

Product cost price

The return on investment (ROI) can be determined by:

$$ROI = \frac{NetEarnings}{TCI} \quad (5)$$

With:

$$NetEarnings = (1 - t) \cdot (S - TPC \cdot -D) \quad (6)$$

Where t is the tax rate (30%), S is the annual sales revenues (keur.yr^{-1}) and D the depreciation (keur.yr^{-1}):

$$S = \frac{ProductionRate \cdot MinimumPCP}{1000} \cdot Operatingtime \quad (7)$$

Where the production rate is the mass flow of phenol in product stream ($kg.h^{-1}$), PCP is the minimum product cost price and the operating time (the hours runtime in a year) is 8000 h.
Depreciation (D) is described by:

$$D = \frac{FCI}{Planteconomicallife} \quad (8)$$

With a plant economical life of 10 years.

By varying the PCP, the product cost price for a ROI of 15% can be determined.

The non-integrated and integrated processes were evaluated to obtain the phenol cost price at a return on investment (ROI) of 15%. The phenol cost price is calculated to be 57 and 18 $€.kg^{-1}$ for the non-integrated and the integrated process, respectively. This is still far from the current phenol market price (approximately 0.6 $€.kg^{-1}$, 2009 ICIS pricing), although phenol is in this work considered a model compound for more valuable fine chemicals.

Process optimization

The economic evaluation described in this paper shows a preference for an integrated process as compared to a non-integrated process for the production of the toxic model component phenol. The total capital investment and the total annual production costs are higher for a non-integrated process as compared to an integrated process. Options for (process) improvement and consequent decrease of the product cost price are considered below. The main cost factors of the integrated process are the costs of the pertraction unit, the glucose costs and the distillation costs (distillation units and steam).

A low aqueous product concentration results in a low driving force for pertraction and consequently to high costs for membrane extraction and distillation units. Using a solvent with a higher partition coefficient for the product, a lower volume of solvent can be used to extract the product from the fermentation broth and the distillation costs can be further decreased. In earlier work[24], it was determined that the rate limiting factor for overall mass transfer in the pertraction process is the membrane resistance. The overall mass transfer for pertraction was already optimized by choosing a thinner membrane fiber (less resistance in the membrane)[30]. Additionally, an alternative solvent with a higher partition coefficient (higher capacity) can improve the overall mass transfer coefficient. A solvent with a higher partition coefficient like methyl isobutyl ketone (MIBK, partition coefficient for phenol ~120) as described by reference [31] or n-butanol [32] will result in a reduced membrane- and

stripping resistance for mass transfer. On the other hand, a solvent with a high partition coefficient usually dissolves well in water and vice versa. MIBK, for example, has a solubility in water of 19 $g.L^{-1}$, while 1-octanol dissolves in water at a maximum concentration of 0.5 $g.L^{-1}$ [33]. This leads to solvent losses into the bioreactor and potentially additional solvent toxicity effects. Experiments were executed with tributylphosphate (TBP), a solvent with a partition coefficient for phenol around 400. This value is comparable with the value reported by Burghoff et al: a partition coefficient for phenol in TBP of 450 [34]. The overall mass transfer coefficient determined in single-fiber modules with TBP and the membrane type used in this study increased with a factor 5 as compared to the overall mass transfer coefficient determined with 1-octanol[30]. Other solvents like Cyanex 923, ionic liquids, trioctylamine (TOA), linear monoalkyl cyclohexane (IMACH), micellar solvents and 1-decanol were also mentioned in literature [12, 35-38]. Optimization studies can be executed with different single-fiber modules and solvents, where the overall mass transfer is the most important parameter to evaluate. Additionally, solubility of solvent in the water phase and vice versa and solvent toxicity should be evaluated.

Alternatively, the process of pertraction and solvent and product recovery as described in this paper can be altered by using another process like emulsion pertraction. Several references describe a simultaneous stripping of product from the solvent stream using a basic stripping solution [12, 37, 39]. A subsequent separation of the solvent from the stripping phase can reduce the total process costs avoiding expensive distillation processes. For the model product phenol the stripping phase can be for example a sodium hydroxide solution, extracting phenol as phenolate from the solvent phase due to the high pH of the stripping solution. Solvent and stripping solution are separated by phase separation based on their difference in density. The solvent can be reused and the stripping phase containing the product can be further purified. A disadvantage of this method is the large salt streams in the process and the additional need for neutralizing agent. Furthermore, once the product is in its neutral form, it still needs to be purified by for example nanofiltration [40, 41]. The system described using emulsion pertraction seems to shift the problem of expensive distillation units to other complicated problems and therefore further research is required.

Besides changing process conditions and the separation process, the micro-organism can be further optimized to a higher production rate, a higher yield of biomass and/or product on substrate and/or a higher solvent/product tolerance. By improving the resistance of the micro-organism to the toxic product, a higher aqueous product concentration can be reached and the costs for pertraction and distillation will be lowered. On the other hand, solvent tolerant *P. putida* tends to have an increased energy metabolism when in contact with toxic solvent[42]. This results in an increase in substrate utilization. Since the costs of the raw material glucose is one of the cost determining factors of the process, it should also be considered to change to a less expensive carbon source like glycerol or lignocelluloses [24, 43]. However, when changing a raw material in a bioprocess, the experimental

(kinetic) data should be studied carefully and extra information should be obtained by running new fermentation and pertraction experiments.

Finally, an integrated pertraction process can be interesting for other bioprocesses besides the model process for phenol production chosen in this paper. Examples of alternative (bio)products are carboxylic acids, amino acids, antibiotics, other organic acids and aromatic carboxylic acids. Acids or salts might be interesting in combination with other solvents and purification techniques in combination with membrane extraction, for example ionic liquids, micellar solvents, regeneration by pH shift, possibility of using ion exchange membranes and more, depending on the system. Other examples of (bio)products which can be separated by (membrane) extraction are described in literature [12, 44, 45]. Alternative bioprocesses besides the model process for phenol, especially those which do not allow for a higher aqueous product concentration due to the high product toxicity and the resulting product inhibition and a low yield on glucose, will probably show even larger benefits in an integrated membrane extraction process.

3.7 Conclusions

In this paper, the (bio)production of the inhibiting model component phenol in a bioreactor by a recombinant strain of the micro-organism *Pseudomonas putida* S12 combined with in-situ product removal by membrane extraction (pertraction) has been described. Continuous fermentation with integrated pertraction is compared to a fed-batch fermentation with a non-integrated pertraction process. The work results in a process design describing fermentation, cell removal, membrane extraction and regeneration of the solvent and product purification by distillation. The design has been made for an annual phenol production of 10 kton.

Results from metabolic models show that at product concentrations above 3-4 mM in the fermentor the growth rate, phenol production rate and the substrate consumption rate decrease. The non-integrated process runs mainly at higher phenol concentrations, therefore the utilization of substrate to produce biomass and phenol will be less efficient. Additionally, the cell separation unit in the non-integrated process requires a large amount of membrane and produces a large amount of waste materials. Furthermore, simulations indicate that the integration of a pertraction unit in a bioreactor decreases the volume of the fermentation broth required. On the contrary, the lower phenol concentration in the reactor and in the solvent causes a higher energy input and larger column costs for distillation as compared to a non-integrated process. On the other hand, the specific membrane area per reactor volume required for pertraction is higher in the integrated process.

Economic evaluation of the two processes show that, at a return of investment of 15%, the phenol cost price of the integrated process is a factor 3 lower as compared to the non-integrated process: 18 versus 57 €.kg^{-1}, respectively. The equipment costs in the non-integrated process is mainly

determined by the reactor costs, while the pertraction unit in the integrated process is the main cost factor. The substrate used for the fermentation process (glucose) is the determining factor in the direct production costs is for both cases.

Optimization and further decrease of the product cost price in the integrated process can be realized by improvement of the pertraction process by for example improved mass transfer using a solvent with a higher partition coefficient. This results in a lower surface area of required membrane and thus lower process costs. The use of alternative processes such as emulsion pertraction might lower the overall process costs to a certain extent. On the other hand, improvement of the microbial metabolism by further optimization of the bacterial strain can result in a higher phenol production rate and/ or a more efficient substrate consumption which in turn can improve the driving force for pertraction and lower the substrate costs, respectively. Additionally, a decrease in raw material cost price or the use of an alternative carbon source will have a significant effect on the phenol cost price. Finally, the integration of a membrane extraction unit in a (bio)production process will show even larger benefits for processes which do not allow for a high product concentration in the fermentation broth due to a high product toxicityas compared to the model process for phenol described in this paper.

References

1. Nijkamp, K.; van Luijk, N.; de Bont, J.; Wery, J., The solvent-tolerant Pseudomonas putida S12 as host for the production of cinnamic acid from glucose. Applied Microbiology and Biotechnology 2005, 69, (2), 170-177.

2. Nijkamp, K.; Westerhof, R. G. M.; Ballerstedt, H.; de Bont, J. A. M.; Wery, J., Optimization of the solvent-tolerant Pseudomonas putida S12 as host for the production of p-coumarate from glucose. Applied Microbiology and Biotechnology 2007, 74, (3), 617-624.

3. Wierckx, N. J. P.; Ballerstedt, H.; De Bont, J. A. M.; Wery, J., Engineering of solvent-tolerant Pseudomonas putida S12 for bioproduction of phenol from glucose. Applied and environmental microbiology 2005, 71, (12), 8221-8227.

4. Lye, G. J.; Woodley, J. M., Application of in situ product-removal techniques to biocatalytic processes. Trends in Biotechnology 1999, 17, (10), 395-402.

5. Lienqueo, M. E.; Asenjo, J. A., Use of expert systems for the synthesis of downstream protein processes. Computers & Chemical Engineering 2000, 24, (9-10), 2339-2350.

6. Groot, W. J.; van der Lans, R. G. J. M.; Luyben, K. C. A. M., Technologies for butanol recovery integrated with fermentations. Process Biochemistry 1992, 27, (2), 61-75.

7. Brink, L. E. S.; Tramper, J., Optimization of organic solvent in multiphase biocatalysis. Biotechnology and Bioengineering 1985, 27, 1258-1269.

8. Buhler, B.; Bollhalder, I.; Hauer, B.; Witholt, B.; Schmid, A., Use of the two-liquid phase concept to exploit kinetically controlled multistep biocatalysis. Biotechnology and Bioengineering 2003, 81, (6), 683-694.

9. Berg, C. v. d.; Roelands, C. P. M.; Bussmann, P.; Goetheer, E. L. V.; Verdoes, D.; van der Wielen, L. A. M., Preparation and analysis of high capacity polysulfone capsules. Reactive and Functional Polymers 2009, 69, (10), 766-770.

10. Stark, D.; Kornmann, H.; Münch, T.; Sonnleitner, B.; Marison, I. W.; Stockar, U. v., Novel type of in situ extraction: Use of solvent containing microcapsules for the bioconversion of 2-phenylethanol from L-phenylalanine by Saccharomyces cerevisiae. Biotechnology and Bioengineering 2003, 83, (4), 376-385.

11. Berg, C. v. d.; Wierckx, N.; Vente, J.; Bussmann, P.; Bont, J. d.; Wielen, L. v. d., Solvent-impregnated resins as an in-situ product recovery tool for phenol recovery from Pseudomonas putida S12TPL fermentations. Biotechnology and Bioengineering 2008, 100, (3), 466-472.

12. Schlosser, S.; Kertesz, R.; Martak, J., Recovery and separation of organic acids by membrane-based solvent extraction and pertraction: An overview with a case study on recovery of MPCA. Separation and Purification Technology 2005, 41, (3), 237-266.

13. Fernandes, P.; Prazeres, D. M.; Cabral, J. M., Membrane-assisted extractive bioconversions. Advances in biochemical engineering/biotechnology 2003, 80, 115-148.

14. Hüsken, L. E.; Oomes, M.; Schroën, K.; Tramper, J.; de Bont, J. A. M.; Beeftink, R., Membrane-facilitated bioproduction of 3-methylcatechol in an octanol/water two-phase system. Journal of Biotechnology 2002, 96, (3), 281-289.

15. Molinari, F.; Aragozzini, F.; Cabral, J. M. S.; Prazeres, D. M. F., Continuous production of isovaleraldehyde through extractive bioconversion in a hollow-fiber membrane bioreactor. Enzyme and Microbial Technology 1997, 20, (8), 604-611.

16. Urbanus, J.; Laven, J.; Roelands, C. P. M.; ter Horst, J. H.; Verdoes, D.; Jansens, P. J., Template Induced Crystallization: A Relation between Template Properties and Template Performance. Crystal Growth & Design 2009, 9, (6), 2762-2769.

17. Buque-Taboada, E. M.; Straathof, A. J. J.; Heijnen, J. J.; van der Wielen, L. A. M., Microbial reduction and in situ product crystallization coupled with biocatalyst cultivation during the synthesis of 6R-dihydrooxoisophorone. Advanced Synthesis and Catalysis 2005, 347, 1147-1154.

18. Urbanus, J.; Roelands, C. P. M.; ter Horst, J. H.; Verdoes, D.; Jansens, P. J., Screening for templates that promote crystallization. Food and Bioproducts Processing 2008, 86, 116-121.

19. Buque-Taboada, E. M.; Straathof, A. J. J.; Heijnen, J. J.; van der Wielen, L. A. M., In situ product recovery (ISPR) by crystallization: basic principles, design, and potential applications in whole-cell biocatalysis. Applied Microbiology and Biotechnology 2006, 71, (1), 1-12.

20. Curcio, E.; Di Profio, G.; Drioli, E., Recovery of fumaric acid by membrane crystallization in the production of -malic acid. Separation and Purification Technology 2003, 33, (1), 63-73.

21. Bouchoux, A.; Roux-de Balmann, H.; Lutin, F., Investigation of nanofiltration as a purification step for lactic acid production processes based on conventional and bipolar electrodialysis operations. Separation and Purification Technology 2006, 52, (2), 266-273.

22. Groot, W. J.; den Reyer, M. C. H.; Baart de la Faille, T.; van der Lans, R. G. J. M.; Luyben, K. C. A. M., Integration of pervaporation and continuous butanol fermentation with immobilized cells I: Experimental results. The Chemical Engineering Journal 1991, 46, (1), B1-B10.

23. Hirata, D. B.; Oliveira, J. H. H. L.; Leão, K. V.; Rodrigues, M. I.; Ferreira, A. G.; Giulietti, M.; Barboza, M.; Hokka, C. O., Precipitation of clavulanic acid from fermentation broth with potassium 2-ethyl hexanoate salt. Separation and Purification Technology 2009, 66, (3), 598-605.

24. Heerema, L.; Wierckx, N.; Roelands, M.; Hanemaaijer, J. H.; Goetheer, E.; Verdoes, D.; Keurentjes, J., In situ phenol removal from fed-batch fermentations of solvent tolerant Pseudomonas putida S12 by pertraction. Biochemical Engineering Journal 2011, 53, 245-252.

25. Heijnen, J. J., Approximative kinetic formats used in metabolic network modeling. Biotechnology and Bioengineering 2005, 91, (5), 534-545.

26. R. Heijmans; M. Boon; Araújo, L. Kinetic modelling of bioproduction process; TNO Science and Industry: 2007.

27. Riet, K. v. t.; Tramper, J., Basic Bioreactor Design. Marcel Dekker, Inc.: 1991; p 465.

28. Matche http://www.matche.com/

29. Coulson, J. M.; Richardson, J. F., Coulson & Richardson's Chemical Engineering: Chemical engineering design 3th ed.; Butterworth-Heinemann: 1999; Vol. 6

30. Heerema, L.; Roelands, M.; Goetheer, E.; Verdoes, D.; Keurentjes, J., Strategies for module design for in-situ product removal from fermentations by membrane extraction To be submitted 2011.

31. Prasad, R.; Sirkar, K. K., Dispersion-free solvent extraction with microporous hollow-fiber modules. AIChE Journal 1988, 34, (2), 177-188.

32. Ruhl, J.; Schmid, A.; Blank, L. M., Selected Pseudomonas putida strains able to grow in the presence of high butanol concentrations. Applied and Environmental Microbiology 2009, 75, (13), 4653-4656.

33. Berg, C. v. d., Personal communication In Delft, 2009; p Table of solvents with their properties.

34. Burghoff, B.; Goetheer, E. L. V.; de Haan, A. B., COSMO-RS-based extractant screening for phenol extraction as model system. Industrial & Engineering Chemistry Research 2008, 47, (12), 4263-4269.

35. Cichy, W.; Schlosser, S.; Szymanowski, J., Extraction and pertraction of phenol through bulk liquid membranes. Journal of Chemical Technology and Biotechnology 2005, 80, 189-197.

36. Marták, J.; Schlosser, S.; Vlcková, S., Pertraction of lactic acid through supported liquid membranes containing phosphonium ionic liquid. Journal of Membrane Science 2008, 318, (1-2), 298-310.

37. Trivunac, K.; Stevanovic, S.; Mitrovic, M., Pertraction of phenol in hollow-fiber membrane contactors. Desalination 2004, 162, 93-101.

38. Heerema, L.; Cakali, D.; Roelands, M.; Goetheer, E.; Verdoes, D.; Keurentjes, J., Micellar solutions of PEO-PPO-PEO block copolymers for in situ phenol removal from fermentation broth. Separation and Purification Technology 2010, 73, (2), 319-326.

39. Boyadzhiev, L.; Dimitrov, K.; Metcheva, D., Integration of solvent extraction and liquid membrane separation: An efficient tool for recovery of bio-active substances from botanicals. Chemical Engineering Science 2006, 61, (12), 4126-4128.

40. Bódalo, A.; Gómez, E.; Hidalgo, A. M.; Gómez, M.; Murcia, M. D.; López, I., Nanofiltration membranes to reduce phenol concentration in wastewater. Desalination 2009, 245, (1-3), 680-686.

41. López-Muñoz, M. J.; Sotto, A.; Arsuaga, J. M.; Van der Bruggen, B., Influence of membrane, solute and solution properties on the retention of phenolic compounds in aqueous solution by nanofiltration membranes. Separation and Purification Technology 2009, 66, (1), 194-201.

42. Blank, L. M.; Ionidis, G.; Ebert, B. E.; Buhler, B.; Schmid, A., Metabolic response of Pseudomonas putida during redox biocatalysis in the presence of a second octanol phase. Febs Journal 2008, 275, (20), 5173-5190.

43. Meijnen, J. P.; de Winde, J. H.; Ruijssenaars, H. J., Engineering Pseudomonas putida S12 for efficient utilization of D-xylose and L-arabinose. Applied and Environmental Microbiology 2008, 74, (16), 5031-5037.

44. Schugerl, K., Integrated processing of biotechnology products. Biotechnology Advances 2000, 18, (7), 581-599.

45. Straathof, A. J. J.; Panke, S.; Schmid, A., The production of fine chemicals by biotransformations. Current Opinion in Biotechnology 2002, 13, (6), 548-556.

Chapter 4

Module design for in-situ product removal from fermentations by membrane extraction

This chapter was submitted as:
Heerema, L.; Roelands, M.; Goetheer, E.; Verdoes, D.; Keurentjes, J., Strategies for module design for in-situ product removal from fermentations by membrane extraction *Submitted* 2011.

Abstract

A strategy for the design of a membrane extraction module for implementation in a bioreactor is proposed by combining experimental and theoretical results. This paper describes the experimental evaluation of in-situ pertraction of the model compound phenol from model fermentation solutions. Overall mass transfer coefficients are determined using hollow fiber modules and rate limiting parameters have been established. The influence of membrane type, solvent and Reynolds number at the shell side (water) and lumen side (solvent) on the overall mass transfer coefficient is investigated and the results are combined with data from pertraction experiments in a bioreactor to determine a strategy to design an integrated membrane module. The calculations and considerations made in this paper show that implementation of an integrated membrane extraction process in fermentation of an inhibiting compound is a realistic perspective.

4.1 Introduction

Environmental issues (closed carbon cycles) and the search for renewable, bio-based fuels and chemicals induced the development of bio-catalytic processes for the sustainable production of chemicals. Often, sustainable processes utilize genetically modified organisms such as yeast, bacteria or fungi. These organisms can give high production rates, however, a major problem in these production processes is the fact that the micro-organisms are often affected by the high product concentrations in the bioreactor [1-4]. The use of in-situ product removal (ISPR) is a useful strategy to overcome this problem. Integration of the first downstream process step with the bioreactor leads to direct removal of product during growth and production reactions, potentially increasing the productivity of the biocatalyst and thus the total yield of product.

Pseudomonas putida is a solvent-tolerant bacterium that is capable to deal with toxic solutes like phenol and 3-methylcatechol to a certain extent and can additionally be used in direct contact with organic solvents [5, 6]. Although these micro-organisms are capable of growing and producing the desired product in the presence of organic solvents like 1-octanol, they are affected by direct contact with the solvent. In addition, such a two-phase extraction process cannot run continuously. An alternative concept for the extraction of toxic products from a bioreactor is in-situ membrane extraction. Membrane extraction (pertraction) enables a large contacting surface area between fermentation broth (aqueous phase) and solvent without the formation of an emulsion and, therefore, it is a useful technique for ISPR [7]. Additional advantages of integrated membrane extraction are lower stress levels for the micro-organisms and the absence of large circulating streams of fermentation broth outside the reactor.

In Figure 1 a schematic representation of an in-situ membrane extraction process is given. The Figure describes a (continuous) fermentation process with a feed containing nutrients. A small bleed stream of fermentation broth is led through a solid-liquid separation unit, for example a microfiltration unit, to maintain a constant reactor volume. Inside the fermentor a membrane extraction unit is integrated and the product of interest is removed from the reactor by membrane solvent extraction. Subsequently, the solvent is regenerated and the product is recovered using for example distillation. Part of the biomass and the aqueous stream of fermentation liquid and the regenerated solvent are recycled to the fermentor and the extraction unit, respectively.

Membrane extraction modules for integration in a bioreactor are not commercially available yet. Therefore, in this work an approach for an integrated module design is described. Mass transfer is studied experimentally for pertraction of the model component phenol in a single-fiber membrane unit using the solvents 1-octanol and tributylphosphate (TBP). The results are compared with the results obtained in earlier work in a bioreactor[1] for a phenol fermentation process and combined to estimate the mass transfer coefficient for an optimized module. Subsequently, calculations are

performed to design a module that is potentially suitable to reach the desired phenol removal rate in a large scale bioreactor. Finally, the possible consequences and bottlenecks of a combined separation and bioproduction process are considered.

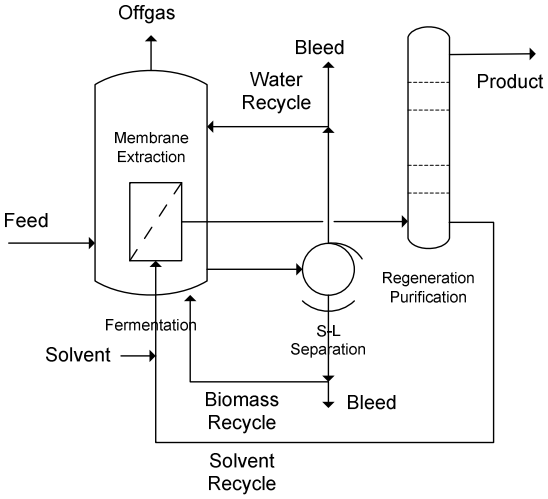

Figure 1. Continuous fermentation with integrated membrane extraction.

4.2 Experimental evaluation of the overall mass transfer coefficient

Bioreactor system

In earlier work[1], mass transfer experiments in a bioreactor system were performed. Pertraction in a bioreactor was carried out with Accurel PP V8/HF polypropylene hollow fiber microfiltration membranes (Membrana), see Figure 2 for a schematic presentation of the experimental setup. The membrane fibers had a pore size of 0.2 µm, outer diameter (d_{out}) of 8.6 mm and inner diameter (d_{in}) of 5.5 mm, see also Table 2 in the supplementary data. The area available for pertraction in all experiments was approximately 0.014 m^2 (~7 $m^2.m^{-3}$). The hollow fiber membrane is mounted as a spiral inside the reactor on the same height as the lower stirrer.

The experiments were carried out in duplicate with an aqueous reactor volume of 2 L. A feed containing phenol was added at a feed rate corresponding to the average production rate in a reference fed-batch fermentation process. Additionally, mass transfer coefficients were determined in experiments with a sterilized membrane, in fermentation medium without cells and with a phenol feed rate of a factor three higher than the average production rate. The temperature in the reactor for the mass transfer experiments was maintained at 30°C, the stirrer speed at 250 rpm with an airflow rate of 1 $L.min^{-1}$ (headspace aeration) and 1-octanol was circulated at a flow rate of 50 $mL.min^{-1}$ (a

superficial solvent velocity of 0.02 $m.s^{-1}$). With a stirrer speed (N) of 250 rpm, a fermentor diameter (D) of 25 cm and a stirrer diameter (D_A) of 0.3*D, the Reynolds number (Re) was $2.3*10^4$ (turbulent flow) while the stirrer tip speed (v_{tip}) in this case was 1.0 $m.s^{-1}$ ($v_{tip} = \pi.N.D_A$).

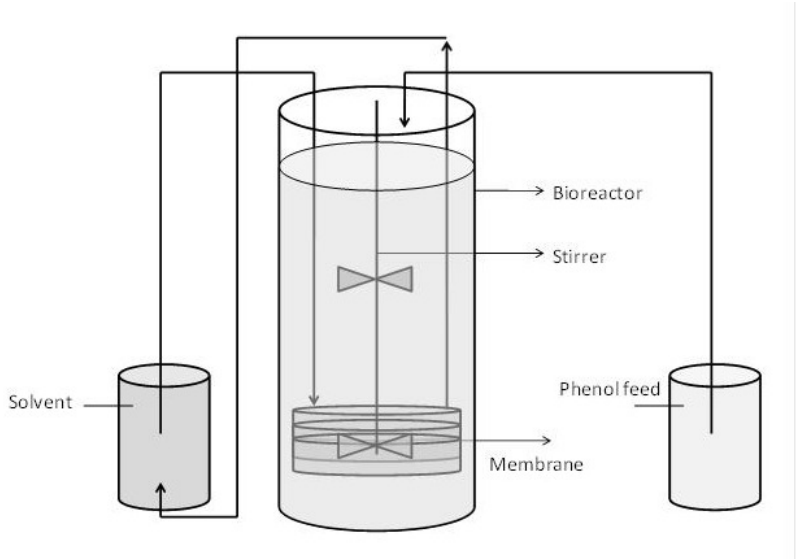

Figure 2. Experimental setup mass transfer experiments: bioreactor setup.

1-Octanol and phenol (analytical grade) were purchased from Sigma-Aldrich and used as delivered, see Table 1 in the supplementary data for properties. The 1-octanol was circulated through the membrane lumen and the solvent volume used was approximately 0.6 L. The membrane was integrated in the reactor and sterilized in the presence of demineralized water at 120°C. For all pertraction experiments, samples were taken in time from the aqueous and the 1-octanol phase to determine the phenol concentration. The phenol concentration was determined by using a UV/Vis spectrophotometer (Ultrospec 2100 pro, Amersham Biosciences) at 270 nm. To determine the amount of phenol in the solvent phase, 1 M NaOH was added to the samples (1 part of solvent with 2 parts of NaOH) and equilibrated overnight. After equilibration, the NaOH phase of the samples was taken and treated as described above.

Single-fiber system

Pertraction in a single-fiber system was carried out using Accurel PP V8/HF and S6/2 polypropylene hollow fiber microfiltration membranes obtained from Membrana, see also Figure 3 for a schematic representation of the experimental setup. An aqueous solution of phenol was pumped through the module and is in contact with the membrane at the shell side. The solvent (1-octanol or tributylphosphate, TBP) was led through the membrane lumen and was regenerated by leading the loaded solvent through a 1 M stripping solution of NaOH. In Table 1 the module specifications are

given. Phenol, 1-octanol, TBP and NaOH pellets used were purchased from Sigma-Aldrich. In Table 1 in the supplementary data the properties of the solvents and phenol used in this study are given. To obtain a higher driving force for pertraction, the solvent was regenerated continuously with 1 M NaOH. The volume of solvent and NaOH used was approximately 0.5 L. The linear modules contained one straight membrane fiber and were mounted in a horizontal direction. The module material is a stainless steel tube (for membrane type S6/2) or polyvinylchloride tube (for membrane type V8/HF) with an inner diameter of 32 and 9 mm, respectively. The membrane lumen contained solvent and the aqueous phenol solution was run co-current at the shell side. The experiments were executed in the laminar regime. The experiments were carried out at different water and solvent flow rates and at least in duplicate. The maximum allowable pressure drop (breakthrough pressure) over the membrane (0.3 bar) results in a maximum superficial solvent flow rate through the tube (v_s) of 0.05 $m.s^{-1}$. Samples were taken from the aqueous, solvent and sodium hydroxide phase in time and the phenol concentration was determined as described above.

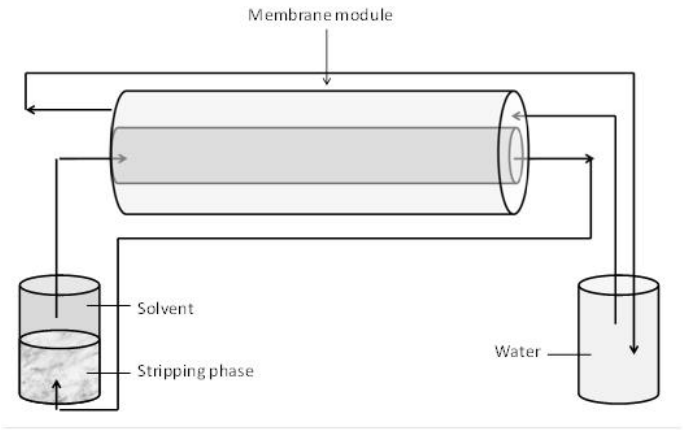

Figure 3. Experimental setup mass transfer experiments: single fiber setup.

Determination of the overall mass transfer coefficient

The overall mass transfer coefficient (K_{ov}, $m.s^{-1}$) can be obtained by using the experimental data combined with a simple model:

$$\frac{dc_{ph,b}}{dt} = \frac{K_{ov} \cdot A \cdot (c_{ph,b} - c_{ph,eq})}{V_{aq}} \quad (1)$$

With $\frac{dc_{ph,b}}{dt}$ the amount of phenol removed from the bulk (aqueous phase) in time ($mM.h^{-1}$), A the outer membrane area (m^2), V_{aq} the water volume (m^3), $c_{ph,b}$ the phenol concentration in de bulk at time t (mM) and $c_{ph,eq}$ the phenol concentration in the water phase at equilibrium (mM). The concentration of phenol in the aqueous phase at equilibrium ($c_{ph,eq}$) was assumed to be zero because

of the constant regeneration of the organic phase. The differential equation was integrated by ODE45 solver in Matlab. By adjustment of K_{ov}, the model was optimized to fit the experimental data.

Determination of the separate mass transfer coefficients

To evaluate the pertraction system, the overall mass transfer coefficient was determined. The K_{ov} can be divided into three partial mass transfer coefficients: the shell side (bulk) mass transfer coefficient (k_b, $m.s^{-1}$), the membrane mass transfer coefficient (k_m, $m.s^{-1}$) and the mass transfer coefficient in the lumen (stripping phase, k_s, $m.s^{-1}$). The solute diffuses first through the boundary layer in the reactor phase, through the membrane and finally through the boundary layer in the stripping phase.

The relation between the overall mass transfer coefficient and de separate mass transfer coefficients is given in Equation 2. From literature [8-17], relations for calculating the separate mass transfer coefficients were analyzed and calculated.

$$\frac{1}{K_{ov}} = \frac{1}{k_b} + \frac{d_{out}}{d_{lm}}\frac{1}{P}\frac{1}{k_m} + \frac{d_{out}}{d_{in}}\frac{1}{P}\frac{1}{k_s} \quad (2)$$

With d_{out} the membrane outer diameter (m), P the partition coefficient of phenol between the aqueous and solvent phase, d_{in} the membrane inner diameter (m) and d_{lm} the logarithmic mean diameter (m), defined as:

$$d_{lm} = \frac{d_{out} - d_{in}}{log d_{out} - log d_{in}} \quad (3)$$

The mass transfer through the membrane, k_m, was calculated according to Equation 4 using the properties given in Table 1 and Table 1 in the supplementary data. The membranes used are hydrophobic and the pores are filled with solvent. The mass transfer through the membrane is not dependent on the aqueous and solvent flow rate.

$$k_m = D_{ps}\frac{\varepsilon}{(d_{out} - d_{in})/_{2\tau}} \quad (4)$$

With D_{ps} the diffusion coefficient of phenol in solvent ($m^2.s^{-1}$) at 30 °C, determined by the Wilke Change method.

Table 1. Specifications of the single fiber membrane modules.

Parameter	**Unit**	**Accurel PP V8/HF**	**Accurel PP S6/2**
Length membrane (L)	m	0.375	0.415
Membrane outer diameter (d_{out})	m	$8.6*10^{-3}$	$2.7*10^{-3}$
Membrane inner diameter (d_{in})	m	$5.5*10^{-3}$	$1.8*10^{-3}$
Diameter module (d_{mod})	m	$3.2*10^{-2}$	$0.9*10^{-2}$
Wall thickness module (λ)	m	$3*10^{-3}$	$0.5*10^{-3}$
Area available for mass transfer	m^2	$1.0*10^{-2}$	$2.9*10^{-3}$

The mass transfer coefficient in the stripping phase (k_s) was given as a function of Reynolds (Re) and Schmidt (Sc) numbers. For laminar flows and Graetz (Gz) number greater than 4, Gabelman [13] states that the mass transfer coefficient in the tube can be calculated using:

$$Sh = \frac{k_s \cdot d_{in}}{D_{ps}} = 1.62 \cdot Gz^{\frac{1}{3}} \quad (5)$$

$$Gz = \frac{d_{in}}{L} \cdot Re \cdot Sc \quad (6)$$

Where Sh is the Sherwood number.

It should be noted that in some of the experiments (at very low Re) the Graetz number can reach values below 4, which may lead to an overestimation of k_s.

The prediction of the mass transfer coefficient in the reactor (k_b) is not as straightforward, because it is depending on the geometry of the system used. Several relations used for the determination of the Sherwood number are proposed by different authors. An overview was presented by Fernandes [16] and Gabelman [13]. The equations used for the prediction of the k_b are usually in the following form:

$$k_b = \frac{Sh \cdot D_{pw}}{\Delta z} \quad (7)$$

And:

$$Sh = a \cdot Re^x \cdot Sc^y \quad (8)$$

With Δz the thickness of the boundary layer (m) and D_{pw} the diffusion coefficient of phenol in water ($m^2.s^{-1}$). The factor *a* is a function of geometry. The coefficients *x* and *y* vary for different setups described by different authors, but are always smaller than unity. Equation 7 cannot be used in this

work to determine the mass transfer coefficient in the reactor due to the missing values for *a*, *x* and *y*. However, using Equation 2 and the experimentally determined overall mass transfer coefficient, k_b can be determined indirectly.

4.3 Results

Mass transfer coefficient in a bioreactor sytem

Experiments were executed to evaluate the overall mass transfer coefficient of phenol from the reactor through the membrane to the 1-octanol phase. In Table 2 the overall mass transfer coefficients determined in a fermentor are given. The membrane used in experiment 1 was not sterilized and the overall mass transfer coefficient was determined to be $4.4*10^{-6}$ $m.s^{-1}$. The membrane used in experiment 2 was sterilized at 120°C in the presence of demineralized water. The membrane in experiment 3 was not sterilized and the experiment was executed in the presence of fermentation medium without cells. The results showed that the sterilization of the membrane had a noticeable effect on the rate of phenol removal from the aqueous phase and on the overall mass transfer coefficient that was reduced to $2.9*10^{-6}$ $m.s^{-1}$. The heating of the membrane probably caused the pores to become smaller and the overall mass transfer coefficient to decrease. Although the melting temperature of polypropylene is approximately 160°C, at a temperature of 120°C significant creep starts to occur. The required force to obtain a given deformation for a given polymer (the tensile modulus E in Nm^{-2}) decreases with temperature [18] and in this case the membrane material is most likely in transition to a solid phase. Additional testing of the sterilized membrane indicated a change in pore size as compared to a non-sterillized membrane by a decrease in bubble size when immersed in water and connected to pressurized air (1.2-1.3 bar).

Table 2. Experimental results overall mass transfer coefficients in a bioreactor with 1-octanol using the V8/HF membrane at phenol production rate (r_p) 0.058 $mmol.L^{-1}.h^{-1}$ (1 and 2) and 0.17 $mmol.L^{-1}.h^{-1}$ (3), for a non-sterilized membrane (1), for a sterilized membrane (2) and for a non-sterilized membrane in the presence of medium components (3).

	r_p ($mmol.L^{-1}.h^{-1}$)	k_{ov} ($m.s^{-1}$)
1	0.058	$4.4*10^{-6}$
2	0.058	$2.9*10^{-6}$
3	0.17	$2.6*10^{-6}$

The overall mass transfer coefficient determined with aqueous phenol solutions in a fermentor using fermentation medium (experiment 3) was $2.6*10^{-6}$ $m.s^{-1}$. This membrane was not sterilized and it was expected that the overall mass transfer coefficient would be comparable to the one of experiment 1.

The results indicate that the medium components present in the reactor have an additional negative effect on the overall mass transfer.

Mass transfer coefficient in a single-fiber system

The overall mass transfer coefficient was determined experimentally for two membrane types (V8/HF and S6/2), using two solvents (1-octanol and TBP) and for varying Reynolds numbers in the solvent (lumen) and aqueous (shell) side of the membrane in single-fiber modules. In Table 3 the results of overall mass transfer coefficients with 1-octanol and TBP using the V8/HF and S6/2 single fiber modules at different water- and solvent Reynolds numbers (Re_w and Re_s, respectively) are given. The value of the mass transfer coefficient is in the order of $3*10^{-7}$ $m.s^{-1}$. It appears that, using 1-octanol and the V8/HF module, both the increase in Reynolds number in the lumen and at shell side did not increase the overall mass transfer coefficient to a large extent. These results indicate that the resistance for mass transfer is not in the bulk side or in the solvent side but in the membrane. To improve the overall mass transfer, the driving force should be increased. This can be achieved by for example choosing a solvent with a high partition coefficient (TBP) and by using a membrane with a smaller wall thickness (Accurel PP S6/2).

Additionally, in Table 3 the results obtained with TBP using membrane V8/HF and TBP using membrane S6/2 are given. Experiments with TBP and membrane V8/HF at different Reynolds numbers resulted in an average K_{ov} between 1.1 and $1.5*10^{-6}$ $m.s^{-1}$, an increase of a factor of approximately 5 as compared to the K_{ov} obtained with 1-octanol with the same membrane type. However, an increase in Reynolds number either in the lumen and at shell side still did not result in an improvement of K_{ov}. Using a thinner membrane type S6/2 with solvent TBP at varying Reynolds numbers results in an average K_{ov} between 2.4 and $3.3*10^{-6}$ $m.s^{-1}$. In this case, the effect of the Reynolds number at the shell side is more obvious. Increasing the Re_w from 5 to 10 gives an increase in K_{ov} of a factor 1.4. Overall, by using TBP and membrane S6/2, K_{ov} can be improved with a factor of 11 as compared to the overall mass transfer coefficient obtained with the V8/HF membrane and 1-octanol.

Additionally, the separate mass transfer coefficients k_m and k_s were determined theoretically using the equations mentioned above and the bulk mass transfer coefficient was determined using these separate mass transfer coefficients in combination with experimentally determined K_{ov} and equation 2. In Table 3 the results from the calculations are given (km, ks and kb-exp). Using the solvent 1-octanol and the V8/HF membrane, the limiting factor is the k_m, as expected. An increase in Re_S or Re_w does not change the K_{ov} to a large extent because the limitation is in the membrane. By changing the solvent the same trend is observed, although the overall mass transfer coefficient is higher due to the higher partition coefficient of TBP. Using TBP and membrane S6/2 shifts the mass transfer limitation from predominantly the membrane to the stripping phase and the bulk phase as well.

Table 3. Experimental results overall mass transfer coefficient (Kov, $m.s^{-1}$) and theoretical results membrane mass transfer coefficient (km, $m.s^{-1}$) and mass transfer coefficient in the strip phase (ks, $m.s^{-1}$) and corresponding experimental bulk mass transfer coefficient (kb-exp, $m.s^{-1}$) determined with equation 1 with 1-octanol and TBP and the V8/HF and S6/2 single fiber modules at different Reynolds numbers in the aqueous phase (Re_w) and solvent phase (Re_S).

		V8/HF	S6/2	V8/HF			S6/2		
		Kov	Kov	km	ks	kb-exp	km	ks	kb-exp
1-octanol									
$Re_w = 6$	$Re_S = 5$	2.6±0.5E-07	ND	2.4E-07	5.4E-07	2.8E-07	7.5E-06	1.1E-06	-
	$Re_S = 26$	3.0±0.3E-07	ND	2.4E-07	9.3E-07	3.2E-07	7.5E-06	1.9E-06	-
$Re_w = 34$	$Re_S = 26$	3.3±0.1E-07	ND	2.4E-07	9.3E-07	3.6E-07	7.5E-06	1.9E-06	-
	$Re_S = 35$	3.5±0.3E-07	ND	2.4E-07	1.0E-06	3.8E-07	7.5E-06	2.1E-06	-
TBP									
$Re_w = 5$	$Re_S = 17$	ND	24.0±5.0E-07	5.1E-07	6.4E-07	-	1.6E-05	1.3E-06	2.4E-06
	$Re_S = 34$	ND	26.0±3.0E-07	5.1E-07	8.0E-07	-	1.6E-05	1.6E-06	2.6E-06
$Re_w = 6$	$Re_S = 46$	11.0±3.0E-07	ND	5.1E-07	8.9E-07	1.1E-06	1.6E-05	1.8E-06	-
	$Re_S = 229$	11.0±1.0E-07	ND	5.1E-07	1.5E-06	1.1E-06	1.6E-05	3.1E-06	-
$Re_w = 10$	$Re_S = 17$	ND	32.8±4.0E-07	5.1E-07	6.4E-07	-	1.6E-05	1.3E-06	3.3E-06
$Re_w = 34$	$Re_S = 229$	11.0±1.0E-07	ND	5.1E-07	1.5E-06	1.1E-06	1.6E-05	3.1E-06	-
$Re_w = 69$	$Re_S = 46$	15.0±3.0E-07	ND	5.1E-07	8.9E-07	1.5E-06	1.6E-05	1.8E-06	-

ND: not determined

4.4 Strategy for module design for integrated pertraction

Mass transfer coefficient integrated membrane module design

Combining the experimental results of the bioreactor system and the single-fiber system, an overall mass transfer coefficient can be estimated to use for calculations for an integrated membrane module. The overall mass transfer coefficient determined in a bioreactor was $4.4*10^{-6}$ $m.s^{-1}$. Sterillization of the membrane decreases the K_{ov} with a factor 1.5 and the presence of medium components decreases the K_{ov} with a factor 1.7. Additionally, the overall mass transfer coefficient determined in a single fiber setup using membrane V8/HF and 1-octanol was approximately $3*10^{-7}$ $m.s^{-1}$. The use of the solvent TBP improves the K_{ov} with a factor 5 and the use of membrane type S6/2 improves the K_{ov} with a factor 2.2. The factors mentioned above are summarized in Table 4. Combining this data, an overall mass transfer coefficient can be estimated for a bioreactor system with membrane S6/2 and TBP: $4.4*10^{-6} * 5 * 2.2 * (1/1.5) * (1/1.7) = 1.9*10^{-5}$ $m.s^{-1}$.

Table 4. Factors to determine K_{ov} for different setups and solvents. The minus sign indicates a decrease in K_{ov} while the plus sign indicates an increase in K_{ov}.

Experimental setup	**Factor**
Fermentor V8/HF 1-octanol sterillization vs non-sterillization	-1,5
Fermentor V8/HF medium components	-1,7
Single V8/HF fiber TBP vs 1-octanol	+5,0
Single fiber S6/2 vs V8/HF (both with TBP)	+2,2

Concept design integrated membrane module

A concept design for an integrated membrane unit in a bioreactor was made, see Figure 4 for a schematic representation of the setup. The membrane unit consists of several membrane module rings in-series that are mounted parallel to each other. The modules are distributed in rings between the agitator and the wall of the fermentor. Assumptions made for the calculations are given in Table 3 in the supplementary data. To obtain optimum driving force for pertraction, the outgoing loaded solvent can be led through a stripping solution before recycled back to the module. A continuous mode of operation was assumed for the membrane contactor.

To determine the key parameters for this design, the required extraction rate (phenol removal rate, E in mol.h^{-1}) is the starting point. The number of membrane fibers (N_{fibers}) and the total membrane area (A, m^2) can be determined from the required phenol removal rate:

$$N_{fibers} = \frac{4 \cdot E}{c_{ph,s} \cdot v_s \cdot \pi \cdot d_{in}^2 \cdot 3600} \quad (9)$$

And:

$$A = N_{fibers} \cdot \pi \cdot d_{lm} \cdot L \quad (10)$$

With v_s the superficial solvent velocity (m.s^{-1}), which should be chosen such that the pressure drop over the membrane does not exceed the breakthrough pressure of either solvent or water.
Additionally, the specific membrane area (a_{sp}, $m^2.m^{-3}$) is determined:

$$a_{sp} = \frac{A}{V_{aq}} \quad (11)$$

The specific membrane area should not exceed the maximum specific membrane area ($a_{sp,max}$, $m^2.m^{-3}$), which is specified by the manufacturer of the membranes, see also membrane characteristics in Table 2 in the supplementary data.

Furthermore, the membrane extraction process should be able to concentrate the product, therefore the concentration factor should be larger than unity:

$$CF = \frac{c_{ph,s}^{x=L}}{c_{ph,b}} \quad (12)$$

With $c_{ph,s}^{x=L}$ the concentration of phenol in the solvent phase at length L in the membrane tube (mM).

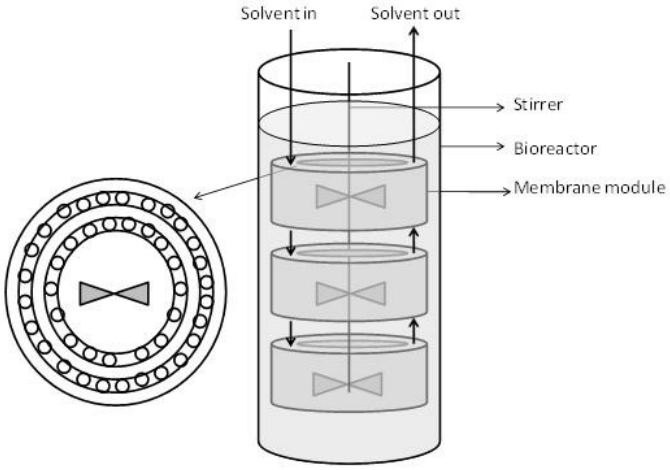

Figure 4. Schematic representation of the concept design for a pertraction module in a bioreactor. Right: front view of the reactor with the membrane module rings surrounding the stirring axis. Left: top view of the membrane module rings around the stirrer.

The maximum superficial solvent velocity, the membrane length and the pressure drop over the membrane influence the breakthrough pressure. The wetting fluid (solvent) should not permeate into the non-wetting phase (water) and vice-versa. When the solvent phase permeates into the water phase, this causes solvent losses and phase toxicity in the aqueous reactor phase in the presence of micro-organisms. The breakthrough of the water phase into the solvent phase causes impurity of the solvent stream and difficulties in further processing of the solvent. The immobilization of the liquid-liquid interface within the membrane surface usually requires a slight overpressure from the non-wetting liquid. However, if the pressure drop over the membrane exceeds 20-30 kPa, this may lead to displacement of the solvent phase and breakthrough of water is likely to occur. Considering the membrane length to be 1 m, the $\Delta P<0.3$ bar and the $CF>1$, the recommended maximum superficial solvent velocity is 0.05 $m.s^{-1}$ for membranes V8/HF and S6/2.

The maximum specific membrane area depends on the membrane outer diameter, the smaller the outer diameter, the higher the transfer area per volume. For membrane type V8/HF and S6/2 the maximum specific area is in the order of 61-166 $m^2.m^{-3}$ and 194-529 $m^2.m^{-3}$, respectively. Finally, the

maximum volume of required membrane module that is assumed to be acceptable is arbitrarily set at 25-30% of the fermentation volume.

In previous work [19], it has been determined that for a large scale annual phenol production of 10 kton, the required phenol removal rate in a fed-batch fermentation process (E) is 1389 $kg.h^{-1}$ (2949 $mol.h^{-1}$). In Table 5 the results are given for the required removal rate using membrane type S6/2, solvent TBP and an overall mass transfer coefficient of $2*10^{-5}$ $m.s^{-1}$. The membrane area required for pertraction (A) was determined to be $8.2*10^{3}$ m^2 per reactor. For the module design, the required area is increased with 20% (overdesign factor, ODF) to compensate for the assumption of a zero phenol concentration in the solvent feed. From the required membrane area the number of membrane fibers needed ($N_{fibers/ferm}$) was determined to be $5*10^{5}$. For a reactor with a volume of 456 m^3, the specific membrane area was determined to be 18 $m^2.m^{-3}$ which is lower as compared to the maximum specific membrane area. Additionally, the solvent flux required to obtain a product removal rate of 1389 $kg.h^{-1}$ was determined to be approximately $3.6*10^{4}$ $kg.h^{-1}$.

Using the assumptions described in Table 3 in the supplementary data, a rough dimensioning of the membrane modules was performed. Assuming membrane bundles of 1000 fibers per bundle and two membrane bundles in series, a total number of 583 parallel modules per fermentor is required. A design consisting of rings of modules with 7 rings in the horizontal direction and 6 rings in the vertical direction is proposed. The volume of one module was determined to be 0.02 m^3, which results in a total module volume of approximately 10 m^3, contributing to 2% of the total reactor volume, which is considered an acceptable value.

Considerations for improvement overall mass transfer coefficient in a bioreactor

Although first rough calculations show potential for an implemented membrane extraction unit, several factors for the possible consequences and bottlenecks of a combined separation and bioproduction process should be considered. The most important factor to address is the mass transfer in the reactor. Both separation and bioproduction processes rely to a large extent on the mass transfer of on the one hand the product from the aqueous broth to the solvent (separation) and on the other hand of the oxygen from the headspace into the reactor broth (biological growth and production). Additionally, the constant availability of substrate for the micro-organisms for growth and product formation is dependent on the mixing quality of the liquid. Obviously, the integration of an extra obstacle into the reactor can give rise to several bottlenecks, mainly caused by the altered mixing patterns. Below, several considerations are described on how to improve the mass transfer coefficients that both processes can run simultaneously in a (sub)optimum matter.

Table 5. Results for the integrated pertraction unit using membrane type S6/2.

Parameter	**Symbol**	**Value**	**Unit**
Fermentor liquid height	H	17.4	m
Fermentor diameter	D	5.8	m
Membrane area required per fermentor	A	$8.2*10^3$	m^2
Number of fibers required for extraction per fermentor	$N_{fibers/ferm}$	$5*10^5$	-
Number of parallel modules per fermentor	$N_{mod/ferm}$	583	-
Number of bundles in series per module	$N_{bundle/mod}$	2	-
Number of bundles per fermentor	$N_{bundles/ferm}$	1166	-
Spare bundles per fermentor	N_{spare}	24 (2%)	-
Space for rings (horizontal)	$S_{ring,H}$	1.13	m
Number of rings (horizontal)	$N_{ring,H}$	7	-
Space for rings (vertical)	$S_{ring,V}$	15.6	m
Number of rings (vertical)	$N_{ring,V}$	6	-

Several factors can be considered to improve the overall mass transfer coefficient for pertraction in the reactor. As described in Equations 7 and 8, the mass transfer coefficient in the bulk (k_b) is a function of Reynolds number (Re), Schmidt number (Sc) and geometry (a). Additionally, the diffusion coefficient of the product in the reactor phase and the thickness of the boundary layer is of importance. The Schmidt number is influenced by the properties of the product and the solvent (viscosity, density and diffusivity of the product). The Schmidt number cannot contribute to improvement of the bulk mass transfer coefficient because the liquid composition in the reactor cannot be altered. The mass transfer coefficient in the bulk is more difficult to improve by changing the reactor geometry because of the limited degrees of freedom. The available volume for a membrane unit in the reactor is small and the liquid flow pattern in the bulk is influenced by the presence of the membrane module and the flow rate at the membrane surface changes for different locations along the surface.

Fouling at the membrane surface and/or in the pores by medium components will increase the boundary layer thickness at the surface and, in addition, it may decrease the available contact area between the solvent and the fermentation broth. To decrease the thickness of this boundary layer, several strategies can be followed. One way to improve the shell-side mass transfer is to increase the turbulence at the membrane surface. However, in a bioreactor, this is not a preferred option because possibilities for changes in the process conditions in the reactor are limited. The liquid flow rate in the reactor is determined by the stirrer speed, which in turn is automated to control the dissolved oxygen level in the reactor. It is impossible to increase the stirrer speed to a very high value because the micro-organisms will be damaged by the high shear forces. Another option to decrease the thickness

of the boundary layer is to design the configuration of the integrated membrane unit such that the water flow rate across the membrane surface becomes more turbulent. Other authors describe, for example, rotating [20] or vibrating [21, 22] membrane modules, the addition of external forces such as ultrasound [23] or membrane surface modification [24-27] to reduce fouling at the membrane surface and to improve the flux in (pressure driven) (micro)filtration processes.

Additionally, computational fluid dynamics (CFD) modeling is recommended to study the flow pattern in the reactor with the integrated membrane module. The impact of the type of stirrer used for example can make a large impact on the liquid flow pattern in the reactor (important for mixing and oxygen transfer) and around the membrane module (important for optimal mass transfer for pertraction), see also Figure 5. Using for example a propeller stirrer with an axial downflow might improve oxygen transfer from the reactor headspace into the broth, depending on the stirrer location in the reactor but might decrease efficiency of the flux around the membrane fibers. A disk turbine stirrer with a radial flow might improve the flux around the membrane but might decrease the efficiency of oxygen transfer into the broth. A combination of stirrers can result in an acceptable flux for both oxygen transfer and flow around the modules. Additionally, the entrance point of the air can be shifted to the bottom of the reactor, using an air sparger below the lower stirrer. A better oxygen transfer can be obtained sparging as compared to when the air entrance is at the top of the reactor in the headspace. A disadvantage of air entering the reactor from the bottom is the possibility of foaming caused by damaged cells due to the high shear forces of the (bursting) bubbles to the micro-organisms.

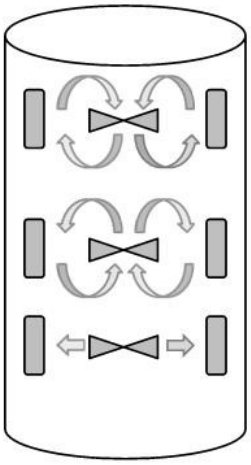

Figure 5. Schematic representation of flow patterns from different stirrers. Upper: propeller stirrer with axial down flow, middle: propeller stirrer with axial up flow and lower: disk turbine stirrer with radial flow.

In earlier work[1], experiments were described that were performed with the experimental setup as given in Figure 2. The standard stirrer configuration in the reactor consists of two rushton stirring blades. To increase mixing efficiency after membrane implementation, the lower stirring blade was replaced by a propeller with axial down flow. The air was fed to the headspace of the reactor. Measurements indicated that the oxygen transfer rate in the reactor did not change with this altered stirrer configuration in the presence of a membrane compared to the standard configuration with two rushton stirring blades in the absence of a membrane. In addition, after the implementation of the membrane in a bioreactor, a fed-batch fermentation was performed in the absence of solvent to study the effect of the membrane on the performance of the micro-organisms. The biomass growth and the phenol production of the recombinant *P. putida* S12 strain in presence of a membrane showed the same trend as the reference experiments where no membrane was present. This indicates that the test setup used has no negative effect on the performance of the micro-organisms. The effect of the stirrer configuration of the test setup on the overall mass transfer coefficient was not tested. A disk turbine stirrer will probably have a positive effect on the overall mass transfer coefficient as compared to a propeller stirrer due to the larger stirrer power output at equal rpm and the fluid flow in the radial direction will be higher decreasing the boundary layer for pertraction. However, very high liquid flows might damage the cells by high shear forces and possibly also the membrane fibers.

The results described in this paper show possibilities for an integrated membrane extraction process. To obtain a better understanding of the dynamics of the system and for an optimal design of the integrated membrane module system, additional experiments and models describing fluid dynamics in the combined systems are needed.

4.5 Conclusions

In this work, a strategy for the design of a membrane extraction module for implementation in a bioreactor is described by combining experimental and theoretical results. Overall mass transfer coefficients are determined experimentally using hollow fiber modules and rate limiting parameters are determined. The influence of membrane type, solvent and Reynolds number at the shell side (water) and lumen side (solvent) on the overall mass transfer coefficient of the model component phenol is investigated. The data is combined with data from pertraction experiments in a bioreactor to determine a strategy to design an integrated membrane module.

Experimental results show that by using the solvent tributylphosphate (TBP) with a higher partitioning coefficient and thinner hollow fiber membrane type S6/2 the K_{ov} can be improved with a factor 11 as compared to the overall mass transfer coefficient obtained with the V8/HF membrane and 1-octanol. The overall mass transfer coefficient in a model bioreactor was higher as compared to the single fiber setup due to the higher Reynolds number in a reactor (turbulent regime). Mass transfer in a reactor is negatively influenced by membrane sterilization and the presence of medium components.

Using overall mass transfer factors from experimental data, the K_{ov} for a membrane type S6/2 with the solvent TBP in a bioreactor was estimated to be $2*10^{-5}$ $m.s^{-1}$. To obtain a phenol removal rate of 1389 $kg.h^{-1}$, the required membrane area for pertraction for the model reactor with a volume of 456 m^3 was determined to be $8.2*10^3$ m^2 per reactor (18 $m^2.m^{-3}$ reactor volume). A membrane module design was proposed with multi-fiber bundles positioned in rings in the horizontal and the vertical direction. The volume requirement of the membrane modules in the reactor was determined to be 2% of the total reactor volume.

The integration of an extra obstacle into the reactor can give rise to several bottlenecks for both the separation process and the biological growth and production processes, mainly caused by the altered mixing pattern. To obtain a better understanding of the dynamics of the system and for an optimal design of the integrated membrane module system, additional experiments and models describing fluid dynamics are needed. Although additional information is needed, the calculations and considerations made in this paper clearly demonstrate possibilities for an integrated membrane extraction process.

References

1. Heerema, L.; Wierckx, N.; Roelands, M.; Hanemaaijer, J.H.; Goetheer, E.; Verdoes, D.; Keurentjes, J., In situ phenol removal from fed-batch fermentations of solvent tolerant Pseudomonas putida S12 by pertraction. Biochemical Engineering Journal 2011, 245-252.
2. Luong, J.H.T., Kinetics of ethanol inhibition in alcohol fermentation. Biotechnology and Bioengineering 1985, 280-285.
3. Mirata, M.A.; Heerd, D.; Schrader, J., Integrated bioprocess for the oxidation of limonene to perillic acid with Pseudomonas putida DSM 12264. Process Biochemistry 2009, 764-771.
4. Qureshi, N.; Maddox, I.S., Reduction in Butanol Inhibition by Perstraction: Utilization of Concentrated Lactose/Whey Permeate by Clostridium acetobutylicum to Enhance Butanol Fermentation Economics. Food and Bioproducts Processing 2005, 43-52.
5. Wierckx, N.J.P.; Ballerstedt, H.; De Bont, J.A.M.; Wery, J., Engineering of solvent-tolerant Pseudomonas putida S12 for bioproduction of phenol from glucose. Applied and environmental microbiology 2005, 8221-8227.
6. Husken, L.E.; Dalm, M.C.F.; Tramper, J.; Wery, J.; de Bont, J.A.M.; Beeftink, R., Integrated bioproduction and extraction of 3-methylcatechol. Journal of Biotechnology 2001, 11-19.
7. Klaassen, R.; Feron, P.H.M.; Jansen, A.E., Membrane contactors in industrial applications. Chemical Engineering Research and Design 2005, 234-246.
8. Asimakopoulou, A.G.; Karabelas, A.J., Mass transfer in liquid-liquid membrane-based extraction at small fiber packing fractions. Journal of Membrane Science 2006, 151-162.

9. Cichy, W.; Schlosser, S.; Szymanowski, J., Recovery of phenol with cyanex 923 in membrane extraction-stripping systems. Solvent extraction and ion exchange 2001, 905-923.
10. Gonzalez-Munoz, M.J.; Luque, S.; Alvarez, J.R.; Coca, J., Recovery of phenol from aqueous solutions using hollow fibre contactors. Journal of Membrane Science 2003, 181-193.
11. Cichy, W.; Szymanowski, J., Recovery of phenol from aqueous streams in hollow fiber modules. Environmental Science and Technology 2002, 2088-2093.
12. Cichy, W.; Schlosser, S.; Szymanowski, J., Extraction and pertraction of phenol through bulk liquid membranes. Journal of Chemical Technology and Biotechnology 2005, 189-197.
13. Gabelman, A.; Hwang, S.-T., Hollow fiber membrane contactors. Journal of Membrane Science 1999, 61-106.
14. Kertesz, R.; Schlosser, S., Design and simulation of two phase hollow fiber contactors for simultaneous membrane based solvent extraction and stripping of organic acids and bases. Separation and Purification Technology 2005, 275-287.
15. Kubisová, L.; Sabolová, E.; Schlosser, S.; Marták, J.; Kertész, R., Membrane based solvent extraction and stripping of a heterocyclic carboxylic acid in hollow fiber contactors. Desalination 2002, 205-211.
16. Fernandes, P.; Prazeres, D.M.; Cabral, J.M., Membrane-assisted extractive bioconversions. Advances in biochemical engineering/biotechnology 2003, 115-148.
17. Han, S.; Ferreira, F.C.; Livingston, A., Membrane aromatic recovery system (MARS) -- a new membrane process for the recovery of phenols from wastewaters. Journal of Membrane Science 2001, 219-233.
18. Mulder, M., Basic principles of membrane technology. Kluwer Academic Publishers: 1991.
19. Heerema, L.; Roelands, M.; Goetheer, E.; Verdoes, D.; Keurentjes, J., In-Situ Product Removal from Fermentations by Membrane Extraction: Conceptual Process Design and Economics. Industrial & Engineering Chemistry Research 2011, 9197-9208.
20. Bouzerar, R.; Ding, L.; Jaffrin, M.Y., Local permeate flux-shear-pressure relationships in a rotating disk microfiltration module: implications for global performance. Journal of Membrane Science 2000, 127-141.
21. Beier, S.P.; Jonsson, G., Separation of enzymes and yeast cells with a vibrating hollow fiber membrane module. Separation and Purification Technology 2007, 111-118.
22. Frappart, M.; Jaffrin, M.Y.; Ding, L.H.; Espina, V., Effect of vibration frequency and membrane shear rate on nanofiltration of diluted milk, using a vibratory dynamic filtration system. Separation and Purification Technology 2008, 212-221.
23. Kyllönen, H.M.; Pirkonen, P.; Nyström, M., Membrane filtration enhanced by ultrasound: a review. Desalination 2005, 319-335.
24. Hilal, N.; Kochkodan, V.; Al-Khatib, L.; Levadna, T., Surface modified polymeric membranes to reduce (bio)fouling: a microbiological study using E. coli. Desalination 2004, 293-300.

25. Hilal, N.; Al-Khatib, L.; Atkin, B.P.; Kochkodan, V.; Potapchenko, N., Photochemical modification of membrane surfaces for (bio)fouling reduction: a nano-scale study using AFM. Desalination 2003, 65-72.

26. Yu, H.-Y.; Hu, M.-X.; Xu, Z.-K.; Wang, J.-L.; Wang, S.-Y., Surface modification of polypropylene microporous membranes to improve their antifouling property in MBR: NH3 plasma treatment. Separation and Purification Technology 2005, 8-15.

27. Taniguchi, M.; Kilduff, J.E.; Belfort, G., Low fouling synthetic membranes by UV-assisted graft polymerization: monomer selection to mitigate fouling by natural organic matter. Journal of Membrane Science 2003, 59-70.

Supplementary data Chapter 4

Table 1. Properties of the solvents and phenol with P the partition coefficient of phenol between water and the solvent (experimentally determined, (mM phenol in solvent)/ (mM phenol in aqueous phase)), MW the molecular weight of the compound ($g.mol^{-1}$), ρ the density ($g.cm^{-3}$) and μ the viscosity (Pa.s).

Parmeter	**1-octanol**	**Tributylphosphate (TBP)**	**Phenol**
Formula	$C_8H_{18}O$	$(C_4H_9)_3PO_4$	C_6H_5OH
P	31.6	417	-
MW	130.2	266.3	94.1
ρ	0.82	0.97	1.07
μ	$6.16*10^{-3}$	$3.7*10^{-3}$	-

Table 2. Membrane characteristics (Accurel PP hydrophobic capillary membrane, Membrana).

Parameter	**Symbol**	**Unit**	**Type V8/2 HF**	**Type S6/2**
Pore size	d_p	mm	0.2	0.2
Internal fiber diameter	d_i	mm	5.5	1.8
Fiber wall thickness	tk	mm	1.55	0.45
Membrane tortuosity	τ	-	2.25	2.25
Membrane porosity	ε_m	-	0.8	0.8
Max. specific membrane area	a_{sp}	$m^2.m^{-3}$	61 – 166	194 – 529
Max. superficial solvent velocity	$v_{s,max}$ [a]	$m.s^{-1}$	0.05	0.05

[a] at CF>1 and ΔP<0.3 bar

Table 3. Assumptions made for the design of the integrated pertraction unit using membrane type S6/2.

Parameter	**Symbol**	**Value**	**Unit**
Overal mass transfer coefficient	K_{ov}	$2*10^{-5}$	$m.s^{-1}$
Required phenol removal rate	E	1389	$kg.h^{-1}$
Solvent superficial flowrate	v_s	0.01	$m.s^{-1}$
Overdesign factor	ODF	1.2	-
Reactor volume	V_R	456	m^3
Diameter fermentor	D	5.8	m
Reactor liquid height/diameter ratio	H/D	3	-
Diameter of agitator	D_A	0.3*D	m
Membrane length in bundle	L_M	1.135	m
Number of fibers per membrane bundle	N_{FB}	1000	-
Area per bundle	A_B	7.9	m^2
Max. specific membrane area	a_{sp}	194 – 529	$m^2.m^{-3}$
Max. specific volume occupancy modules	V_{sp}	25-30	%
Distance between fibers	df	0.0012	m
Module diameter	dm	0.10	m
Module length	L_{module}	2.4	m
Distance from the wall	dw	0.3	m
Distance from the agitator	ds	0.5	m
Distance between rings	dbr	0.09	m
Distance between rings in height	dr	0.47	m
Distance between modules in horizontal	dbm	0.05	m
Distance from bottom and top	de	0.87	m

Chapter 5

Micellar solutions of PEO-PPO-PEO block copolymers for in situ phenol removal from fermentation broth

This chapter was published as:
Heerema, L.; Cakali, D.; Roelands, M.; Goetheer, E.; Verdoes, D.; Keurentjes, J., Micellar solutions of PEO-PPO-PEO block copolymers for in situ phenol removal from fermentation broth. *Sep. Purif. Technol.* 2010, 73, 319-326.

Abstract

The applicability of aqueous solutions of Pluronics for the removal of the model product phenol was evaluated. Phenol is a chemical that can be produced by a recombinant strain of the solvent tolerant bacterium *Pseudomonas putida* S12. However, the growth of the micro-organisms and the phenol production is inhibited at low phenol concentrations. The solubility of phenol in aqueous solutions containing micelles of Pluronics F108, F68, P105, L64, P104, P85, P103 and L122 was determined. Additionally, the regeneration behavior of the Pluronics was studied by determining the solubility of phenol in Pluronic unimers after lowering the temperature of the solution to below critical micelle temperature. The phase behavior of Pluronics in the presence of fermentation broth and the growth of *P. putida* S12 in the presence of Pluronics were studied. Finally, the results obtained in this study were used to estimate the amount of cooling energy needed to obtain one gram of phenol using Pluronic P85 and P103.

5.1 Introduction

Over the past years, the "green" production of (fine) chemicals gained significant interest. Reasons for this are for example environmental issues (closed carbon cycles) and the search for renewable, bio-based fuels and chemicals. As a result, bio-catalytic processes are being developed for the sustainable production of chemicals. Often genetically modified organisms such as yeast, bacteria or fungi are used. High production rates can be achieved as long as toxic or inhibitory effects of the chemicals on the growth and production processes can be avoided. Therefore, it is important that product concentrations in the production medium remain below a certain level. To maintain a low product concentration in the reactor, in-situ product removal (ISPR) can be applied. ISPR can be described as a separation method that is integrated into the (bio)reactor to selectively remove a certain component from the broth. ISPR can have many advantages such as reduced reactor volume, easier downstream processing and reduced substrate costs [1]. A well-described example of an ISPR technique is membrane extraction (pertraction) [2].

Continuous membrane extraction provides a large and stable contacting surface area between the aqueous fermentation broth and the solvent without the formation of an emulsion and is therefore useful for ISPR [3-7]. The solvents selected in this study are polymeric micelles solubilized in water. The micelles are formed of poly(ethylene oxide)-poly(propylene oxide) (PEO-PPO-PEO) block copolymers, commercially known as Pluronics. Pluronics are water-soluble, non-ionic macromolecular surface active agents. They are environmentally mild and hardly toxic to micro-organisms. The molecular characteristics of Pluronics can vary according to the PPO/PEO ratio and molecular weight [8].

The core of a micelle forms a hydrophobic micro-environment, which can be used for removal of dissolved organics like phenol [9-11], p-xylene, n-butyl acetate and 1-butanol [12], naphthalene [13], 1-naphtol [9] and for water-insoluble hydrophobic compounds [8].

Temperature dependent micellization is the key factor for solvent regeneration. When decreasing the solution temperature below the critical micelle temperature (CMT), the micelles will disintegrate and the desired product is released. An example of a process based on membrane extraction with micellar solvents is given in Figure 1. The Pluronics are separated from the bioreactor by a membrane permeable for water and the product of interest but not for the copolymers. Continuous circulation of a micellar solution through a membrane will result in a continuous removal of the product and the concentration in the reactor phase can be maintained below the inhibition level. The micellar solution containing the extracted product is regenerated by cooling and the product can be purified from the unimeric solution by for example membrane filtration.

For the use in a bioprocess the Pluronics should meet certain requirements. The first criterion is that the Pluronic micelles should have a solubility ratio that is comparable to the partition coefficient of the product in conventional organic solvents and a reasonable capacity for the product of interest. The second criterion concerns the critical micelle concentration (CMC) and the CMT. A bioreactor (fermentor) runs at a fixed temperature, usually around 30°C. To be able to extract the product, the concentration of Pluronics should be high enough to form micelles at this temperature. In other words, the concentration should be above CMC at fermentation temperature. For the regeneration of the Pluronics it is important that the micelles can be broken up in unimers by means of a relatively small decrease of the temperature. Preferably, the regeneration temperature is in the range of 10-20°C. The third criterion is the mutual compatibility of Pluronics and the fermentation broth. The broth contains several components like sugar, minerals, salts and micro-organisms. Pluronics can be toxic and/or inhibiting on the growth and production of the micro-organisms. Vice versa, the components present in the broth can have an effect on the (phase) behavior of the Pluronics.

In this paper, the model component phenol is used to illustrate the applicability of Pluronic micelles as novel solvent for fermentation processes. Phenol can be produced by the solvent tolerant micro-organism *Pseudomonas putida* S12 [14] and is inhibiting at concentrations around 2 mM. In this model process, 2 mM is the maximum allowable concentration of product in the aqueous reactor phase and the phenol removal with Pluronic micelles should be such that this concentration in the reactor is not exceeded. The extraction of phenol from aqueous solutions with several Pluronics will be evaluated. In addition, the influence of Pluronics on the growth of the micro-organisms, the influence of fermentation medium on the CMC and the energy needed for regeneration of the solvent will be evaluated.

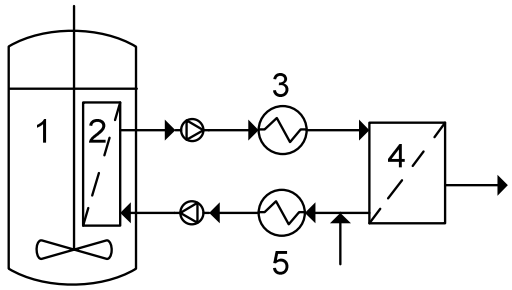

Figure 1. An example of a continuous membrane extraction process using Pluronic micelles. The bioreactor (left) contains components such as micro-organisms and the desired product (1). The reactor contains an integrated membrane unit (2). An aqueous solution of Pluronic micelles is circulated through the integrated membrane unit. The micellar solvent containing the extracted product is cooled to below CMT (3) and the product is separated from the Pluronics by for example a membrane unit (4). The Pluronics are heated to above CMT (5) and recycled to the integrated membrane unit after water is added to compensate for the loss in the product stream.

5.2 Experimental

Chemicals

All reagents were used as received without further purification. Pluronic L64, Synperonic P94, Synperonic P105, Synperonic L122 and Pluronic F68 10 wt% solution were purchased from Sigma-Aldrich. Pluronic P84, Pluronic P103, Pluronic P104 and Pluronic F108 were donated by BASF (Antwerp). The physical properties of the Pluronics used in this study are given in Table 1. Analytical grade phenol was purchased from Sigma-Aldrich. A water-insoluble hydrophobic dye, 1-(2-pyridylazo)-2-naphthol (PAN), was used as a spectroscopic probe to determine CMC and CMT of the Pluronics. The PAN dye was supplied by Sigma Aldrich. The water used in this study was demineralized water.

Table 1. Properties of the selected Pluronics. A: molecular weight, B: % w/w PEO, C: cloud point (°C) of 1 wt% solution, D: molecular weight of PPO block, E: ratio PPO/PEO, F: specific gravity, G: viscosity (cps) for L(25°C), P(70°C),F(95°C), H: hydrophilic-lypophilic balance. Data were taken from Alexandridis et al., 1995.

	Formula	**A**	**B**	**C**	**D**	**E**
F108	EO132PO50EO132	14600	80	>100	0.19	>24
F68	EO76PO29EO76	8400	80	>100	0.19	>24
P105	EO37PO56EO37	6500	50	91	0.76	12-18
L64	EO13PO30EO13	2900	40	58	1.15	12-18
P104	EO27PO61EO27	5900	40	81	1.13	12-18
P85	EO26PO40EO26	4600	50	85	0.77	12-18
P103	EO17PO60EO17	4950	30	86	1.76	7-12
L122	EO11PO69EO11	5000	20	19	3.14	1-7

Membranes

Regenerated cellulose (RC) ultrafiltration (UF) disc membranes, with a Molecular Weight Cut Off (MWCO) of 1, 3, 10 and 30 kD and a membrane area of 13.4 cm^2 were supplied by Millipore. Ultrafree-MC RC microcentrifuge filters with a MWCO 5 kD and an area of 0.2 cm^2 were supplied by Sigma Aldrich. For the disk membranes, filtration was carried out by either applying a transmembrane

pressure (TMP) of 4 bar to reach a filtrate flux of approximately 0.003 $ml.cm^{-2}.min^{-1}$. For the centrifuge filters, a centrifugal field, with a maximum g force rate of 5000 g was applied. RC Spectra/Por Dialysis Membranes with a MWCO of 12-14 kD, a diameter of 16 mm, a volume to diameter ratio of 2.0 ml/cm and a wall thickness of 45 µm were used as tubular dialysis membranes. The membrane area used for these experiments was approximately 110 cm^2.

Pluronics and Pseudomonas putida fermentations

In shake flask fermentations containing growth medium, cells of phenol producing recombinant *P. putida* S12 were grown at 30°C in the presence of 5 wt% Pluronics F108, P104 and P85 and 5, 10 and 15 wt% F108. The cell density in the fermentation broth was monitored in time with a Unicam Helios spectrophotometer at 600 nm. Control shake flasks were incubated to compare normal biomass growth to growth in the presence of Pluronics and all experiments were executed in duplicate.

Determination of the solubility ratio and phenol uptake by Pluronics

Stock solutions were prepared from the eight selected Pluronics (F108, F68, P105, L64, P104, P85, P103 and L122) and phenol in water. The stock solutions of Pluronics and phenol were mixed to give a final solution containing 2.5 wt% Pluronics and 3.5 mM phenol. The solutions were equilibrated at 30°C, 21°C and 10°C. After equilibration, the samples were filtered over either a 3 kD disc membrane or a 5 kD microcentrifuge filter at the chosen temperature (30°C, 21°C or 10°C). The phenol concentration in the filtrate was determined using an UV/Vis spectrophotometer (Ultrospec 2100 pro, Amersham Biosciences) at 270 nm. Another set of experiments was executed with 3.5 mM phenol in presence of different concentrations of Pluronic P103 (0 - 10 wt%) at 30°C. Additional experiments were done with solutions containing P103 and phenol, equilibrated in presence of dialysis membrane tubes (Spectra/Por Dialysis Membranes, see 2.2). These experiments were executed to rule out the effects of pressure (disc membrane) or centrifugal forces (microcentrifuge filter) on the extraction behavior of the Pluronics. The membrane tubes, containing the Pluronic solution, were sealed and incubated in demi-water containing phenol at 10°C and 30°C. After equilibration, the solution outside the membrane tube was sampled and the phenol concentration was measured as mentioned before. Figure 3 illustrates the two Pluronic states that were tested in abovementioned experiments: micelles at 30°C and unimers at 10°C. The solutions prepared at room temperature consist of a mixture of micelles and unimers. Additionally, the phenol concentration in the aqueous phase ($C_{p,aq}$) and in the pluronic phase ($C_{p,pl}$) are indicated in Figure 3. $C_{p,aq}$ was measured and $C_{p,pl}$ was calculated, see below.

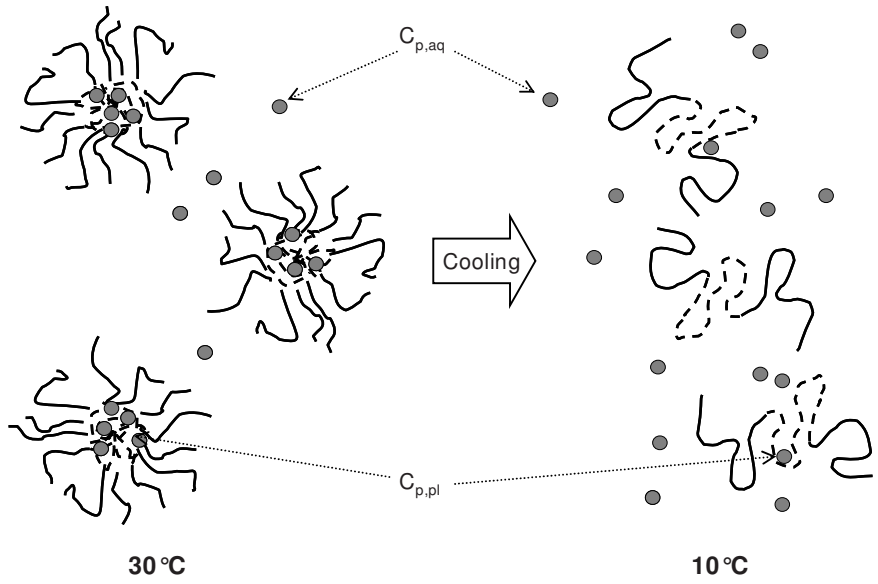

Figure 2. Extraction with Pluronic micelles at 30°C (left) and regeneration of the pluronics by unimerization at 10°C (right). The phenol concentrations in the aqueous and in the pluronic phases are illustrated ($C_{p,aq}$ and $C_{p,pl}$) where $C_{p,pl}$ is either the concentration of phenol in the micelles at 30°C or adsorbed to the unimers at 10°C. The phenol concentration in the total stripping phase ($C_{p,strip}$, mM) is the total amount of phenol present in the strip phase (aqueous phase and pluronic phase) divided by the total volume of the stripping phase.

The solubility ratio of phenol in the Pluronics (S) was determined for temperatures above and below the CMT where the Pluronics are in the form of micelles and unimers, respectively. The solubility ratio is defined as the ratio of the concentration of phenol in the stripping phase ($C_{p,strip}$, mM) to the concentration of phenol in the aqueous phase ($C_{p,aq}$, mM):

$$S = \frac{C_{p,strip}}{C_{p,aq}} \quad (1)$$

It was assumed that the retentate only contains Pluronics and phenol and that the retention of the Pluronic micelles and unimers is 100%. The phenol concentration in the aqueous phase is assumed to be equal to the phenol concentration in the filtrate. The concentration phenol in the Pluronic phase (micelles or unimers) ($C_{p,pl}$, mM) is determined from the difference between the initial phenol concentration in the aqueous phase ($C_{p,in}$, mM) and the concentration of phenol in the filtrate ($C_{p,f}$, mM):

$$C_{p,pl} = \frac{C_{p,in} - C_{p,f} \cdot (1-\phi)}{\phi} \quad (2)$$

With ϕ the weight percentage of Pluronic in the stripping solution, defined as the ratio of the volume of Pluronic (V_{pl}, L) to the total volume of the solution (V_{tot}, L). It was assumed that the density of Pluronic is equal to the density of water:

$$\phi = \frac{V_{pl}}{V_{tot}} \quad (3)$$

The concentration of phenol in the stripping phase will become:

$$C_{p,strip} = C_{p,pl} \cdot \phi \quad (4)$$

The uptake of phenol by the Pluronic micelles (U, g phenol/g Pluronic) is defined as the ratio of the amount of phenol removed by Pluronics to the amount of Pluronics used:

$$U = \frac{M_{p\_removed}}{M_{pl}} \quad (5)$$

Where $M_{p\_removed}$ is the mass of phenol removed by the Pluronic (g of phenol) and M_{pl} the mass of Pluronic used in the experiments (g of Pluronic).

Additional experiments were executed to study the effect of the phenol concentration on the phase behavior of Pluronic solutions. Solutions of 2.5 wt% Pluronic P103 were incubated at 30°C in the presence of different concentrations of phenol (3.5 - 35 mM). All mixtures were mixed and settled overnight and the solubility ratio and capacity were determined as described above.

Critical micelle concentration and critical micelle temperature

To determine the CMC and CMT, the water insoluble dye PAN was dissolved in acetone and absorbed in a strip of filter paper. The acetone was evaporated from the filter paper and the paper was placed into a flask that contains a certain amount of water. At specified time intervals, 1 mL of Pluronic solution with a known concentration was added to the mixed flask. Samples were taken before the addition of each portion of the Pluronic solution and the absorption was measured at 470 nm in a UV/VIS spectrophotometer (Ultrospec 2100 pro, Amersham Biosciences). The experiment was continued until the majority of the dye was solubilized in the micelles. The absorption data were plotted as a function of the logarithm of the Pluronic concentration. Two straight lines were drawn

before and after the first inflection point of the absorbance versus concentration curve. The intercept of the two lines represents the CMC value of the Pluronic at that temperature.

To evaluate the CMC of Pluronics in the presence of the complex growth medium used for fermentations, experiments were executed with Pluronics, aqueous phenol solutions and fermentation medium. The exact composition of the fermentation medium was described by reference [14]. The experiments were executed as described above with fermentation medium, Pluronics P103 and P104 and at a temperature of 30°C. For comparison, reference experiments with demineralized water and Pluronics were executed in parallel.

Energy requirement for regeneration of the micellar solvent

To evaluate the potential of Pluronics as alternative solvent, calculations for the phenol extraction with Pluronics P103 and P85 and subsequent regeneration of the solvent were executed. On the one hand it is important that a high amount of phenol can be removed (ΔM, g), this is determined by the solubility ratio (S). On the other hand the cooling energy needed for solvent regeneration (ΔQ, kJ), determined by the CMC and CMT, plays an important role. For the evaluation, the amount of energy needed for the removal of 1 gram of phenol ($\Delta Q.\Delta M^{-1}$) will be determined for P103 and P85.

The calculations were performed assuming a maximum phenol concentration in a reactor ($c_{ph,b}$) of 2 mM (0.19 $g.L^{-1}$) and 1 L (V_{strip}) Pluronic solutions at 30°C. A schematic representation of the extraction and regeneration process as given in Figure 1 is illustrated in Figure 3. For the calculations, the reactor- and stripping phase are separated by an UF dialysis membrane that is permeable for phenol but not for Pluronics. Phenol diffuses over the membrane and is extracted into the micelles (extraction). After extraction, the stripping solution is cooled down to below CMT and phenol will be released (regeneration). To separate the phenol from the unimers, a second UF dialysis membrane is placed between the stripping solution and 1 L clean water. The phenol diffuses to the water phase and the unimers will not pass the membrane.

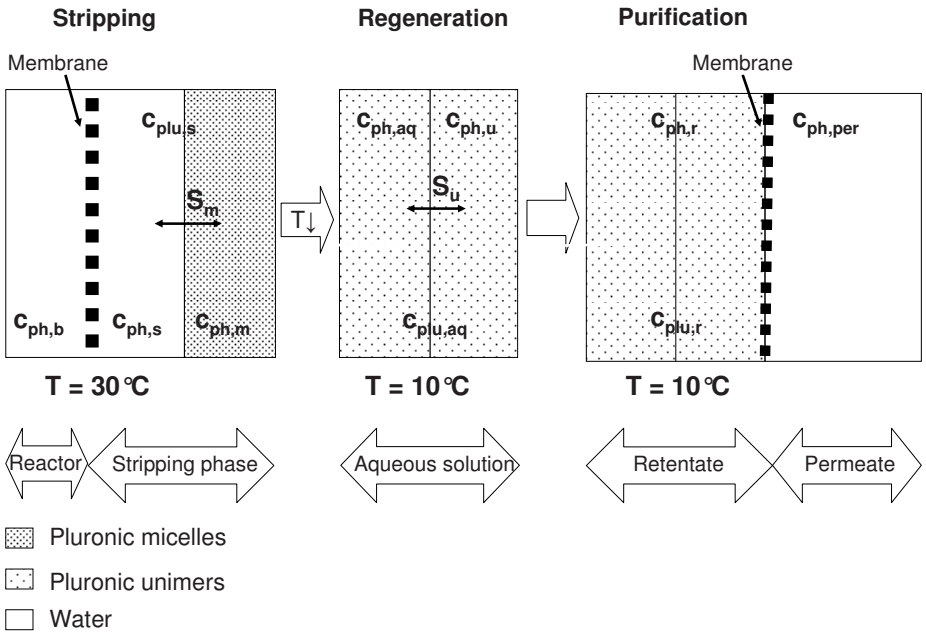

Figure 3. Schematic representation of the process used for the calculations. The process is divided into three parts: stripping, regeneration and purification. Explanation of the terms in the Figure: $c_{ph,b}$ – concentration of phenol in the reactor (bulk) phase ($g.L^{-1}$), $c_{ph,s}$ – concentration of phenol in the stripping phase ($g.L^{-1}$), $c_{ph,m}$ – concentration of phenol in the micellar phase ($g.L^{-1}$), $c_{plu,s}$ – the concentration of Pluronic in the stripping phase (wt%) is equal to the Pluronic concentration in the unimer solution ($c_{plu,aq}$) and to the concentration of Pluronic in the retentate ($c_{plu,r}$), S_m – solubility ratio of phenol in the micellar phase, T – Temperature (°C), $c_{ph,aq}$ – concentration of phenol in the water phase in the unimeric solution ($g.L^{-1}$), $c_{ph,u}$ – concentration of phenol in the Pluronic unimers ($g.L^{-1}$), S_u – solubility ratio of phenol in the Pluronic unimer phase, $c_{ph,r}$ – concentration of phenol in the retentate ($g.L^{-1}$) and $c_{ph,per}$ – concentration of phenol in the permeate.

The solubility ratio was determined experimentally for 2.5 wt% solutions using dead-end filtration or centrifugal filtration (see 2.4). Additionally, the solubility ratio was determined for P103 in a dialysis system. The solubility ratios used for the calculations were corrected for the method used and for the concentration of Pluronics used. In this case, the dialysis values are used for both the micellar and unimeric solutions and a Pluronic concentration of 20 wt%.

The concentration of phenol in the total stripping (micellar) phase ($c_{ph,s}$, $g.L^{-1}$) was determined by multiplying the phenol concentration in the reactor phase with the solubility ratio of phenol in the micellar solution (S_m):

$$c_{ph,s} = c_{ph,b} \cdot S_m \quad (6)$$

After cooling the solution for regeneration, the phenol is removed by dialysis with 1 L water ($V_{dialysis}$). Assuming the volumes at both sides of the membrane will remain constant, the diffusion of phenol from the retentate to the permeate is considered. The total amount of phenol (g) in the stripping phase is equal to the sum of the amount of phenol in the dialysis phase (permeate) and the amount of phenol in the retentate. The amount of phenol in the permeate (ΔM) in equilibrium can be determined by using the following mass balance:

$$c_{ph,s} \cdot V_{strip} = V_{dialysis} \cdot c_{ph} + V_{strip} \cdot S_u \cdot c_{ph} \quad (7)$$

With c_{ph} the total phenol concentration in the regeneration solution ($g.L^{-1}$).

And:

$$\Delta M = c_{ph} \cdot V_{dialysis} \quad (8)$$

Finally, the cooling energy needed (ΔQ, kJ) to cool down the stripping solution from 30 °C to below CMT was determined:

$$\Delta Q = m \cdot c_p \cdot \Delta T \quad (9)$$

Where m is the mass of the solvent (g), c_p the specific heat capacity ($J.g^{-1}.K^{-1}$) which is 4.2 for water and assumed 2.3 for Pluronic. ΔT corresponds to the temperature difference between the stripping solution (30°C) and the regeneration temperature (°C).

5.3 Results and discussion

Pluronics and *Pseudomonas putida* fermentations

In Figures 4 and 5 the growth of *Pseudomonas putida* S12 in the presence of different types of Pluronics and at different concentrations is illustrated. For Pluronic F108, the differences in cell growth for 5 wt% F108 in both figures are caused by the differences in the initial amount of cells in the experiments which was lower for the experiment shown in Figure 5: an OD600 of 0.06 compared to an OD600 of 0.3. The results show that Pluronics in general do not seem to affect the growth of the micro-organisms negatively. Figures 4 and 5 seem to indicate that higher biomass concentrations are

reached in the presence of Pluronics. A first explanation for this phenomenon is suppressed product inhibition due to the extraction of phenol into the micelles. It is expected that the micro-organisms produce phenol during growth because a genetically modified and phenol-producing strain of *P. putida* S12 was used in these experiments. Alternative explanations for the higher biomass concentration in the presence of Pluronics are the protection of the cells by the Pluronics or consumption of the Pluronics by the micro-organisms. Reference [8] describes the use of Pluronics as a protection agent for micro-organisms, insect- and mammalian cells that are very sensitive to shear . In a bioreactor, high shear forces can be exhibited on the cells by for instance stirring or air sparging. The addition of Pluronics to the culture medium caused the cells to be less vulnerable to the shear forces in the reactor, which resulted in a better cell growth.

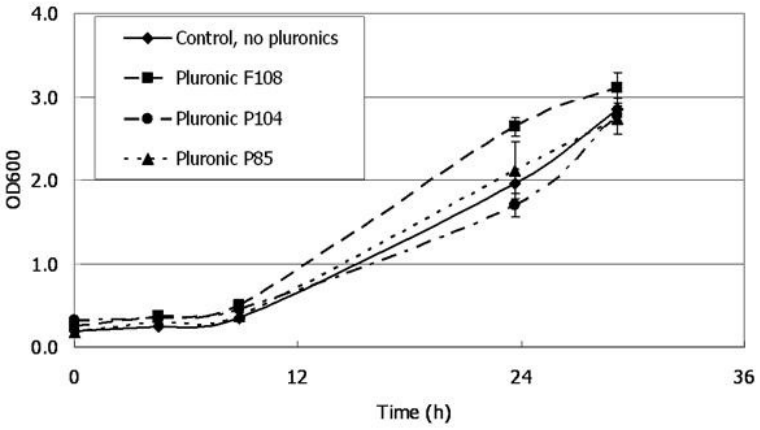

Figure 4. Growth of Pseudomonas putida S12 in presence of 5 wt% Pluronics F108, P104 and P103.

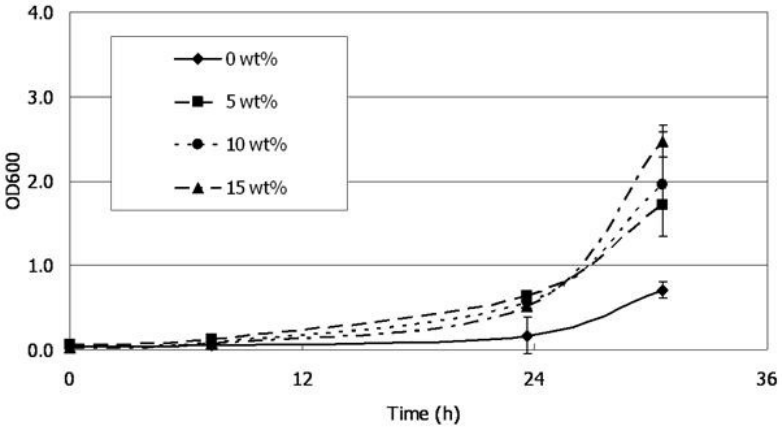

Figure 5. Growth of *Pseudomonas putida* S12 in presence of 0, 5, 10 and 15 wt% Pluronic F108.

Screening of Pluronics for the removal of phenol from aqueous solutions

In Table 2 an overview of the measured solubility ratios for 3.5 mM phenol in solutions containing 2.5 wt% Pluronics is given. At 30°C the solubility ratios vary from 0.58 to 1.75. The highest values for the solubility ratio were measured for Pluronics P103 and L122, which thus seem to be suited best for the extraction of phenol from aqueous solutions at 30°C, the temperature at which fermentations are typically executed. The values in Table 2 are corrected for the total stripping solution with the weight percentage of Pluronic present. It must be noted that the solubility of phenol in the micellar phase is much higher. The solubility of phenol in the total strip solution containing 2.5 wt% P103 micelles at 30°C for example was determined to be 1.70. According to Equation 4, the solubility of phenol in the P103 micelles is calculated to be 68.

Pluronics P103 and L122 have a relatively high PEO/PPO ratio compared to the other investigated Pluronics. Our measurements reveal that all Pluronics with a PEO/PPO ratio lower than 1 (P85, F108, F68 and P105) have a relatively low solubility ratio at 30°C. The low solubility ratio could be caused by the fact that these Pluronics have a CMT value higher than 30°C at the concentration used. If the Pluronics are present in a concentration below CMC at the temperatures used, no micelles are present in solution and the solubility ratio for phenol remains low. These Pluronics will show a higher solubility ratio for phenol when the concentration in the solution is increased. For illustration, Table 3 gives the (estimated) CMC values for all pluronics except Pluronic L122 at 30°C taken from reference [15]. Pluronics F68 and L64 show CMC values comparable to or higher than the concentration used for the experiments. Furthermore, Pluronics L64 with a PEO/PPO ratio of 1.15 has a relatively low solubility ratio, whereas Pluronic P104 has a higher solubility ratio but a comparable PEO/PPO ratio of 1.13. In summary it can be stated that the PEO/PPO ratio and CMC are important, but not the only factors explaining the affinity of a certain Pluronic for phenol at the conditions used.

Table 2 shows that the solubility ratios decrease with decreasing temperature. At room temperature (21°C) the relative decrease of the solubility ratio depends on the type of Pluronic, but at 10°C the solubility ratios are comparable for all Pluronics. In the temperature range from 30 to 10°C the solutions of the investigated Pluronics switch from the micellar form into the unimeric form. The unimers have a lower affinity for phenol than the micelles, which explains the comparable and low solubility ratios at 10°C. Another possibility to switch between micelles and unimers is to decrease the concentration of the Pluronic solution at a fixed temperature.

Pluronic L122 has a high affinity for phenol at 30°C, but it shows a different behavior compared to the other Pluronics at lower temperatures. The decrease in temperature leads to emulsion formation in the Pluronic L122 solution. The temperature of the separation of the copolymer phase from water is

denoted as the cloud point. In general Pluronics with a low PEO content have low cloud points, whereas Pluronics with a high PEO content could have cloud points above 100°C. Due to its relatively low PEO content (20 wt%) it can be expected that the cloud point for L122 should be low. Alexandridis reported that a 1 wt% L122 solution has a cloud point around 19°C [8], see also Table 1. This value was also given by BASF. At higher concentrations, the cloud point usually decreases a few degrees. BASF reported a cloud point of 13°C for a 10 wt% L122 solution. In numerous articles [8, 12, 16-24] it has been mentioned that additives like salts or alcohols can affect the phase behavior as well as the cloud point of Pluronics. For these reasons L122 cannot be regenerated by a simple temperature switch and is therefore not suited for the *in-situ* recovery of phenol from a fermentation process.

It must be noted that the methods used here for determining solubility ratios either use dead-end filtration or centrifugal filtration. Both methods gave similar results with respect to the final value of the solubility ratios. For the Pluronic with the highest solubility ratio, P103, additional experiments were performed in dialysis tubes to rule out the effects of pressure (disc membrane) or centrifugal forces (microcentrifuge filter) on the extraction behavior. From the measured partition coefficients with Pluronic P103, the average solubility ratios determined in the dialysis experiments were 1.13 at 30°C and 0.18 at 10°C. These values are lower than those determined by the two other methods (1.75 and 0.35 at 30 and 10°C respectively). A possible explanation is the occurrence of concentration polarization on the membrane surface or a significant change in Pluronic concentration at the retentate side when adding an external force such as pressure or centrifugal force. The Pluronics layer on the membrane will reduce the amount of phenol going through the filter and consequently the corresponding solubility ratio will be higher.

To evaluate the potential of Pluronic micelles as a solvent for phenol, the measured solubility ratio of phenol in the micelles for the Pluronic solutions at fermentation temperature was compared to the partition coefficient of phenol in organic solvents like 1-octanol [14]. The solubility ratios are lower compared to the partition coefficients of 1-octanol. The average partition coefficient for phenol in 1-octanol is 30. Pluronic solutions, however, show more favorable regeneration behavior as compared to conventional organic solvents. The regeneration of conventional solvents is usually accomplished by distillation processes. Distillation is not the preferred option for regeneration of 1-octanol due to the presence of multiple azeotropes in the mixture (water-octanol, phenol-water, phenol-octanol, data obtained from Dechema). This leads to large column(s), a high energy consumption and large reflux ratio(s). To strip phenol from 1-octanol, usually a basic solution is used to increase the pH and convert phenol into phenolate, which has a low partition coefficient in 1-octanol. However, this leads to additional salt streams in the process. The fact that phenol can be released from the Pluronic micelles by a simple and small temperature decrease is an important advantage of the use of this alternative type of solvent.

Table 2. Solubility ratios of phenol at 30, 21 and 10°C using different Pluronics. Pluronic concentration was 2.5 wt% and phenol concentration 3.5 mM for all experiments.

	30°C	**21°C**	**10°C**
F108	0.58	0.46	0.34
F68	0.93	0.30	0.38
L64	0.70	0.57	0.29
P85	0.94	0.81	0.34
P104	1.29	1.24	0.35
P105	0.90	0.59	0.27
P103	1.71	1.47	0.36
L122	1.74	-	-

A Pluronic P103 solution of 2.5 wt% was contacted with phenol in concentrations ranging from 3.5 to 35 mM at 30°C. Figure 6 reveals that the solubility ratio for phenol of the 2.5 wt% P103 solution did not change significantly for the investigated phenol concentrations and that the phenol uptake by P103 increased linearly with increasing phenol concentrations. Kandori et al. [25] studied the solubility of phenol in polyethoxylated micelles, observing a remarkable difference in interaction of the phenol with cationic and nonionic surfactants that could be explained by the hydrophilic structures of these surfactants. The longer ethylene oxide chains in nonionic surfactants offered more binding sites for phenol than the hydrophilic charged heads of cationic surfactants. Since Pluronics are nonionic surfactants with variable hydrophilic PEO domains, a high amount of phenol can be extracted and saturation was not reached in our experiments.

Table 3. Critical micelle concentration of the Pluronics at 30°C, taken from Alexandridis et al, 1994.

	CMC at 30°C
F108	~ 1.0 wt%
F68	10 - 15 wt%
L64	1.0 - 2.5 wt%
P85	~ 1.0 wt%
P104	0.025-0.05 wt%
P105	0.025 wt%
P103	~ 0.01 wt%
L122	-

Solubility ratios and phenol uptake were also determined using aqueous solutions with concentrations up to 510 mM using microcentrifuge filters. The trend of constant solubility ratio and increasing phenol uptake remained the same, but a change in phase behavior was observed. At phenol concentrations above 40 mM the solution became turbid, which indicates the occurrence of a cloud point. Increasing the concentration of phenol above 210 mM resulted in another phase separation. A turbid upper layer that had a milky-color (whiter at increasing concentrations) and a small and clear lower layer appeared which became larger in volume when the phenol concentration increased to 510 mM. The phenol concentration in the upper phase was determined to be lower than the initial concentration, which indicates that phenol was also present in the lower gel-like layer. No further analysis was done on these samples. For application purposes, a maximum allowable phenol concentration of 40 mM should be used when a 2.5 wt% P103 solution is used as extractant.

Another set of experiments was executed with 3.5 mM phenol in the presence of different concentrations of Pluronic P103 (0 - 10 wt%) at 22°C. Figure 7 shows that the effect of the Pluronic concentration on the solubility ratio is negligible and that the corresponding phenol uptake decreases at higher Pluronic concentrations. The decrease in uptake is caused by the increase in Pluronic concentration while the solubility ratio remains constant.

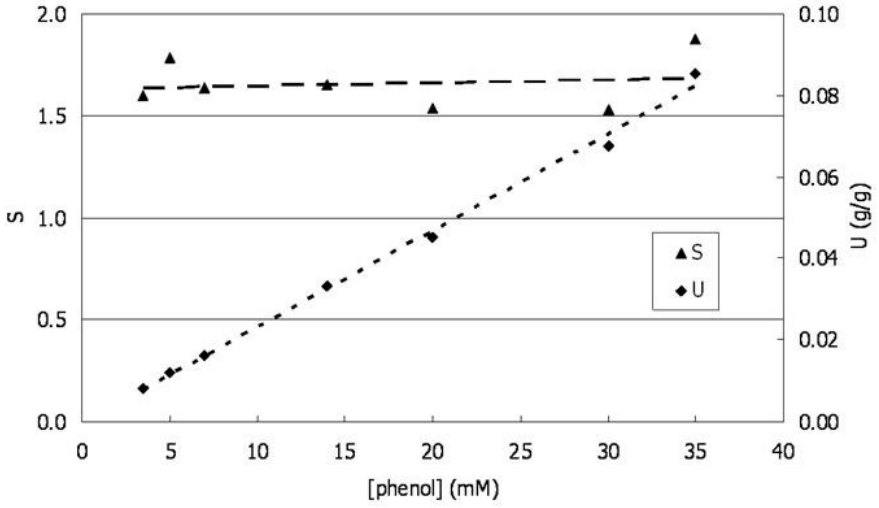

Figure 6. Solubility ratio and phenol uptake (g/g) of phenol in 2.5 wt% P103 solutions at different phenol start concentrations (mM) at 30 °C.

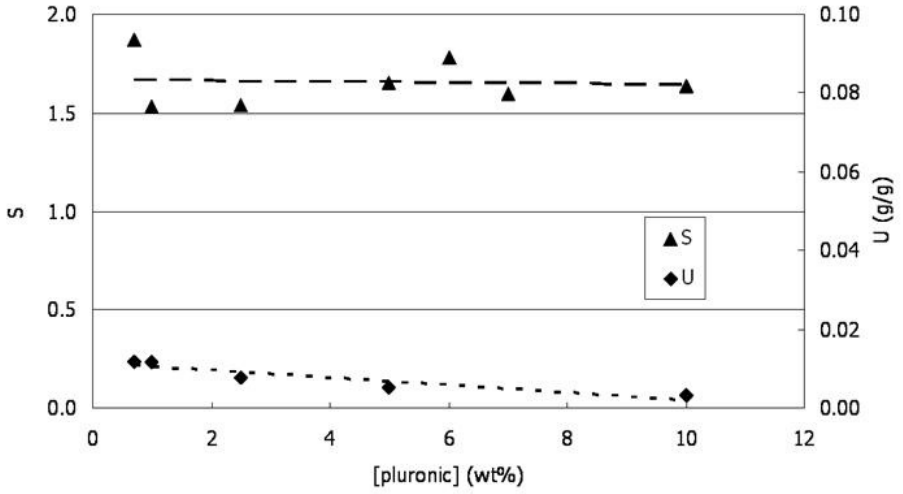

Figure 7. Solubility ratio and phenol uptake (g/g) of solutions with 3.5 mM phenol start concentration at different P103 concentrations (wt%) at 22 °C.

Determination of CMC and CMT

The CMC was determined at three different temperatures for Pluronics P103, P104 and P85. These Pluronics have the highest solubility ratio for phenol and can be regenerated by means of a thermal swing. In Figure 8, the logarithmic CMC is plotted against the CMT. The results agree well with those found by Alexandridis [26]. This phase diagram gives an indication whether these Pluronics will be present as unimers or micelles at a certain temperature and concentration. Below the lines, the Pluronics will be present in the form of unimers, while above the line the Pluronics are present in the form of micelles.

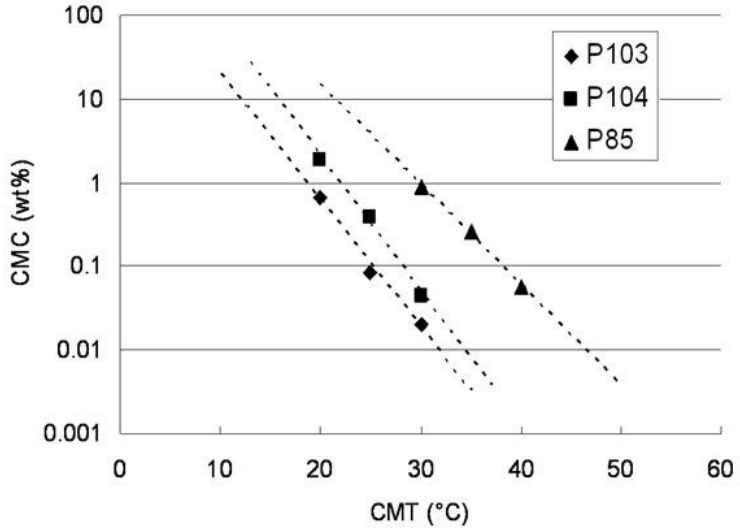

Figure 8. CMC versus CMT for P103, P104 and P85.

Comparing the phase diagrams of the three Pluronics, it can be seen that the CMC value decreases at increasing PPO/PEO ratio. This means that a more hydrophobic Pluronic forms micelles at lower temperatures. Therefore, at a fixed concentration the Pluronics with a higher weight percentage of PEO form micelles at higher temperatures. Furthermore, at a fixed temperature Pluronics with an increased hydrophilic content will switch to the micellar form at a higher concentration (CMC).

Pluronic P103 has the lowest CMC at fermentation temperature of about 30 °C, whereas P85 has the highest CMC under these conditions. The CMT of for example a 1 wt% aqueous solution of Pluronics is 20°C for P103, 22°C for P104 and 30°C for P85. On the other hand, when using for example 10 wt% solutions of these Pluronics, the CMT for P85 is higher than the CMT for P103. As a consequence, when these micellar solutions are regenerated, the P103 solution should be cooled to a much lower temperature compared to the P85 solution to form unimers. In other words, the energy needed for regeneration is higher for P103 compared to P85. This point will be discussed further on in this paper.

Block copolymers can have a complex phase behavior. They can form micelles in aqueous solutions, but they can also form lyotrophic liquid crystalline structures such as lamellar, cylindrical, hexagonal or cubic (gel) structures [8, 12, 27]. One should always take into account that numerous factors can influence this phase behavior in all directions. All species present in a fermentation broth can have a significant effect on the block copolymer structure and phase behavior or could be co-extracted together with the desired product. Therefore the evaluation of Pluronics as solvent for use in a certain bioprocess should

be performed in a realistic medium containing the components that can be expected during production. So, the effect of the fermentation medium used for the growth of *Pseudomonas putida* S12 and the production of phenol on the performance of Pluronics P103 and 104 was investigated. The lines in Figure 9 before and after the first inflection point of the absorbance versus concentration curve for both P103 and P104 are comparable in water and in fermentation medium. So, the CMC of P103 and P104 at 30°C did not change when using the fermentation medium. The medium components do not affect the phase behavior of the Pluronics at the investigated concentrations.

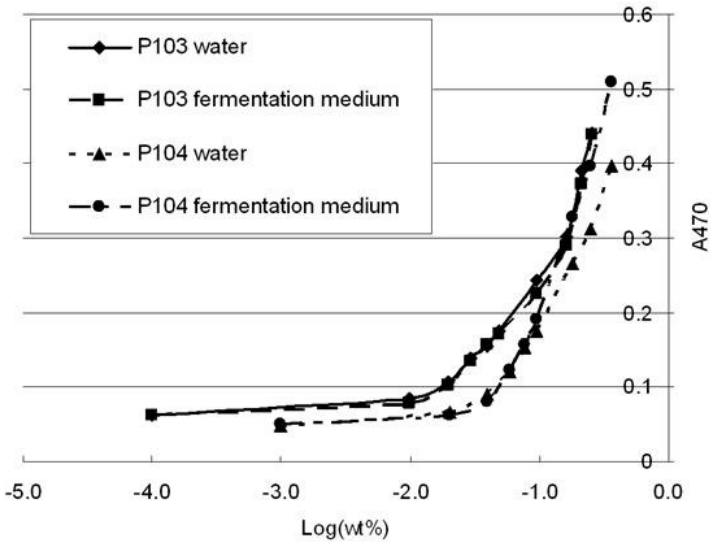

Figure 9. CMC of P103 and P104 at 30°C in water and in fermentation medium.

Energy requirement for regeneration of the micellar solvent

To combine and evaluate the results described above, calculations for the extraction of phenol by P103 and P85 and subsequent regeneration of the solvent were executed. From Figure 8, the unimerization or regeneration temperature of 20 wt% solutions of P103 and P85 can be estimated to be approximately 5 and 15°C respectively. This indicates that the total solvent phase of P103 has to be cooled down to a much lower temperature compared to P85 as mentioned before. For comparison, the amount of phenol removed (ΔM) and the cooling energy needed (ΔQ) were calculated for phenol extraction and solvent regeneration using both Pluronics.

The solubility ratio was determined experimentally for 2.5 wt% P103 and P85 solutions using dead-end filtration or centrifugal filtration at 30° C and 10°C (see Table 2) and for P103 in a dialysis system

at 30° C and 10°C (see paragraph 3.2). For P85, the solubility ratio for a dialysis system at 30° C and 10°C was obtained with the factor for both methods for P103. The results are summarized in Table 4.

Table 4. The amount of energy needed for the separation of phenol with 1 L Pluronic solutions of 20 wt% P103 and P85.

	P103		**P85**	
	S_m (30°C)	S_u (10°C)	S_m (30°C)	S_u (10°C)
UF	1.71	0.36	0.94	0.34
Dialysis	1.13	0.17	0.62	0.16
Factor	1.5	2.2	1.5	2.2

In addition, the solubility ratios were corrected for the Pluronic concentration in the stripping phase (20 wt%). The solubility ratios calculated for 20 wt% solutions of P103 and P85 in a dialysis system were a factor 8 higher compared to the values given in Table 4. The final solubility ratios used for the calculations were 9.0 and 5.0 for P103 and P85 respectively at 30°C and 1.4 for both Pluronics at 10°C. Using these solubility ratios, the phenol concentration in the stripping phase ($c_{ph,s}$, $g.L^{-1}$) and the amount of phenol in the permeate was determined. In Table 5, the results of the calculations are given.

Table 5. The amount of energy needed for the separation of phenol with 1 L Pluronic solutions of 20 wt% P103 and P85.

Parameter	**P103**	**P85**
$c_{ph,s}$, $g.L^{-1}$	1.71	0.94
$\Delta T_{regeneration}$	25	15
ΔQ (kJ)	95.4	57.2
ΔM (g)	0.73	0.41
$\Delta Q.\Delta m^{-1}$ ($kJ.g^{-1}$)	130.5	138.2

From Table 4 it becomes clear that Pluronic P103 can remove a larger quantity of phenol from the reactor phase, due to its higher solubility ratio. The ΔM for P103 is almost twice as high compared to the ΔM for P85. The concentration of phenol in the total stripping phase reaches 1.71 and 0.94 $g.L^{-1}$ for P103 and P85 respectively. Additionally, although more energy is needed to cool down a stripping solution containing 20 wt% P103 compared to a solution containing 20 wt% P85 (95.4 kJ for P103 versus 57.2 kJ for P85) due to the lower CMT for P103. The amount of energy needed per gram of phenol released is lower for P103 solutions. It should be noted that the price of cooling water needed to cool a solution to 5°C is higher compared to that of cooling water needed for cooling to 15°C. This could influence the overall process cost and it should be taken into account when designing a process

based on micellar solvents. The energy needed for the removal of 1 gram phenol ($\Delta Q.\Delta M^{-1}$) was calculated to be 130.5 and 138.2 kJ respectively. The calculated energy was based on a process without heat regeneration. The energy needed for regeneration can be decreased heat integration. In a continuous process, cooling and heating is needed to form unimers and micelles respectively. In a paper to be published in the near future, the process will be further optimized and evaluated [28]. Finally, it should be noted that the separated phenol in our case is still solubilized in water and has to be separated to obtain a pure component.

5.4 Conclusions

Pluronics are attractive solvents for in-situ product removal of toxic compounds like phenol from aqueous fermentation broths. The major advantage of Pluronics is that they can be easily regenerated by a mild temperature-switch.

Experimental results showed that 2.5 wt% Pluronic solutions have solubility ratios for phenol ranging from 0.58 to 1.75 at fermentation temperature (30°C), whereas the solubility ratios at 10°C are significantly lower, ranging from 0.28 to 0.38. The solubility ratio of phenol in a 2.5 wt% P103 solution remained constant at different phenol concentrations and the phenol uptake of P103 for phenol increased linearly with increasing phenol concentrations. The maximum concentration of phenol in a 2.5 wt% P103 solution was found to be 40 mM. Above this concentration, the cloud point of the Pluronic solution was reached and at phenol concentrations above 210 mM a gel-like phase was observed. For practical applications this causes no limits as phenol already causes product inhibition for *Pseudomonas putida* S12 cells at concentrations around 2 mM. Furthermore, it was shown that for 3.5 mM phenol solutions the solubility ratio for phenol in P103 solutions at increasing concentrations remained constant and that the phenol uptake slightly decreased.

For the three most promising Pluronics (P103, P104 and P85) the CMC and the CMT were determined. It can be concluded that the CMC at 30°C was lowest for P103 and highest for P85. This results in a lower CMT of P103 compared to P85 at equal concentrations in micellar form. As a consequence, the cooling energy needed for regeneration of a P103 solution is higher compared to P85.

Experiments revealed that there is no influence of the fermentation medium on the CMC of P103. Finally, it was demonstrated that Pluronics have no negative influence on the growth of *Pseudomonas putida* S12 cells.

Calculations were made to illustrate the amount of energy needed for the separation of one gram of phenol using Pluronics P103 and P85. The calculations show that a large amount of energy is required

for the regeneration of the micellar solution. For the regeneration of Pluronic P103 and P85 solutions, the calculated energy requirement was 130.5 and 138.2 $kJ.g^{-1}$ phenol respectively. Using Pluronic P103, the lowest amount of energy per gram of phenol is needed. However, the regeneration temperature of a micellar P103 solution is lower compared to P85 resulting in a more expensive cooling method.

References

1. Stark, D.; von Stockar, U., In Situ Product Removal (ISPR) in Whole Cell Biotechnology During the Last Twenty Years. In Process Integration in Biochemical Engineering, 2003; pp 149-175.
2. Klaassen, R.; Feron, P.H.M.; Jansen, A.E., Membrane contactors in industrial applications. Chemical Engineering Research and Design 2005, 234-246.
3. Heerema, L.; Roelands, M.; Hanemaaijer, J.H.; de Bont, J.; Verdoes, D., In-situ phenol removal from fermentation broth by pertraction. Desalination 2006, 485-487.
4. Boyadzhiev, L.; Dimitrov, K.; Metcheva, D., Integration of solvent extraction and liquid membrane separation: An efficient tool for recovery of bio-active substances from botanicals. Chemical Engineering Science 2006, 4126-4128.
5. Schlosser, S.; Kertesz, R.; Martak, J., Recovery and separation of organic acids by membrane-based solvent extraction and pertraction: An overview with a case study on recovery of MPCA. Separation and Purification Technology 2005, 237-266.
6. Trivunac, K.; Stevanovic, S.; Mitrovic, M., Pertraction of phenol in hollow-fiber membrane contactors. Desalination 2004, 93-101.
7. Galaction, A.I.; Cascaval, D.; Nicuta, N., Selective removal of Gentamicin C1 from biosynthetic Gentamicins by facilitated pertraction for increasing antibiotic activity. Biochemical Engineering Journal 2008, 28-33.
8. Alexandridis, P.; Alan Hatton, T., Poly(ethylene oxide)---poly(propylene oxide)---poly(ethylene oxide) block copolymer surfactants in aqueous solutions and at interfaces: thermodynamics, structure, dynamics, and modeling. Colloids and Surfaces A: Physicochemical and Engineering Aspects 1995, 1-46.
9. Choi, Y.-k.; Lee, S.-B.; Lee, D.-J.; Ishigami, Y.; Kajiuchi, T., Micellar enhanced ultrafiltration using PEO-PPO-PEO block copolymers. Journal of Membrane Science 1998, 185-194.
10. Adak, A.; Pal, A., Removal of phenol from aquatic environment by SDS-modified alumina: Batch and fixed bed studies. Separation and Purification Technology 2006, 256-262.
11. Mata, J.P.; Majhi, P.R.; Kubota, O.; Khanal, A.; Nakashima, K.; Bahadur, P., Effect of phenol on the aggregation characteristics of an ethylene oxide-propylene oxide triblock copolymer P65 in aqueous solution. Journal of Colloid and Interface Science 2008, 275-282.
12. Alexandridis, P.; Holmqvist, P.; Lindman, B., Poly(ethylene oxide)-containing amphiphilic block copolymers in ternary mixtures with water and organic solvent: effect of copolymer and solvent type on phase behavior and structure. Colloids and Surfaces A: Physicochemical and Engineering Aspects 1997, 3-21.
13. Lebens, P.J.M.; Keurentjes, J.T.F., Temperature-induced solubilization of hydrocarbons in aqueous block copolymer solutions. Industrial and Engineering Chemistry Research 1996, 3415-3421.
14. Wierckx, N.J.P.; Ballerstedt, H.; De Bont, J.A.M.; Wery, J., Engineering of solvent-tolerant *Pseudomonas putida* S12 for bioproduction of phenol from glucose. Applied and environmental microbiology 2005, 8221-8227.

15. Alexandridis, P.; Holzwarth, J.F.; Hatton, T.A., Micellization of Poly(ethylene oxide)-Poly(propylene oxide)-Poly(ethylene oxide) Triblock Copolymers in Aqueous Solutions: Thermodynamics of Copolymer Association. Macromolecules 1994, 2414-2425.
16. Ivanova, R.; Alexandridis, P.; Lindman, B., Interaction of poloxamer block copolymers with cosolvents and surfactants. Colloids and Surfaces A: Physicochemical and Engineering Aspects 2001, 41-53.
17. Rao, I.V.; Ruckenstein, E., Micellization behavior in the presence of alcohols. Journal of Colloid and Interface Science 1986, 375-387.
18. Nakashima, K.; Bahadur, P., Aggregation of water-soluble block copolymers in aqueous solutions: Recent trends. Advances in Colloid and Interface Science 2006, 75-96.
19. Desai, P.R.; Jain, N.J.; Bahadur, P., Anomalous clouding behavior of an ethylene oxide-propylene oxide block copolymer in aqueous solution. Colloids and Surfaces A: Physicochemical and Engineering Aspects 2002, 19-26.
20. Mata, J.P.; Majhi, P.R.; Guo, C.; Liu, H.Z.; Bahadur, P., Concentration, temperature, and salt-induced micellization of a triblock copolymer Pluronic L64 in aqueous media. Journal of Colloid and Interface Science 2005, 548-556.
21. Mata, J.; Joshi, T.; Varade, D.; Ghosh, G.; Bahadur, P., Aggregation behavior of a PEO-PPO-PEO block copolymer + ionic surfactants mixed systems in water and aqueous salt solutions. Colloids and Surfaces A: Physicochemical and Engineering Aspects 2004, 1-7.
22. Adak, A.; Pal, A.; Bandyopadhyay, M., Removal of phenol from water environment by surfactant-modified alumina through adsolubilization. Colloids and Surfaces A: Physicochemical and Engineering Aspects 2006, 63-68.
23. Desai, P.R.; Jain, N.J.; Sharma, R.K.; Bahadur, P., Effect of additives on the micellization of PEO/PPO/PEO block copolymer F127 in aqueous solution. Colloids and Surfaces A: Physicochemical and Engineering Aspects 2001, 57-69.
24. Jain, N.J.; Aswal, V.K.; Goyal, P.S.; Bahadur, P., Salt induced micellization and micelle structures of PEO/PPO/PEO block copolymers in aqueous solution. Colloids and Surfaces A: Physicochemical and Engineering Aspects 2000, 85-94.
25. Kandori, K.; McGreevy, R.J.; Schechter, R.S., Solubilization of phenol in polyethoxylated nonionic micelles. Journal of Colloid and Interface Science 1989, 395-402.
26. Alexandridis, P.; Athanassiou, V.; Fukada, S.; Hatton, T.A., Surface activity of poly(ethylene oxide)-block-poly(propylene oxide)-block-poly(ethylene oxide) copolymers. Langmuir 1994, 2604-2612.
27. Hamley, I.W., Introduction to block copolymers. In Developments in block copolymer science and technology, Hamley, I.W., Ed. Leeds, 2004.
28. Heerema, L.; Cakali, D.; Roelands, M.; Goetheer, E.; Verdoes, D.; Keurentjes, J., Evaluation of an integrated separation- and regeneration process for *in-situ* phenol removal from fermentation broth by extraction with micellar solutions of PEO-PPO-PEO block copolymers. In preparation.

Chapter 6

Evaluation of an integrated extraction process for in-situ phenol removal with micellar solutions of PEO-PPO-PEO block copolymers

This chapter was published as:
Heerema, L.; Cakali, D.; Roelands, M.; Goetheer, E.; Verdoes, D.; Keurentjes, J., Evaluation of an integrated extraction process for in-situ phenol removal with micellar solutions of PEO-PPO-PEO block copolymers. *Sep. Purif. Technol.* 2010, 74, 55-63.

Abstract

This paper evaluates the applicability of aqueous solutions of Pluronics for the removal of phenol in a separation and regeneration process. Experimental results show that Pluronic P103 micelles allow extraction of phenol from aqueous solutions at 30°C. The phenol can be released due to the transition of the Pluronic micelles into unimers with a mild temperature switch from 30 to 8°C. Ultrafiltration membranes provide a barrier between the aqueous Pluronic stripping solution and the aqueous solution in a (bio)reactor containing the desired product. Additionally, a similar UF membrane is used to separate the micelles and unimers from water. Steady state model analysis of the proposed separation and regeneration process are performed to obtain a phenol mass flow rate in the product stream equal to the phenol production rate in the (bio)reactor. Furthermore, the process is analyzed for different process configurations and a cost estimation is made. The results show that for the model product phenol, the process costs are mainly determined by the required membrane area.

The proposed process can be suited for products that allow for a higher critical concentration in the (bio)reactor as compared to phenol. The resulting higher driving force for membrane extraction will result in a decrease of the overall process costs. For products with a lower solubility in water, recovery is easy after regeneration of the micellar solvent.

6.1 Introduction

Product inhibition is one of the major problems in the bioproduction of chemicals. To overcome this problem, the toxic product should be removed from the bioreactor during growth and production. Membrane extraction (pertraction) is an example of a process that can be integrated in a bioreactor and can be useful for *in-situ* product removal (ISPR). A new type of solvent that can be used for ISPR is based on micelles solubilized in water. Micelles formed by Pluronics can be used to extract various solutes [1-4]. Using the unique temperature-dependent micellization behaviour, a decrease of the solution temperature below the critical micelle temperature (CMT) results in the release of the extracted product. For the removal and release of a certain product from a bioproduction process, a membrane-based separation- and regeneration process is proposed.

This paper describes the use of Pluronic block copolymers as a novel "solvent" in bioprocesses in an integrated separation and regeneration process. The model product used to illustrate this process is phenol. Phenol can be produced by the solvent tolerant micro-organism *Pseudomonas putida* S12 and is inhibiting at concentrations around 2 mM [5]. In previous work [6], it has been demonstrated that phenol can be extracted with aqueous micellar solutions and that the solvent can be regenerated by a mild temperature switch. The Pluronic solutions are not toxic to the micro-organisms and the presence of components like salts, sugars and minerals in the reactor show no effect on the phase behavior of the Pluronic solutions. Additionally, calculations have been performed to evaluate the amount of energy needed for the separation of phenol using Pluronic P85 and P103 micellar solutions. Results show the lowest amount of energy per gram of phenol purified is needed for Pluronic P103.

A separation- and regeneration process is proposed for the *in-situ* removal of phenol with Pluronic P103 micellar solutions. The proposed separation- and regeneration process is illustrated in Figure 1. The unit illustrated at the left side in the box in Figure 1 represents a reactor with an integrated membrane unit (units 1 and 2). Micelles are circulated inside the lumen of a tubular ultrafiltration (UF) membrane that provides a barrier between the aqueous block copolymer extraction solution and the aqueous solution in the bioreactor containing the desired product. Phenol diffuses through the membrane pores into the stripping phase and is extracted into the micelles. The second step is the regeneration or unimerization unit (unit 3). In this unit, the temperature of the stripping phase is decreased below the CMT and the micelles disintegrate into unimers resulting in the release of the extracted product. Next, the product is separated from the unimers by another UF membrane (unit 4). The permeate of unit 4 is the product stream and phenol can be further purified from this stream. A possible extraction- and purification (e.g. distillation) step is illustrated in Figure 1. The purification of the product stream will not be discussed in detail in this paper. The retentate of the unimer separation unit is heated to 30°C to form micelles (unit 5) which are subsequently recycled to the first UF unit.
In this paper, the proposed process is evaluated. For this evaluation, several parameters are determined experimentally and by model calculations. The first parameter determined is the total

membrane area needed for the separation of a certain amount of product. Membranes are used for the removal of the product from the bioreactor and to separate the Pluronics from the aqeous phase. The removal of the product from the bioreactor should be fast enough to keep the concentration in the reactor at a certain level. Furthermore, the loss of Pluronics in the product stream should be as small as possible. Additionally, the stream sizes in the process and the fluxes of phenol, water and Pluronic in the different streams and the cooling energy needed for the regeneration of the micellar solvent are calculated. Finally, a cost estimation is made to compare different process configurations.

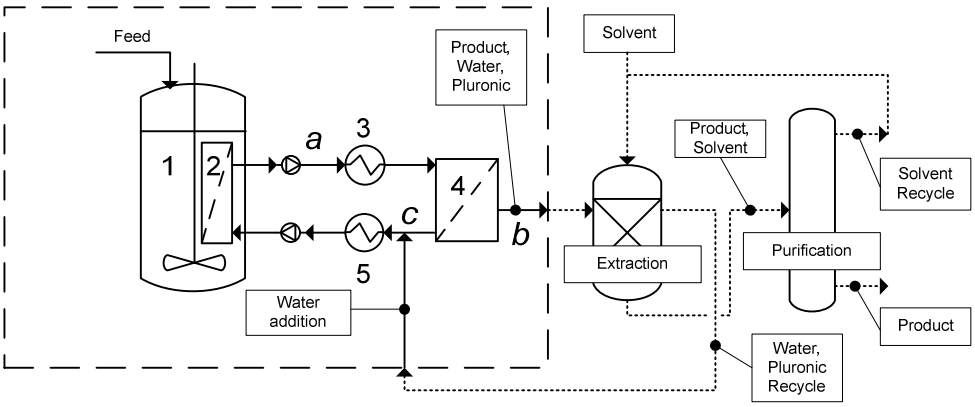

Figure 1. Representation of the proposed process for in-situ phenol removal from a bioreactor with Pluronic micelles. The part illustrated in the box will be discussed in more detail in this paper.

6.2 Experimental

Chemicals

All reagents were used as received without further purification. Pluronic P103 was obtained as a gift sample from BASF (Antwerp). Phenol, analytical grade, and 1-(2-pyridylazo)-2-naphthol (PAN) were supplied by Sigma Aldrich. The water used in this study was demineralised water.

Membranes

The tubular ultrafiltration (UF) membranes used for the integrated membrane unit (unit 2 in Figure 1) were Regenerated Cellulose (RC) Spectra/Por Dialysis Membranes with a Molecular Weight Cut Off (MWCO) 3.5 kD, 6-8 kD and 12-14 kD. The membrane area used for the experiments was in the range of 0.008-0.012 m^2.

RC UF disc membranes with a MWCO of 1, 3, 10 and 30 kD and a membrane area of 13.4 cm^2 were supplied by Millipore. Ultrafree-MC RC microcentrifuge filters with a MWCO of 5 kD and an area of 0.2 cm^2 were supplied by Sigma Aldrich. The disc membranes and the microcentrifuge filters were used to evaluate the unimer separation unit (unit 4 in Figure 1). Based on this, the optimum temperature for regeneration in unit 3 from Figure 1 was determined. For the disk membranes, filtration was carried out by applying a transmembrane pressure (TMP) of 4 bar to reach a filtrate flux (F_{max}) of approximately 0.003 $mL.cm^{-2}.min^{-1}$. For the centrifuge filters, a centrifugal field, with a maximum g force rate of 5000 g was applied.

Experimental evaluation of the process units

Figure 2 illustrates a schematic representation of the proposed process. All units were evaluated separately. The integrated membrane unit was evaluated with 10 wt% aqueous P103 (micellar) solutions (0.25 L) as solvent for phenol. The aqueous reactor phase (0.75 L) contained 5 mM phenol. For this unit, three membranes with different pore sizes were tested: MWCO 3.5, 6-8 and 12-14 kD (Spectra/Por, see 2.2). The micellar solution was pumped though the membranes at 70 $mL.min^{-1}$ and samples were taken from the micellar- and aqueous phase in time. The phenol concentration was determined from the samples using an UV/Vis spectrophotometer (Ultrospec 2100 pro, Amersham Biosciences). Phenol absorbance was measured at 270 nm with an accuracy between 5 and 10%. From the phenol profile in the aqueous phase ($c_{ph,bulk}$, mM) the overall mass transfer coefficient (K_{ov}) was determined. The determination of the K_{ov} will be described further on in this paper (3.1).

The regeneration unit was evaluated by studying the phase behavior of Pluronic P103 and by measuring the solubility ratio of phenol in Pluronics. To study the phase behavior of P103, the critical micelle concentration (CMC) was determined at different temperatures (20, 25 and 30°C). The determination of the CMC is based on the absorption of a water-insoluble hydrophobic dye, 1-(2-pyridylazo)-2-naphthol (PAN). At a fixed temperature, a known amount of P103 was added to an aqueous solution containing PAN. The concentration of P103 in solution increased until the CMC is reached and micelles start to form. The dye solubilized in the micelles leads to a yellow color that was measured at 470 nm in an UV/VIS spectrophotometer (Ultrospec 2100 pro, Amersham Biosciences). The absorption data were plotted as a function of the logarithm of the Pluronic concentration. Two straight lines were drawn before and after the first inflection point of the absorbance versus concentration curve. From the intercept of the two lines the CMC value of the Pluronic at that temperature can be determined.

To study the solubility ratio of phenol in Pluronic, solutions were prepared containing 10 wt% P103 at 30°C and 5 mM phenol. The temperature was decreased in steps from 30 to 5°C and the solubility ratio was determined at different temperatures. The solution was equilibrated and the samples were filtered using either a 3 kD disc membrane or a 5 kD microcentrifuge filter (both methods referred to

as UF from this point on) at the chosen temperature. The phenol concentration in the filtrate was determined as described above.

The solubility ratio of phenol in the Pluronic micelles (S_m) or unimers (S_u) is described as the ratio of the concentration phenol in the Pluronic phase ($c_{ph,m}$ or $c_{ph,u}$) and the concentration phenol in the aqueous phase, which is denoted as $c_{ph,s}$ (mM) in case of micelles and $c_{ph,aq}$ (mM) in case of unimers, see also Figure 2:

$$S_m = \frac{c_{ph,m}}{c_{ph,s}}$$
$$S_u = \frac{c_{ph,u}}{c_{ph,aq}} \quad (1)$$

The phenol concentration in the aqueous phase was assumed to be equal to the phenol concentration in the filtrate. The concentration phenol in the micelles or unimers ($c_{ph,m}$ or $c_{ph,u}$ mM) was determined by the difference between the initial phenol concentration in the aqueous phase ($c_{ph,in}$, mM) and the concentration of phenol in the filtrate after filtration ($c_{ph,f}$, mM). The initial phenol concentration is the phenol concentration in the aqueous solution before contact with the solvent/Pluronics. The phenol concentration in the filtrate was corrected with the weight percentage of Pluronics in the solution (ϕ), defined as the ratio of the volume of Pluronic (V_{pl}, L) to the total volume of the solution (V_{tot}, L):

$$\phi = \frac{V_{pl}}{V_{tot}} \quad (2)$$

$$c_{ph,m} = \frac{c_{ph,in} - c_{ph,f}(1-\varphi)}{\varphi} \quad \textit{and} \quad c_{ph,u} = \frac{c_{ph,in} - c_{ph,f}(1-\varphi)}{\varphi} \quad (3)$$

The solubility ratio at different temperatures indicates the optimum temperature for extraction (above CMT) and regeneration (below CMT). To obtain the solubility ratio for the total stripping phase (Pluronics and water), a correction for the weight percentage of Pluronic in the solution is made:

$$S_{strip,m} = S_m \cdot \phi$$
$$S_{strip,u} = S_u \cdot \phi \quad (4)$$

The unimer separation unit was evaluated using two UF membrane types with MWCO 1 and 3 kD (UF disk membranes, see 2.2). Samples containing 5 mM phenol and 10 wt% P103 were filtered at 4 bar and 10°C. The final filtrate sample was analyzed on phenol content ($c_{ph,f}$, see Figure 2).

For all membrane units, the amount of Pluronic in the filtrate was determined by Total Organic Carbon (TOC) analysis.

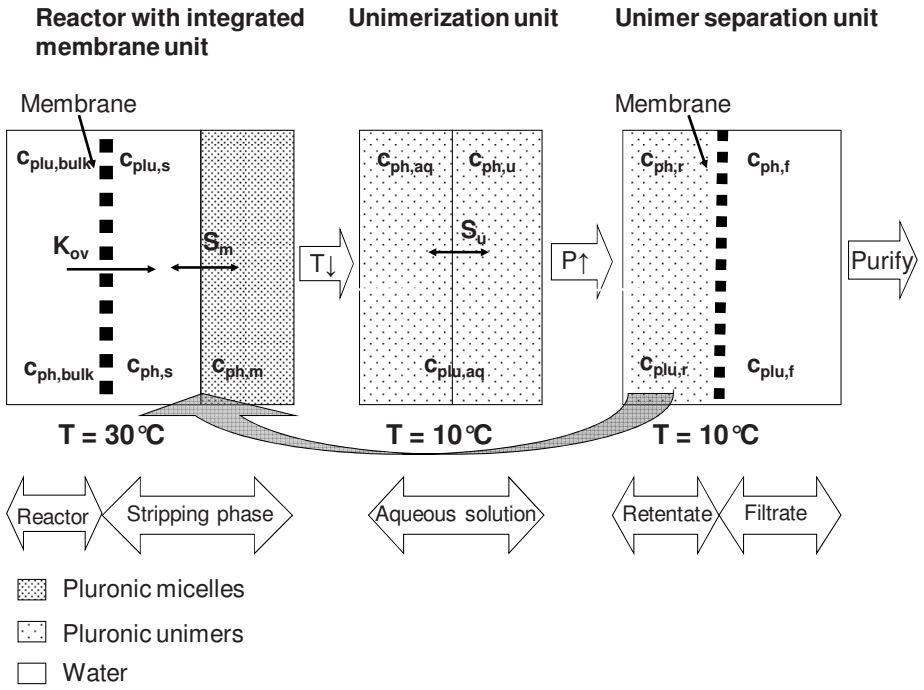

Figure 2. Schematic representation of the proposed process: reactor with integrated membrane unit (left), regeneration or unimerization unit (centre) and unimer separation unit (right).

6.3 Modeling of the phenol production, extraction and regeneration process

Simulation of the phenol concentration profile in the reactor and stripping phase

The phenol concentration in a bioreactor with an integrated membrane unit was modeled by describing the phenol production rate in the reactor, combined with product inhibition. It was assumed that the maximum phenol concentration that can be reached in the reactor ($c_{ph,bulk,max}$) was 2 mol.m^{-3} (0.19 kg.m^{-3}). Reference [5] describes that phenol is inhibiting the biomass growth and the phenol production by a genetically modified phenol producing strain of *Pseudomonas putida* S12 for a phenol concentration above this value. The mass balance for phenol in the reactor without product removal can be described by a simplified equation for production rate, described by Luong et al. [7]:

$$\frac{d}{dt} c_{ph,bulk} = r_{p,max} \left[1 - \left(\frac{c_{ph,bulk}}{c_{ph,bulk,max}} \right)^{\alpha} \right] \quad (5)$$

Where $r_{p,max}$ is the maximum production rate, assumed to be 0.1 $mol.m^{-3}.h^{-1}$. The maximum production rate was estimated from several references that use similar bacteria [5, 8, 9]. Additionally, $c_{ph,b}$ corresponds to the concentration of phenol in the reactor or bulk ($mol.m^{-3}$), see also Figure 2. For the exponent α a value of 4 was assumed. In reference [10] it was stated that when $\alpha > 1$, a slow initial drop in growth and production rate occurs followed by a rapid decrease to zero occurs. This nonlinear behavior expresses a concavity downward and is similar to the type of inhibition occurring in the case of phenol. At low phenol concentrations in the bulk the exponential term is low and the phenol production rate in the bulk is close to the maximum production rate. At phenol concentrations in the bulk approaching the maximum phenol concentration the exponential term approaches unity and the phenol production rate in the bulk is a small fraction of the maximum production rate. An α-value of 4 was assumed to describe the phenol inhibition process because the production rate will decrease rapidly only at concentrations close to the maximum concentration.

The mass balance for phenol in the reactor with product removal can be written as the difference between production and removal:

$$\frac{d}{dt}c_{ph,bulk} = r_{p,max}\left[1-\left(\frac{c_{ph,bulk}}{c_{ph,bulk,max}}\right)^4\right] - \left[K_{ov}\cdot\frac{A}{V_R}\cdot\left(c_{ph,bulk}-\frac{c_{ph,strip}}{S_m\cdot\varphi+(1-\varphi)}\right)\right] \quad (6)$$

Where K_{ov} is the overall mass transfer coefficient ($m.s^{-1}$), A the area of the integrated membrane unit (m^2), V_R the volume of the aqueous phenol solution in the reactor (m^3) and $c_{ph,strip}$ the phenol concentration in the stripping phase ($mol.m^{-3}$).

The phenol mass balance in the micellar extraction stream can be written as the sum of the amount of phenol entering the extraction stream, the amount of phenol transferred from the reactor and the amount of phenol leaving the extraction stream:

$$\frac{d}{dt}c_{ph,stip} = \frac{Q}{V_s}\cdot\left(c_{ph,strip(0)}-c_{ph,strip}\right)+\left[\left[K_{ov}\cdot\frac{A}{V_s}\cdot\left(c_{ph,bulk}-\frac{c_{ph,strip}}{S_m\cdot\varphi+(1-\varphi)}\right)\right]\right] \quad (7)$$

Where Q is the volumetric flow rate of the stripping phase ($m^3.s^{-1}$). The initial concentration of phenol in the stripping phase ($c_{ph,strip(0)}$, mM) was assumed to be zero. The phenol concentration profiles in the reactor and the extraction stream were modeled as a function of time by solving the two ordinary differential equations 6 and 7.

The overall mass transfer coefficient (K_{ov}) was determined experimentally by monitoring the phenol concentration decrease in the reactor in time after addition of a certain amount of phenol. This experiment was executed without phenol production. Consequently, Equation 6 was simplified to the following equation:

$$\frac{d}{dt} c_{ph,bulk} = -\left[K_{ov} \cdot \frac{A}{V_R} \cdot \left(c_{ph,bulk} - \frac{c_{ph,strip}}{S_m \cdot \varphi + (1-\varphi)}\right)\right] \quad (8)$$

The differential equation was integrated by ODE45 solver in Matlab. By adjustment of K_{ov}, the model was optimized to fit the experimental data. With this method, the optimized overall mass transfer coefficient was determined.

Process evaluation

The calculations for the process evaluation comprised solving the phenol and Pluronic mass balances around the different units as given in Figure 1 without recycles. The process model was evaluated and a sensitivity analysis was performed. The phenol mass flow in the product steam (ΔM, $g.min^{-1}$ in stream b) was set to the maximum phenol production rate in the bioreactor (0.0016 $g.min^{-1}$). The Pluronic concentration in the stripping phase was varied between 10 and 20 wt%.

The output parameters considered for the evaluation were the flow rate of the extraction and the product stream (ΦV_a and ΦV_b, $mL.min^{-1}$), the loss of energy in the process ($kJ.g^{-1}$ phenol), the membrane area for the integrated membrane unit and the unimer separation unit (units 2 and 4) (m^2), the mass flow rate of Pluronic in the product stream ($M_{plu,b}$, $g.min^{-1}$) and the phenol concentration in the permeate and the retentate of the unimer separation unit (unit 4 in Figure 3) ($c_{ph,b}$ and $c_{ph,c}$, $g.L^{-1}$).

The energy needed to cool down the micellar solution in stream a was determined by calculating the cooling energy (ΔE, $kJ.min^{-1}$) needed to cool the stripping solution to the regeneration temperature:

$$\Delta E = m \cdot c_p \cdot \Delta T \quad (9)$$

With m the mass flow of the solvent ($g.min^{-1}$), c_p the specific heat capacity ($J.g^{-1}.K^{-1}$) which is 4.2 for water. Meilleur et al. [11] determined that the apparent specific heat capacities for 10 wt% solutions of Pluronic P103 vary between 5 to 25°C from approximately 3.3 to approximately 6.0 $J.g^{-1}.K^{-1}$ respectively. For our calculations, we assume the average of these two values for the c_p for P103 (4.7 $J.g^{-1}.K^{-1}$). ΔT corresponds to the temperature difference between the stripping solution and the regeneration temperature. The density of Pluronic was assumed to be equal to the density of water. ΔE was calculated as the sum of the ΔE for the water and the ΔE for the Pluronic present in stream a. By combining the cooling energy and the mass flow of phenol (ΔM, $g.min^{-1}$), the energy needed per g phenol removed can be calculated (ΔE. ΔM^{-1}, $kJ.g^{-1}$). After regeneration and separation of the Pluronics from the product stream, the recycle stream (stream c), containing unimers, is heated again to form micelles. Using a heat exchanger and heat integration for the cooling and heating of the Pluronic solution, the amount of energy required can be minimized. Although the amount of energy

needed for heating is equal to the required cooling energy, there is always a loss in energy using such a heat exchanger. It is assumed that the energy loss using a heat exchanger for cooling and heating is 20%. For the process evaluation the energy loss taken into account was 20% of the ΔE. ΔM^{-1}.

A micelle concentration unit was added (unit 6 in Figure 3), in order to further evaluate the model. This UF unit between the integrated membrane unit and the regeneration unit has the function to concentrate the micellar stream and to remove some of the impurities. The influence of the micelle concentration unit for concentrating 10 and 20 wt% P103 solutions to 25 wt% was evaluated.

The membrane area needed for the integrated membrane unit (A_{unit2}, m^2) was determined from the phenol mass flow rate in the permeate ($M_{ph,permeate}$, $g.s^{-1}$), the overall mass transfer coefficient (K_{ov}, $m.s^{-1}$) and the concentration difference (driving force) between the two sides of the membrane (dc, $g.m^{-3}$). The membrane area for the other UF membrane units (A_{unit4} and A_{unit6}, m^2) was determined from the total flux of the filtrate ($Q_{filtrate}$, $m^3.s^{-1}$) and the flux through the membrane per area (F_{max}, $m^3.m^{-2}.s^{-1}$):

$$A_{unit2} = \frac{M_{ph,permeate}}{K_{ov} \cdot dc} \quad \text{and} \quad A_{unit4,6} = \frac{Q_{filtrate}}{F_{max}} \tag{10}$$

Using short-cut models and the results obtained from the calculations described above, cost estimations were made. It was assumed that the phenol production is comparable to a large-scale production process: 10 $kton.yr^{-1}$ with a production time of 8000 hours per year. The cost-factors that were evaluated were: the energy loss in the process, the total required membrane area and the Pluronic losses in the product stream. Additionally, the purification of phenol from the product stream was evaluated by determining the amount of the solvent diisopropylether (DIPE) required to maintain an equal phenol production. The first three factors were obtained by making the following assumptions: the average costs for ultrafiltration membranes is 800 $euro.m^{-2}$ [12], the energy loss is 20% of the energy input by unit 3 and the Pluronic costs are 100 $euro.kg^{-1}$ (BASF).

From the volume flow rate of stream d, the amount of cooling energy needed to cool down the solution to below CMT was determined (see Equation 9). The estimated cost of the energy loss was assumed to be 0.05 $euro.kWh^{-1}$.

To complete the process, phenol should be purificated from the (aqueous) product stream (see the part outside the box in Figure 1). This can be accomplished by solvent extraction with a low boiling solvent, for example DIPE. This solvent has a partition coefficient (P) for phenol of 15, a cost price of 5.5 $euro.L^{-1}$ [13] and a boiling point of 68°C [14]. The flow rate of DIPE ($\Phi V_{solvent}$, $mL.min^{-1}$) required to maintain an equal phenol mass flowrate (10 $kton.yr^{-1}$) and, subsequently the amount of solvent per kg phenol produced ($L.kg^{-1}$) can be determined with help of the partition coefficient, see Equation 11.

This information can add to the evaluation of the total estimated process costs for the different process configurations.

$$\phi V_{solvent} = \frac{M_{ph,b}}{c_{ph,b} \cdot P} \qquad (11)$$

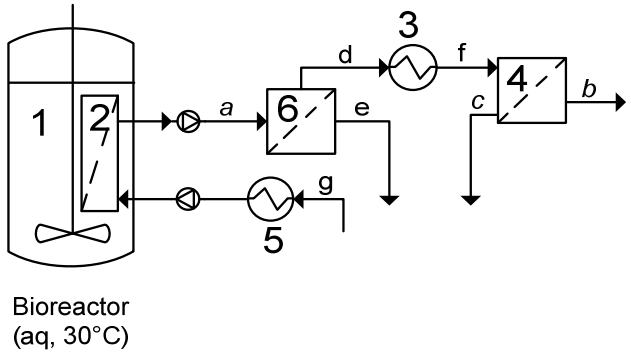

Figure 3. Adjusted scheme for evaluation of the total extraction, regeneration and purification process.

6.4 Results and discussion

Experimental evaluation of the process units

Phenol permeation

The integrated membrane unit (unit 2 in Figure 1) has been evaluated experimentally for three different membrane pore sizes (MWCO 3.5, 6-8 and 12-14 kD). This evaluation includes the determination of the overall mass transfer coefficient of phenol from the reactor to the stripping phase (K_{ov}). Figure 4 illustrates a typical result for the phenol concentration profile in the reactor. The illustrated experiment was performed using a 12-14 kDa membrane of 0.01 m^2 with a flow rate of the stripping phase of 70 $ml.min^{-1}$. The K_{ov} in the integrated membrane unit has been determined with help of Equation 8. Using solutions of 10 wt% P103, the K_{ov} has been determined to be $1.3*10^{-6}$ $m.s^{-1}$ for all membranes used. The overall mass transfer coefficients found in the experiments are comparable with those found in literature, between 10^{-7} - 10^{-5} $m.s^{-1}$. These values are reported for membrane extraction of phenol with various solvents and membranes and for similar process conditions as used here [15-18].

The unimer separation unit (unit 4 in Figure 1) has been evaluated using UF membranes with a MWCO 1 and 3 kD at 10 °C. Solutions containing 10 wt% P103 and 5 mM phenol were filtered and the phenol concentration in the filtrate has been determined. The amount of phenol in the filtrate has been determined to be approximately 50% of the initial amount in this unit.

A micelle concentration (UF) unit was added to the process for the model calculations (unit 6 in Figure 3). This unit was evaluated using disk membranes with MWCO 3, 10 and 30 kD. Solutions containing 10 wt% P103 and 5 mM phenol were filtered at 30°C and the phenol concentration has been determined in the filtrate and compared to the initial concentration, from which it can be concluded that the retention of phenol in the micelle concentration unit is approximately 85%.

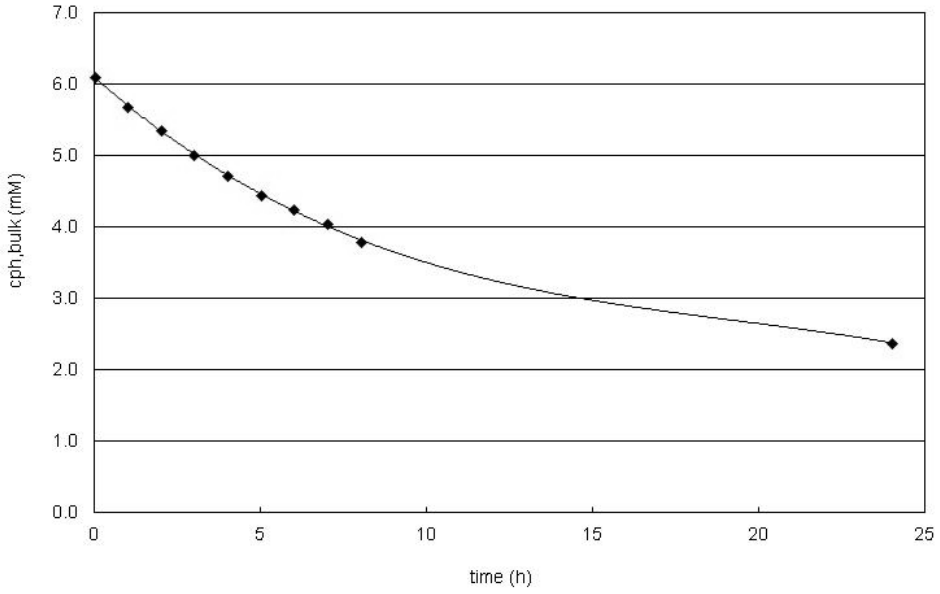

Figure 4. A typical result for the phenol concentration profile in the reactor.

Pluronic permeation

The losses of Pluronic from the stripping phase to the reactor in the integrated membrane unit have been determined. The initial Pluronic concentration in the strip phase is 10 wt% P103. The maximum Pluronic concentration measured in the reactor is 0.07 wt% after 24 hours, which is less than the CMC (0.7 wt% at 30°C). This concentration is not toxic for the micro-organisms in the reactor. In previous work [6] it has been concluded that Pluronics in concentrations up to 15 wt% have no effect on the growth of *Pseudomonas putida* S12 cells in the reactor. Choi et al. [19] concluded that the maximum MWCO of the membrane in similar dialysis experiments with 2 wt% solutions of Pluronic P103 at 25°C is 10 kD. At pore sizes above this value an increase in Pluronic concentration in the reactor was found. The concentration of Pluronic in the reactor is expected to increase in time until equilibrium is reached.

The average Pluronic concentration in the filtrate of the unimer separation unit has been determined to be 1.2 and 1.3 wt%, using membranes with a MWCO of 1 and 3 kD, respectively, and an initial P103 concentration of 10 wt%, which is lower as compared to the CMC at 10°C (approximately 30 wt%).

The concentration of Pluronic in the filtrate of the micelle concentration unit has been determined to be between 1.4 and 1.7 wt% for MWCO ranging from 3 – 30 kD, which is higher than the CMC of P103 at 30°C (approximately 0.01 wt%). In centrifugal ultrafiltration experiments, Sabate et al. [20] observed a similar behavior of surfactants permeating through the membrane. This behavior was found to be independent of the MWCO of the membranes used. The unimers are flexible enough to be deformed and driven through the membrane when applying an external force such as pressure or a centrifugal force. In addition, using 10 wt% P103 solutions, it was determined that 90% of the Pluronics were retained by the membranes in the micelle concentration unit. The difference in retention between Pluronics and phenol was probably caused by the fact that the P103 unimers still have a small solubility for phenol. As a result, the P103 unimers drag phenol through the membrane. Additionally, the concentration phenol determined in the filtrate is higher as compared to when no Pluronics permeates the filter. This will result in a higher aqueous phenol concentration (equal to the concentration in the filtrate) and subsequently a lower solubility ratio will be calculated.

Pluronic phase behaviour and solubility ratio of phenol

To evaluate the regeneration unit (unit 3 in Figure 1), the phase behaviour of P103 and the solubility ratio of phenol in Pluronics were investigated at different temperatures. In Figure 5, the critical micelle concentration versus the critical micelle temperature for Pluronic P103 is illustrated. This phase diagram gives an indication at what temperatures and concentrations the Pluronic will be present in either unimeric (below the line) or micellar (above the line) form. Additionally, Figure 5 illustrates the solubility ratio of phenol in a 10 wt% solution of Pluronic P103 at different temperatures. It is clear that the solubility ratio becomes larger when the solution temperature is above the CMT, due to the presence of micelles. Moreover, the phenol solubility ratio is dependent on the amount of micelles present. The figure shows optimum phenol extraction (indicated by highest solubility ratio) at the fermentation temperature of 30°C and for regeneration of a 10 wt% P103 solution, the optimum temperature is around 8°C. For this process, a temperature-switch from 30°C to 8°C can be applied to extract and release the product.

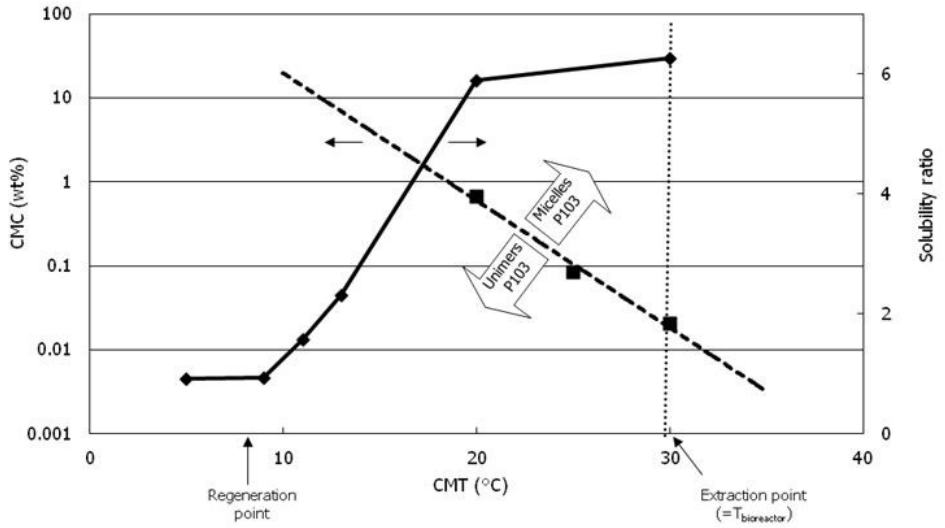

Figure 5. Critical micelle concentration (CMC) as a function of critical micelle temperature (CMT) for Pluronic P103 (EO17PO60EO17) (■) and solubility ratio for phenol in an aqueous 10 w/v% Pluronic P103 solution at different temperatures (♦). The vertical dotted line indicates the fermentation temperature (30 °C) and the extraction point. The regeneration point illustrates the temperature at which the partitioning of the phenol in the Pluronics is lowest.

6.5 Modeling of the phenol production, extraction and regeneration process

The process was evaluated by solving the phenol and Pluronic mass balances around the different units without recycles and a sensitivity analysis was performed. In the steady state model, the goal was to reach a phenol mass flow in the product stream (stream b in Figures 1 and 3) equal to the phenol production rate in the bioreactor (0.1 $mM.h^{-1}$ or 0.0016 $g.min^{-1}$ for a 10 L bioreactor). The parameters that were used for the calculations are given in Table 1. The variables for the evaluation were the concentration of Pluronic in stream a (extraction stream) and the flow rate of stream a. Additionally, the effect of concentrating the micellar stream with an extra UF unit before regeneration (micelle concentration unit, unit 6 in Figure 3) was evaluated. In Table 2 the results of the model calculations are given.

Table 1. Constants used for the model calculations

Parameter	**Value**	**Unit**
Reactor volume (V_r)	10	L
Max. phenol concentration in reactorphase ($c_{ph,bulk,max}$)	0.19	$g.L^{-1}$
Max. phenol production rate ($r_{p,max}$)	0.0016	$g.min^{-1}$
Specific heat capacity water	4.2	$J.g^{-1}.K^{-1}$
Specific heat capacity Pluronic	4.7	$J.g^{-1}.K^{-1}$
Concentration Pluronic in stream e	1.5	wt%
Concentration Pluronic in stream c	30	wt%
Concentration Pluronic in stream b	1.2	wt%
Solubility ratio at 30°C and 10 wt% P103 ($S_{strip,m,10}$)	6.8	-
Solubility ratio at 30°C and 20 wt% P103 ($S_{strip,m,20}$)	13.7	-
Solubility ratio at 10°C and 10 wt% P103 ($S_{strip,u,10}$)	1.4	-
Solubility ratio at 10°C and 20 wt% P103 ($S_{strip,u,20}$)	2.9	-

For the process illustrated in Figure 1, a higher percentage of Pluronic in the stripping phase results in a more optimal process. This is a result of the fact that the flow rate of the stripping phase (ΦV_a), the area needed for the integrated membrane unit (A_{unit2}), the area needed for the unimer separation unit (A_{unit4}), the energy loss for the regeneration of the stripping solution ($20\%.\Delta E.\Delta M^{-1}$) and the Pluronic mass flow rate in the product stream ($M_{plu,b}$) all decrease with an increase in Pluronic concentration in the stripping phase (see Table 2). Additionally, the phenol concentration in the product stream ($c_{ph,b}$) and the phenol concentration in the retentate of the unimer separation unit ($c_{ph,c}$) are higher with a higher Pluronic concentration in the stripping phase. The phenol concentration in the permeate of the unimer separation unit, the product stream, should be as high as possible, however, the phenol concentration in the retentate of the unimer separation unit should not be too high. This stream will be recycled back to the integrated membrane unit and a high phenol concentration in the extraction stream will cause a lower driving force for extraction.

Table 2. Results from the calculations with phenol and Pluronic P103 assuming a phenol mass flow in the product stream (stream b) equal to the phenol production rate in the reactor (0.0016 $g.min^{-1}$) in a 10 L reactor.

	No micelle separation unit		Micelle separation unit		Micelle separation unit and higher solvent flow rate	
Parameter	10wt%	20wt%	10wt% +unit6	20wt% +unit6	10wt% +unit6	20wt% +unit6
ΦV_a ($ml.min^{-1}$)	4.6	3.7	4	4	10	10
ΦV_b ($ml.min^{-1}$)	3.1	1.2	0.3	0.5	0.7	1.3
$20\%.\Delta E.\Delta M^{-1}$ ($kJ.g^{-1}$)	78	62	19	38	47	95
A_{unit2} (m^2)	0.076	0.053	0.060	0.058	0.15	0.15
A_{unit4} (m^2)	0.102	0.041	0.009	0.018	0.022	0.044
A_{unit6} (m^2)	-	-	0.053	0.107	0.13	0.27
$M_{plu,b}$ ($g.min^{-1}$)	0.037	0.015	0.0032	0.0064	0.0080	0.018
$c_{ph,b}$ ($g.L^{-1}$)	0.52	1.32	6.0	3.0	2.4	1.2
$c_{ph,c}$ ($g.L^{-1}$)	1.51	1.90	2.0	1.0	0.8	0.4

The addition of a micelle concentration unit in the process resulted in a high phenol concentration in the product stream due to the small volume flow rate of this stream (see also Table 2). The phenol concentration in the retentate of the unimer separation unit (stream c) does not differ to a large extent from the case without the addition of this unit. Concentrating the strip phase results in a smaller and more concentrated volume to be regenerated and, subsequently, the energy input per gram of phenol, and thus the energy loss, is much lower compared to the situation without the addition of unit 6. This effect is larger when the initial Pluronic concentration in the strip phase is 10 wt%.

Using a higher flow rate of the strip phase (10 $mL.min^{-1}$ instead of 4 $mL.min^{-1}$) causes a substantial increase in the total required membrane area. Additionally, a higher flow rate of the strip phase leads to a higher energy loss per gram phenol. For the two cases without the micelle concentration unit and the two cases with this unit with a flow rate of the strip phase of 4 $mL.min^{-1}$, a cost estimation was made and the most important cost factors were determined.

For the estimation of the process costs for the different process configurations, the factors that were evaluated (in euro.kg^{-1} phenol) were the energy loss, the total required membrane area and the

Pluronic losses in the product stream. Futhermore, the purification of phenol from the product stream was evaluated by determination of the flow rate of solvent required to maintain an equal phenol mass flow ($\Phi V_{solvent}$, mL.min^{-1}). It was assumed that the phenol production ($M_{ph,b}$) is comparable to a large-scale production process: 10 kton.yr^{-1} with a production time of 8000 hours per year. With an average production rate of 0.1 mM.h^{-1} (75.3 kg.m^{-3}.yr^{-1}), the reactor volume needed is 1.3*10^{5} m^{3}. In Table 3 the results for the cost estimation for the different process configurations are given. The overall costs seem to be mainly influenced by the Pluronic losses and the total membrane costs.

The energy costs for regeneration of the micellar solvent vary between 0.1 and 0.3 euro.kg^{-1} phenol. These costs can be reduced by for example choosing another Pluronic with a higher CMT at comparable concentrations and a comparable solubility ratio for phenol. P85 for example has a CMT of 15°C at a concentration of 20 wt% whereas the CMT for P103 was 5°C at the same concentration. The solubility ratio for phenol, however, is lower for P85 compared to P103. In previous work [6], the required cooling energy for regeneration per gram phenol using P103 and P85 was determined. The energy requirement was determined to be comparable although the quality of cooling was higher for P103 because the solution should be cooled down to 5°C instead of 15°C. The energy needed for heating the unimeric solution to form micelles before recycling back to the reactor (unit 5) for P85 solutions will be lower compared to the case described in this paper. This indicates that using P85 can decrease the regeneration costs to a certain extend. As described before, using a heat exchanger and heat integration for the cooling and heating of the Pluronic solution, the amount of energy required can be minimized. Finally, it should be mentioned that the energy requirements do not appear to be the main cost driver for this process and the other factors should be addressed to achieve a large decrease in the process costs.

The total membrane area was determined for the production of 0.016 g.min^{-1} phenol in a 10 L bioreactor. From these values the area required for a production of 10 kton phenol per year was determined. The calculated costs for the required membrane area for the different process configurations vary between 100 and 200 euro.kg^{-1} phenol. The lowest membrane costs are obtained in the processes with a high Pluronic concentration in the strip phase. The addition of the extra micelle concentration unit results in an increase of the total membrane costs. In the presence of the extra unit, the costs are lower with a low Pluronic concentration in the strip phase. This is caused by the lower flow rate of stream d in Figure 3. Table 2 also shows this effect, a larger membrane area is required when using a 20 wt% solution as strip phase. To reduce the required membrane area in this process and thus the overall process costs, the overall mass transfer coefficient in the integrated membrane extraction unit (unit 2) should be improved. The K_{ov} determined in this paper was 1.3*10^{-6} m.s^{-1}, this can be further improved by, for example, optimization of the rate limiting factor, i.e. mass transfer of phenol through the membrane (k_{mem}). The membrane mass transfer coefficient is dependent on the diffusion coefficient of phenol in water and by membrane properties like wall thickness. To improve the k_{mem}, an alternative membrane can be used with a smaller wall thickness.

The driving force for phenol transport over the membrane, which is caused by diffusion in this process. The driving force can be improved by applying a small pressure over the membrane, either by a pressure slightly higher than atmospheric pressure at the reactor side or slightly below atmospheric pressure at the solvent side. The low driving force for extraction is due to a low critical concentration of phenol in the reactor (0.19 $g.L^{-1}$). For this reason, a large membrane area will be required even though the K_{ov} is increased. This indicates that such a process is more suited when higher critical concentrations can be reached in the reactor. This allows a higher driving force and therefore less membrane is required.

With an annual production of 10 kton phenol, the amount of Pluronic in the product stream was calculated to be a significant loss. This is caused by the high Pluronic concentration in the product stream (1.2 wt%) compared to the phenol concentration (varying from 0.5 to 6 $g.L^{-1}$). If all Pluronics can be recycled after the purication of phenol from the product stream by extraction with DIPE (see also Figure 1), this cost factor can be eliminated and the total process costs can be decreased significantly to 100 - 200 $euro.kg^{-1}$ phenol. If Pluronics show no interaction with DIPE (e.g. no coextraction), the extraction step can even be performed directly after regeneration of the micellar solvent and unit 4 can be removed from the process. This will subsequently cause a decrease in the total membrane costs. Stejskal et al. studied the behavior of polystyrene-block-poly(ethylene-co-propylene) (PS-PEP) in the presence of DIPE and observed no structural changes of the micelles or interaction between these components [21]. To confirm a similar behavior in our process, experiments should be performed to determine the (phase) behavior of Pluronics in combination with phenol and DIPE.

Another option to remove the Pluronics from the product stream is for example a chemical treatment to obtain the Pluronic from the product stream given by Purkait et al. [22]. The addition of a salt can lead to precipitation of the surfactant. The aqueous product stream can be separated and further purified. Subsequent dilution of the Pluronic stream will dissolve the Pluronics again and the solution can be recycled to the integrated membrane unit. The salt used can be chosen similar to those present in the fermentation medium, for example by using one of the buffer salts (sodium- or potassium-phosphate). The water in the product stream can be recycled to the Pluronic stream after phenol has been extracted from this stream, see also the part outside the box given in Figure 1.

The volumetric flow rate of DIPE required maintaining an equal phenol mass flowrate (10 $kton.yr^{-1}$) was determined with help of the partition coefficient (see Equation 12). The amount of solvent required to extract phenol from stream b varied between 11 and 128 L per kg phenol. The large amount of solvent needed is caused by the rather low phenol concentration in the product stream. Furthermore, the energy needed to purify phenol from DIPE by distillation will add to the total purification costs. However, the solvent can be recycled after regeneration and only a small amount is needed to replenish the loss of solvent in the distillation process and in the water phase of the

recycled Pluronic stream after extraction. The trend shows that the higher the phenol concentration in the product stream, the lower the amount of DIPE needed for extraction and the less energy is required for distillation.

Table 3. Cost estimation for the different process configurations. The data is based on a production of 10 kton phenol per year with a production time of 8000 hours per year and in euro.kg^{-1} phenol.

	10wt%	**20wt%**	**10wt% +unit6**	**20wt% +unit6**
Energy loss	0.32	0.24	0.10	0.21
Membrane	185	98	127	191
Pluronic losses	2308	909	200	400
Total	$2.5*10^3$	$1.0*10^3$	$0.3*10^3$	$0.6*10^3$

6.7 Conclusions

The results show that mildly thermo reversible Pluronics can be used as alternative solvents for *in-situ* product removal from aqueous solutions. Phenol has been used as a model component to show experimentally that Pluronic P103 can extract and release the model product from aqueous solutions with a mild temperature switch from 30°C to 8°C. In an integrated membrane unit, the phenol is extracted to the Pluronic phase with an overall mass transfer coefficient of $1.3*10^{-6}$ $m.s^{-1}$. The micelles are regenerated after a concentration step by cooling down the solution leading to the release of phenol to the aqueous phase. The unimers and phenol could be separated with the help of a pressurized UF membrane.

Different process parameters were compared and a rough cost estimate has been made for the most important cost factors in this process: energy loss, membrane costs, Pluronic losses and the purification of phenol from the product stream. To obtain similar phenol mass flow rates in the product stream, the use of a high Pluronic concentration in the extraction liquid gives lowest total costs for the selected parameters. The calculated overall costs are still far from the current phenol market price. The calculated process costs can be further decreased by optimization, for example by improvement of the overall mass transfer coefficient in the integrated membrane unit, and recycling of for example the Pluronic in the product stream.

The low driving force for extraction is a problem that can not be solved easily due to the maximum allowable phenol concentration in the reactor. Therefore, the proposed process is interesting for

products that allow for a higher concentration in the reactor. Additionally, if these products exceed solubility after regeneration of the micellar solvent by a temperature-switch, a phase separation (e.g. crystallization) can be an interesting option for low cost purification.

List of symbols

Symbol	Description	Unit
K_{ov}	Overall mass transfer coefficient	$m.s^{-1}$
CMC	Critical micelle concentration	mM
CMT	Critical micelle temperature	°C
S_m	Solubility ratio of phenol in Pluronic micelles	-
S_u	Solubility ratio of phenol in Pluronic unimers	-
$c_{ph,bulk}$	Phenol concentration in the aqueous (bulk) phase	mM
$c_{plu,bulk}$	Pluronic concentration in the aqueous (bulk) phase	wt%
$c_{ph,m}$	Phenol concentration in the micelles	mM
$c_{ph,u}$	Phenol concentration in the unimers	mM
$c_{ph,s}$	Phenol concentration in aqueous phase of micellar solution	mM
$c_{ph,aq}$	Phenol concentration in aqueous phase of unimeric solution	mM
$c_{ph,in}$	Initial phenol concentration in the aqueous phase	mM
φ	Weight percentage (fraction) of Pluronics in the solution	-
V_{pl}	Volume of Pluronic	L
V_{tot}	Volume of total solution	L
$S_{strip,m}$	Solubility ratio of phenol in total micellar solution	-
$S_{strip,u}$	Solubility ratio of phenol in total unimeric solution	-
$c_{ph,f}$	Phenol concentration in the filtrate	mM
T	Temperature	°C
P	Pressure	bar
$c_{ph,bulk,max}$	Maximum phenol concentration in the reactor	mM
$r_{p,max}$	Maximum phenol production rate	$mol.m^{-3}.h^{-1}$
α	Exponent used to describe phenol production	-
A	Membrane area	m^2
V_R	Volume of aqueous phenol solution in the reactor	m^3
$c_{ph,strip}$	Phenol concentration in the stripping phase	mM
Q	Volumetric flow rate of the stripping phase	$m^3.s^{-1}$
$c_{ph,strio(0)}$	Initial phenol concentration in the stripping phase	mM
ΔM	Phenol mass flow in the product stream	$g.min^{-1}$
$M_{plu,b}$	Pluronic mass flow in the product stream	$g.min^{-1}$

φV_a	Flow rate of the extraction stream	$ml.min^{-1}$
φV_a	Flow rate of the product stream	$ml.min^{-1}$
$c_{ph,b}$	Phenol concentration in permeate unimer separation unit	$g.L^{-1}$
$c_{ph,c}$	Phenol concentration in retentate unimer separation unit	$g.L^{-1}$
ΔE	Cooling energy	$kJ.min^{-1}$
c_p	Specific heat capacity	$J.g^{-1}.K^{-1}$
m	Mass flow of the solvent	$g.min^{-1}$
A_{unit2}	Membrane area integrated membrane unit	m^2
A_{unit4}	Membrane area unimer separation unit	m^2
A_{unit6}	Membrane area micelle separation unit	m^2
$Q_{filtrate}$	Filtrate volumetric flux	$m^3.s^{-1}$
F_{max}	Filtrate flux per membrane area	$m^3.m^{-2}.s^{-1}$
$M_{ph,permeate}$	Phenol mass flow permeate of integrated membrane unit	$g.s^{-1}$
dc	Driving force integrated membrane unit	$g.m^{-3}$
P	Partition coefficient	-
$\varphi V_{solvent}$	Solvent flow rate	$ml.min^{-1}$

Subsripts:

ph	Phenol
plu	Pluronic
b	Bulk (reactor)
s	Stripping phase
m	Micellar phase
aq	Aqueous phase
u	Unimeric phase
r	Retentate
f	Filtrate

References

1. Tsurumi, D.; Yoshimura, T.; Esumi, K., Adsolubilization of 2-naphthol into adsorbed layer of PEO-PPO-PEO triblock copolymers on hydrophilic silica. Journal of Colloid and Interface Science 2006, 465-469.

2. Nagarajan, R., Solubilization of hydrocarbons and resulting aggregate shape transitions in aqueous solutions of Pluronic(R) (PEO-PPO-PEO) block copolymers. Colloids and Surfaces B: Biointerfaces 1999, 55-72.

3. Lebens, P.J.M.; Keurentjes, J.T.F., Temperature-induced solubilization of hydrocarbons in aqueous block copolymer solutions. Industrial and Engineering Chemistry Research 1996, 3415-3421.

4. Wang, Y.D.; Gan, Q.; Shi, C.Y.; Zheng, X.L.; Yang, S.H.; Li, Z.M.; Dai, Y.Y., Separation of phenol from aqueous solutions by polymeric reversed micelle extraction. Chemical Engineering Journal 2002, 95-101.

5. Wierckx, N.J.P.; Ballerstedt, H.; De Bont, J.A.M.; Wery, J., Engineering of solvent-tolerant *Pseudomonas putida* S12 for bioproduction of phenol from glucose. Applied and environmental microbiology 2005, 8221-8227.
6. Heerema, L.; Cakali, D.; Roelands, M.; Goetheer, E.; Verdoes, D.; Keurentjes, J., Micellar solutions of PEO-PPO-PEO block copolymers for *in-situ* phenol removal from fermentation broth. Separation and Purification Technology Accepted for publication.
7. Luong, J.H.T., Kinetics of ethanol inhibition in alcohol fermentation. Biotechnology and Bioengineering 1984, 280-285.
8. Berg, C.v.d.; Wierckx, N.; Vente, J.; Bussmann, P.; Bont, J.d.; Wielen, L.v.d., Solvent-impregnated resins as an in-situ product recovery tool for phenol recovery from *Pseudomonas putida S12TPL* fermentations. Biotechnology and Bioengineering 2008, 466-472.
9. Heerema, L.; Wierckx, N.; Roelands, M.; Hanemaaijer, J.H.; Goetheer, E.; Verdoes, D.; Keurentjes, J., Pertraction for *in-situ* phenol removal from fed-batch fermentations of solvent tolerant *Pseudomonas putida* S12. In preparation.
10. Luong, J.H.T., Kinetics of ethanol inhibition in alcohol fermentation. Biotechnology and Bioengineering 1985, 280-285.
11. Meilleur, L.; Hardy, A.; Quirion, F., Probing the structure of pluronic PEO-PPO-PEO block copolymer solutions with their apparent volume and heat capacity. Langmuir 1996, 4697-4703.
12. Intelligen Superprodesigner, 7.5; 1991.
13. Berg, C.v.d., Personal communication In Delft, 2009; p Table of solvents with their properties.
14. Lide, D.R., CRC Handbook of Chemistry and Physics. 89th Edition ed.; CRC Press/Taylor and Francis: Boca Raton, FL, Vol. Version 2009 of the Internet Edition.
15. Gonzalez-Munoz, M.J.; Luque, S.; Alvarez, J.R.; Coca, J., Recovery of phenol from aqueous solutions using hollow fibre contactors. Journal of Membrane Science 2003, 181-193.
16. Xiao, M.; Zhou, J.; Tan, Y.; Zhang, A.; Xia, Y.; Ji, L., Treatment of highly-concentrated phenol wastewater with an extractive membrane reactor using silicone rubber. Desalination 2006, 281-293.
17. Han, S.; Ferreira, F.C.; Livingston, A., Membrane aromatic recovery system (MARS) -- a new membrane process for the recovery of phenols from wastewaters. Journal of Membrane Science 2001, 219-233.
18. Gonzalez-Munoz, M.J.; Luque, S.; Alvarez, J.; Coca, J., Simulation of integrated extraction and stripping processes using membrane contactors. Desalination 2004, 1-12.
19. Choi, Y.-k.; Lee, S.-B.; Lee, D.-J.; Ishigami, Y.; Kajiuchi, T., Micellar enhanced ultrafiltration using PEO-PPO-PEO block copolymers. Journal of Membrane Science 1998, 185-194.
20. Sabate, J.; Pujola, M.; Centelles, E.; Galan, M.; Llorens, J., Determination of equilibrium distribution constants of phenol between surfactant micelles and water using ultrafiltering centrifuge tubes. Colloids and Surfaces A: Physicochemical and Engineering Aspects 1999, 229-245.
21. Stejskal, J.; Hlavatá, D.; Sikora, A.; Konnák, C.; Plestil, J.; Kratochvíl, P., Equilibrium and non-equilibrium copolymer micelles: polystyrene-block-poly (ethylene-co-propylene) in decane and in diisopropylether. Polymer 1992, 3675-3685.
22. Purkait, M.K.; DasGupta, S.; De, S., Separation of aromatic alcohols using micellar-enhanced ultrafiltration and recovery of surfactant. Journal of Membrane Science 2005, 47-59.

Chapter 7

Discussion and future perspectives

7.1 Integrated membrane extraction as an in-situ product recovery tool

Bio-catalytic processes for the sustainable production of chemicals focus on the transition from the use of fossil-based raw materials to renewable bio-based materials. Although the micro-organisms that are used in these processes can reach high production rates, they are often limited by product inhibition or toxicity. The use of in-situ product removal (ISPR), the removal of the inhibiting products from the bioreactor during growth and production reactions, is a useful strategy to overcome this problem. This thesis describes the evaluation of the potential of integrated membrane extraction for the removal of toxic or inhibiting products from a fermentation broth. The production of phenol by a recombinant strain of *Pseudomonas putida* S12 was used as a model process for experimental and theoretical studies. This chapter discusses the main findings of the work described in this thesis and, additionally, presents a novel concept that could be interesting for future work in this field.

The work presented in this thesis shows that biomass growth and phenol production are inhibited at low phenol concentrations (2 mM) in fed-batch fermentations. After implementation of in-situ pertraction, a lower maximum aqueous phenol concentration is reached and the total phenol production is increased. The volumetric productivity appears to slightly increase while the specific productivity of phenol remains constant. However, the removal rate of phenol from the reactor in the experiments described in chapter 3 was not high enough to maintain the phenol concentration below limiting values. Therefore, a large improvement by applying ISPR could not yet be demonstrated.

A conceptual process design and economical evaluation illustrate the benefits and disadvantages of ISPR with an implemented membrane extraction unit in a bioreactor as compared to ISPR with a membrane extraction unit outside the reactor. Running the fermentation process at a lower product concentration results in a more efficient substrate utilization into biomass and phenol. The disadvantage of the integrated process, however, is the need for large distillation columns and a high energy input for solvent regeneration due to the low product concentration in the solvent and the high solvent flows.

Mass transfer studies in model fermentation systems and single-fiber modules result in a membrane extraction module design for implementation in a large scale bioreactor. Factors that are found to influence the overall mass transfer coefficient are the membrane (wall thickness), solvent (partition coefficient), sterilization and fouling. Furthermore, the presence of a membrane module in the reactor can give rise to several bottlenecks for both the separation process and biological growth and production processes, mainly caused by the altered mixing pattern.

Additionally, this thesis describes the use of alternative solvents of polymeric micelles solubilized in water in a membrane extraction process. Experimental results show that Pluronic micelles allow extraction of phenol from aqueous solutions at 30 °C (fermentation temperature). The phenol is

released due to the transition of the Pluronic micelles into unimers with a mild temperature switch from 30 to 8 °C. Steady state model analysis and cost estimation show that the process costs are mainly determined by the required membrane area.

The integration of a membrane extraction unit in a bioreactor can lead to several process constraints. The conditions for the pertraction process are equal to the conditions of the bioprocess because both processes take place in the same environment. The fermentation broth, for example, has a temperature of 30 °C and a pH of 7 at atmospheric pressure. At this temperature, the micro-organisms have optimal growth and/or production although the pertraction process is more effective at higher temperatures. In addition, the pH of the broth determines the charge of the product of interest, depending on its isoelecric point, which can cause difficulties in the extraction process. Additionally, a bioreactor has a certain volume occupied by stirrers, air and electrodes, while additional volume is required for the membrane module. Furthermore, the level of oxygen in the liquid phase of a fermentation process has to be maintained at a certain level to keep the micro-organisms active. A membrane module might alter the liquid flow pattern and, consequently, the oxygen transfer pattern and the performance of the micro-organisms. Additional experiments and models describing fluid dynamics will gain a better understanding of the dynamics of the system and allow for an optimal design of the integrated fermentation-pertraction system. Various examples describing fluid dynamics in bioreactors can be found in literature [1-3].

Furthermore, it has to be considered that a fermentation broth contains numerous components besides the product of interest. These components can be co-extracted which can lead to impurity of the product stream or to poor performance of the micro-organisms by depletion of essential components from the reactor. The products inside the reactor, e.g. sugars, salts, minerals and micro-organisms, can additionally lead to fouling of the membrane surface or the pores which can cause decreased transport of the desired product from the reactor to the stripping (solvent) phase. In this thesis, it was demonstrated that the sterilization of the membrane in the reactor combined with the presence of medium components has a negative effect on the overall mass transfer coefficient.

Optimization and further decrease of the product cost price for an integrated pertraction process can be realized by improvement of the pertraction process, e.g. by improved mass transfer using a solvent with a higher partition coefficient, decreasing the membrane wall thickness or using a larger membrane area. A solvent with higher partition coefficient will reduce the overall mass transfer coefficient, however, such a solvent usually dissolves well in water and vice versa. This can lead to additional solvent toxicity and to more difficult and expensive solvent regeneration processes. Pluronic solvents are an alternative due to the mild regeneration conditions and low toxicity, although these solvents have low partition coefficients as compared to organic solvents. The Pluronic process has potential for products that allow for a high concentration in the reactor, especially when exceeding solubility after regeneration causes a phase separation of the product. Additionally, improvement of

the microbial metabolism by further optimization of the bacterial strain can result in a higher phenol production rate and/or a more efficient substrate consumption. In turn, this can improve the driving force for pertraction and lower the substrate costs. Furthermore, a decrease in raw material cost price or the use of an alternative carbon source will have a significant effect on the phenol cost price.

The overall mass transfer coefficient in the reactor can be improved relatively easy by changing the membrane type, by increasing the membrane area or by choosing another solvent. However, the decrease in the mass transfer due to the presence of components in the reactor is a challenge to be handled. In the following section, a novel concept to deal with this challenge will be described: a discontinuous moving membrane module for improvement of the shell-side mass transfer coefficient.

7.2 Discontinuous moving membrane module

Fouling of micro-organisms and medium components at the aqueous (shell) side of the membrane has a negative effect on the overall mass transfer coefficient. The fouling at the membrane surface and/or in the pores will increase the boundary layer thickness at the surface and, as a consequence, the overall mass transfer coefficient will decrease. Additionally, due to the blockage of pores, which are filled with solvent, fouling can decrease the available contact area between the solvent and the fermentation broth. To decrease the thickness of the boundary layer and to avoid pore blockage, several strategies can be followed, for example by increasing the turbulence at the membrane surface. Increased turbulence can be achieved by applying a higher stirring rate in the reactor or by the use of alternative membrane modules which cause high surface shear rates along the membrane. Different authors describe rotating [4] or vibrating [5, 6] membrane modules, the addition of external forces such as ultrasound [7] or membrane surface modification [8-11] to reduce fouling at the membrane surface and to improve the flux in (pressure driven) (micro)filtration processes. Although the driving force for a membrane extraction process is mainly the concentration difference instead of pressure, it is worthwhile to investigate the possibility to use a technique comparable to the concepts mentioned above for the processes described in this thesis. This paragraph describes the experimental evaluation of an integrated membrane module with a high and turbulent water flow along the membrane surface.

Description of the novel membrane module

A membrane module has been developed that moves up and down discontinuously. Due to the movement of the module the thickness of the boundary layer at the membrane surface can be decreased and the overall mass transfer coefficient is expected to improve. In Figure 1 a schematic representation and a photograph of the module is given. The module consists of vertically mounted polypropylene membrane tubes in a PVC housing. The inside of the membrane tubes is contacted with the aqueous phase in the solution. The module has a central connection with a stainless steel tube

where the filtrate is removed by applying a constant pressure (0.1 bar). In Table 1 the membrane module properties are summarized. The membrane module was tested in a microfiltration setup using *Sacheromyces cerevisiae* solutions.

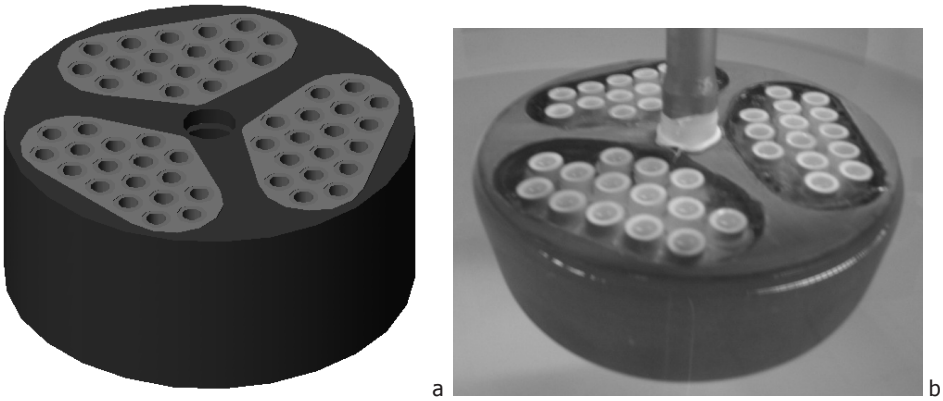

a b

Figure 1. Schematic representation of the membrane module design (a) and a photograph of the experimental module (b).

Table 1. Module properties.

Property	**Value**	**Unit**
Module total height	50	mm
Membrane height	40	mm
Surface topside module	78.5	cm^2
Volume module	392	cm^3
Membrane (outer) diameter	8,6	mm
Cross sectional area membrane tube	58	mm^2
Number of membranes	42	-
Filtration area per membrane	691	mm^2
Filtration area	290	cm^2

Description of the microfiltration experiments

A yeast solution containing 175 $g.L^{-1}$ of wet *S. cerevisiae* (equal to a dry weight of approximately 60 $g.L^{-1}$) was filtered using the module in stationary mode and with a discontinuous moving module (1 s^{-1}). In stationary mode the process is a dead-end filtration with a liquid flow perpendicular to the membrane (see Figure 2a). In the discontinuous moving mode the process is a cross flow filtration with the liquid flow parallel to the membrane surface (see Figure 2b). The yeast concentration in the

reactor was maintained at a constant level by addition of a feed of medium (physiological salt) at room temperature and the reactor volume used was 3 L (small space of 5 mm between module and reactor wall) and 10 L (large space between module and reactor wall), respectively. In Figure 3 a schematic presentation of the experimental setup is given. During the experiments the filtrate volume is monitored in time.

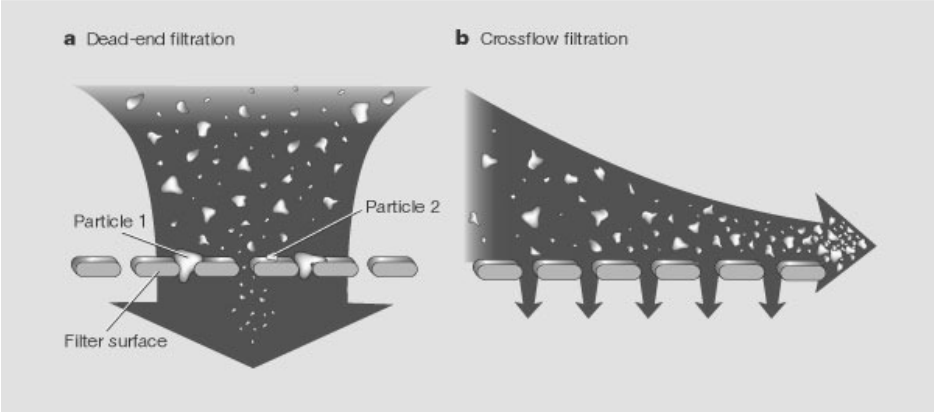

Figure 2. Dead-end filtration (a) and crossflow filtration (b).

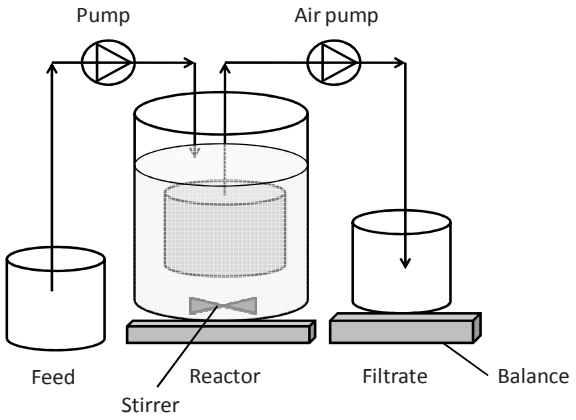

Figure 3. Experimental setup.

Results and discussion microfiltration experiments

In Figure 4 the experimental results are given for the microfiltration module in stationary and moving mode. Additionally, the results of filtration of water is given. Figure 4a illustrates the filtration of water at room temperature which is constant in time. The clean water flux was determined to be approximately 1000 $L.m^{-2}.bar^{-1}.h^{-1}$. Figure 4b illustrates filtration of water after a yeast filtration experiment after removal of the filter cake by back flushing with air, rinsing with water and without treatment with cleaning chemicals. An increase in time per total volume shows that fouling occurred in the membrane pores and that chemical cleaning with 1 M sodium hydroxide solution is necessary after each experiment to reach the original clean water flux. Figure 4c illustrates a stationary filtration of a yeast solution. Fouling by yeast cells on the membrane surface and in the pores causes a cake formation and the flux decreases in time until the cake prevents water to pass (zero flux). Figure 4d illustrates the filtration of a yeast solution in a 3 L reactor with a discontinuous moving membrane module. The time needed to reach a certain filtrate volume is much lower as compared to the time needed to reach comparable filtrate volume in the stationary mode. By the movement in a small reactor, the liquid was forced through the membrane tubes with a high flow rate (approximately 0.04 $m.s^{-1}$) and thus a high shear force. The high shear force reduced the fouling and thus a higher flux was reached as compared to the stationary mode. Figure 4d additionally shows a decrease in slope with higher filtrate volumes which indicates the existence of an equilibrium between particles that are kept on the membrane causing fouling and particles that are removed from the membrane decreasing fouling. Using the derivative of the filtration line, it was determined that after 10 L filtrate volume and approximately 3.4 hours of filtration this equilibrium was reached. The equilibrium flux is approximately 50 $mL.min^{-1}$, which is 148 $L.m^{-2}.bar^{-1}.h^{-1}$, approximately 15% of the clean water flux.

The filtration of a yeast solution in a 10 L reactor with a discontinuous moving membrane module showed the same trend as compared to the 3 L reactor but reached a lower equilibrium flux. Using a larger reactor, the flow rate through the membrane tubes was lower (approximately $7*10^{-3}$ $m.s^{-1}$). The equilibrium value of the flux was reached after 2 L filtrate volume and is approximately 22 $mL.min^{-1}$, which is 63 $L.m^{-2}.bar^{-1}.h^{-1}$, approximately 6% of the clean water flux.

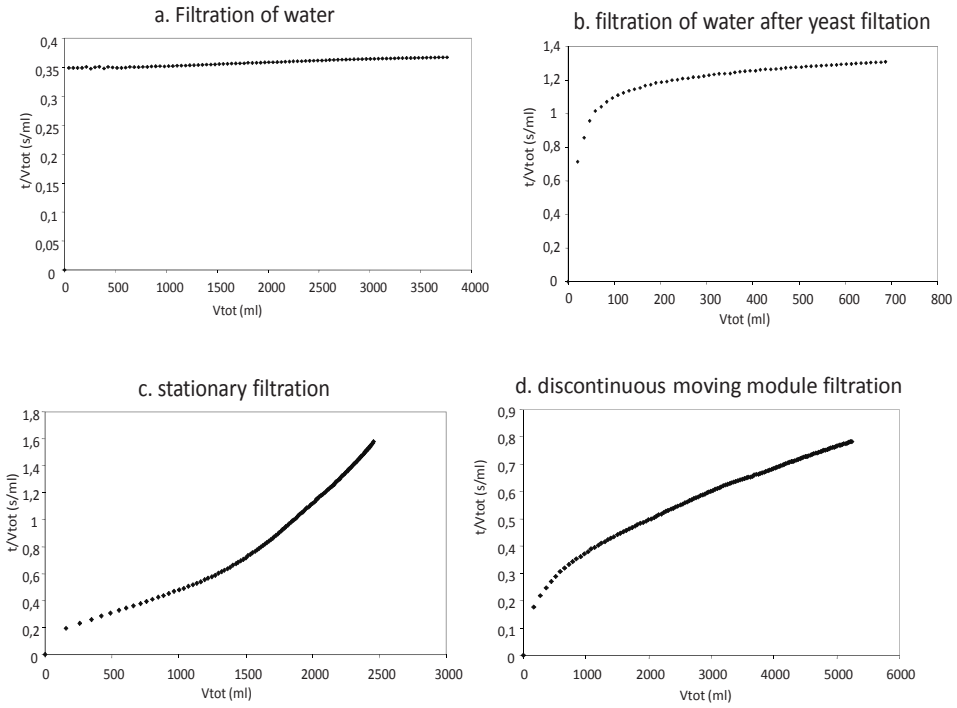

Figure 4. Filtration of water (a and b), stationary flux (c) and flux at discontinuous movement (d).

Conclusion microfiltration experiments

In the previous paragraph a novel microfiltration membrane module that can reduce the fouling and improve the filtrate flux by moving discontinuously was described. This concept can possibly be used for the membrane extraction processes described in this thesis. Using a discontinuously moving membrane extraction module, the boundary layer at the membrane surface can be minimized and the overall mass transfer coefficient can be improved. However, when using the membrane module in an extraction setup, the solvent in the moving membrane module might leak into the aqueous phase. Additional research should therefore be executed to explore the possibilities of the module for membrane extraction purposes. Alternatively, using the module in microfiltration mode in the reactor with a membrane extraction unit outside the reactor is another option to remove the product of interest. Using the module as an in-situ microfiltration unit, the shear-sensitive cells remain in the reactor without pumping around large fermentation streams. To minimize the fouling at the membrane surface and in the membrane pores, the membrane should always be cleaned after use with cleaning chemicals before a new process can be initiated.

Finally, it should be considered how the fluid dynamics in the reactor change when using a discontinuous moving membrane module instead of a standard stirrer configuration. Mixing properties will change and thus the oxygen transfer coefficient into the broth should also be studied. Also, energy requirement may become a part of attention.

7.3 Concluding remarks

This thesis illustrates the potential of integrated membrane extraction as a tool for in-situ product removal. The implementation of pertraction in a fermentation process for the production of an inhibiting compound is a realistic perspective. Although several improvement strategies are necessary, the work described in this thesis may contribute to the knowledge on the possibilities and constraints of the integration of a separation process in a bioproduction process and may be helpful for future work in developing and implementing such processes.

References

1. Ahmed, S.U.; Ranganathan, P.; Pandey, A.; Sivaraman, S., Computational fluid dynamics modeling of gas dispersion in multi impeller bioreactor. Journal of Bioscience and Bioengineering 2010, 588-597.
2. Andreas, L., Advanced methods for bioreactor characterization. Journal of Biotechnology 1992, 145-182.
3. Gogate, P.R.; Beenackers, A.A.C.M.; Pandit, A.B., Multiple-impeller systems with a special emphasis on bioreactors: a critical review. Biochemical Engineering Journal 2000, 109-144.
4. Bouzerar, R.; Ding, L.; Jaffrin, M.Y., Local permeate flux-shear-pressure relationships in a rotating disk microfiltration module: implications for global performance. Journal of Membrane Science 2000, 127-141.
5. Beier, S.P.; Jonsson, G., Separation of enzymes and yeast cells with a vibrating hollow fiber membrane module. Separation and Purification Technology 2007, 111-118.
6. Frappart, M.; Jaffrin, M.Y.; Ding, L.H.; Espina, V., Effect of vibration frequency and membrane shear rate on nanofiltration of diluted milk, using a vibratory dynamic filtration system. Separation and Purification Technology 2008, 212-221.
7. Kyllönen, H.M.; Pirkonen, P.; Nyström, M., Membrane filtration enhanced by ultrasound: a review. Desalination 2005, 319-335.
8. Hilal, N.; Kochkodan, V.; Al-Khatib, L.; Levadna, T., Surface modified polymeric membranes to reduce (bio)fouling: a microbiological study using E. coli. Desalination 2004, 293-300.
9. Hilal, N.; Al-Khatib, L.; Atkin, B.P.; Kochkodan, V.; Potapchenko, N., Photochemical modification of membrane surfaces for (bio)fouling reduction: a nano-scale study using AFM. Desalination 2003, 65-72.
10. Yu, H.-Y.; Hu, M.-X.; Xu, Z.-K.; Wang, J.-L.; Wang, S.-Y., Surface modification of polypropylene microporous membranes to improve their antifouling property in MBR: NH3 plasma treatment. Separation and Purification Technology 2005, 8-15.
11. Taniguchi, M.; Kilduff, J.E.; Belfort, G., Low fouling synthetic membranes by UV-assisted graft polymerization: monomer selection to mitigate fouling by natural organic matter. Journal of Membrane Science 2003, 59-70.

Curriculum Vitae

Louise Heerema was born on the 23th of September 1979 in Den Haag. She finished the secondary school at the Scholengemeenschap Alverna in Leiden in 1998. That same year she started her Bachelor of Life Science and Technology with specialization biochemistry and biotechnology which she successfully finished with a thesis research in fermentation technology at Unilever R&D in Vlaardingen. In 2002 she received her BSc degree after which she started working as a technician fermentation at DSM Food Specialties in Delft. In 2003 she started her Master of Life Science and Technology with the profile Cell Factory at the TU Delft. Her thesis research at former Diosynth/ Organon in Oss at the Department Quality & Regulatory Unit/ Analytical Development and the Department Research & Development/ Down Stream Processing was focused on analytical aspects of micro chip technology and the improvement of the refolding kinetics of a particular protein. In August 2005 she started her PhD research at TNO Separation Technology which is described in this thesis. Currently, she is working as a project leader at Sanquin Plasmaproducts at the department of process development and support working on the production and separation processes of proteins from human blood plasma.

Publications

Heerema, L.; Roelands, M.; Hanemaaijer, J. H.; de Bont, J.; Verdoes, D., In-situ phenol removal from fermentation broth by pertraction. *Desalination* 2006, 200, 485-487.

Heerema, L.; Cakali, D.; Roelands, M.; Goetheer, E.; Verdoes, D.; Keurentjes, J., Micellar solutions of PEO-PPO-PEO block copolymers for in situ phenol removal from fermentation broth. *Sep. Purif. Technol.* 2010, 73, 319-326.

Heerema, L.; Cakali, D.; Roelands, M.; Goetheer, E.; Verdoes, D.; Keurentjes, J., Evaluation of an integrated extraction process for in-situ phenol removal with micellar solutions of PEO-PPO-PEO block copolymers. *Sep. Purif. Technol.* 2010, 74, 55-63.

Heerema, L.; Wierckx, N.; Roelands, M.; Hanemaaijer, J. H.; Goetheer, E.; Verdoes, D.; Keurentjes, J., In situ phenol removal from fed-batch fermentations of solvent tolerant Pseudomonas putida S12 by pertraction. *Biochem. Eng. J.* 2011, 53, 245-252.

Heerema, L.; Roelands, M.; Goetheer, E.; Verdoes, D.; Keurentjes, J., In-Situ Product Removal from Fermentations by Membrane Extraction: Conceptual Process Design and Economics. Industrial & Engineering Chemistry Research 2011, 50, 9197-9208.

Heerema, L.; Roelands, M.; Goetheer, E.; Verdoes, D.; Keurentjes, J., Strategies for module design for *in-situ* product removal from fermentations by membrane extraction *Submitted* 2011.

Dankwoord

Na vier jaar van experimenten uitvoeren, opstellingen in elkaar knutselen, modellen in elkaar zetten en nog twee extra jaar schrijfwerk naast mijn huidige baan is mijn proefschrift nu eindelijk af! Ik ben erg blij dat het nu klaar is en ik mag zeggen dat ik veel heb geleerd tijdens mijn tijd bij TNO Scheidingstechnologie. Met dit dankwoord wil ik een aantal mensen graag bedanken voor hun bijdrage aan het tot stand komen van dit proefschrift.

Allereerst wil ik mijn promotor Jos Keurentjes bedanken voor het vertrouwen in mij en de steun en discussies tijdens de besprekingen die we tussendoor in hebben kunnen plannen van Apeldoorn tot Eindhoven en sinds je baan bij Akzo voornamelijk via de telefoon. Ook Luuk van der Wielen wil ik bedanken om mijn promotie in Delft mogelijk te maken. Mijn (dagelijkse) begeleiders van TNO Mark, Dirk en Earl wil ik graag bedanken voor hun geduld, vertrouwen, steun en de levendige discussies met veel goede ideeën over en voor mijn werk en/of mijn artikelen. Voor Mark een extra bedankje voor zijn hulp in het laatste stadium tijdens de afronding van mijn proefschrift.

Mijn mede scheidings-aio's Corjan en Jan Harm wil ik ook bedanken voor onze nuttige discussies over het ISPR werk en hun gezelligheid als kamergenoten. We hebben samen leuke jaren meegemaakt. Corjan de deeltjes-man, bedankt voor je gezelligheid, enthousiasme en het feit dat je altijd klaar stond voor discussie of hulp. Jan Harm, bedankt voor je hulp, rust, nuchterheid, gezelligheid en scherpe opmerkingsvermogen. Ook de rest van de Apeldoornse en Delftse (ex)collega's van Scheidingstechnologie wil ik bedanken voor hun hulp en de leuke herinneringen aan de koffiepauzes, borrels, uitjes, sinterklaas- en kerst feestjes, Wageningen party's en etentjes. Dank je hiervoor Sanaz ("roomie"), Arjen, Mohammad, Peter(tje), Hannie, Peter Jan, Eva, Jitske, Jan Henk en Hans (van der Meer, de Jong en Brouwer). Ook wil ik de "bio-aio's" en medewerkers van TNO Bioconversie bedanken: Luaine, Nick, Frank, Jean-Paul, Suzanne, Rita, Karin, Maaike, Harald, Jan Wery, Jan de Bont voor de discussies, gezelligheid, de borrels en feestjes en het geduld met mijn altijd naar octanol stinkende fermentoren.

Mijn stagiaires Marcel, Doga en Xin wil ik bedanken voor hun input en enthousiasme. Jullie werk heeft mij stuk voor stuk bruikbare informatie opgeleverd voor mijn artikels. Ook de twaio's Laura en Leila wil ik graag bedanken voor hun bijdrage aan de uitgebreide Matlab modellen.

Marcel Jansen, bedankt dat je me tijdens mijn baan bij Sanquin de ruimte hebt gegeven die ik nodig had voor de afronding van mijn proefschrift.

Ook wil ik graag mijn ketel vrienden en in het bijzonder Droes, Henny en Wietske bedanken. Zonder jullie luisterend oor, kracht en de nodige "duwtjes" zou ik het afronden van dit proefschrift

waarschijnlijk nog langer hebben uitgesteld. Ik ben zoveel veranderd en sterker geworden sinds ik twee jaar terug als half overspannen aio binnen kwam lopen!

Als laatste wil ik graag mijn ouders Thelma en Peter, Barend, Granny, de rest van mijn familie en vrienden bedanken voor hun steun en hun altijd aanwezige interesse in de voortgang van mijn promotiewerk.
Voor iedereen die ik nog ben vergeten: bedankt. Nu is het klaar, het is gedaan! Punt!

Louise

Supplementary data Chapter 3

Appendix 1 – Supplementary data Chapter 3

Table 1. Battery limits

ISBL	**OSBL**
Fermentation unit	Raw materials treatment and storage
Biomass concentration unit	Product storage and distribution
ISPR unit (integrated case)	Utilities
Product concentration unit (non-integrated case)	Waste treatment and disposal
Auxiliary phase regeneration and product purification units (if applicable)	Piping and electrical equipment
Temperature change (heat exchangers)	Basic instrumentations and control
Pressure change (compressors, pumps)	Civil and structural design aspects
Phase change (evaporators, condensers)	Plant layout
Transport (conveyors, pumps, compressors) equipment	

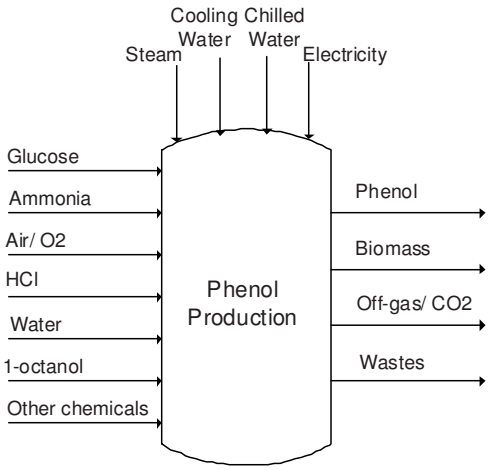

Figure 1. Representation of most important in and outgoing streams of the non-integrated and integrated processes for the phenol production plants. Raw materials (left) and utilities (top) fed to the process and product (phenol), by-products (biomass and Off-gas/ CO_2) and wastes (right) resulting from the process operation are depicted.

Table 2. Microbial kinetic model equations in the fermentation section

Parameter	Equation*	Unit
Biomass growth	$\mu = \mu^{max} \cdot \frac{C_S}{k_S + C_S} exp\left(-\frac{C_P}{k_{tox}}\right)$	h^{-1}
Phenol production	$q_P = \frac{q_p^{\max} \cdot \mu}{\beta + \mu} \cdot \left[1 - \exp\left(-\left(\frac{C_P}{\varepsilon}\right)^{-\delta}\right)\right]$	$mol.mol^{-1}.h^{-1}$
Biomass death/ inactivation	$K_{death}(C_p) = k_d \cdot \exp\left(\frac{C_p}{k_{cd}}\right)$	h^{-1}
Glucose consumption	$q_s = -\left(\frac{1}{Y_{sx}^{\max}} \cdot \mu + \frac{1}{Y_{sp}^{\max}} \cdot q_p + m_s\right)$	$mol.mol^{-1}.h^{-1}$
Oxygen consumption	$q_O = -\left(\frac{1}{Y_{ox}^{\max}} \cdot \mu + \frac{1}{Y_{op}^{\max}} + m_o\right)$	$mol.mol^{-1}.h^{-1}$

*The first 3 equations were derived from literature, TNO internal reports on kinetic modeling and internal communication within the TNO bioconversion group (for example J. Wery, N.Wierckx). Equations and constants were based on actual experimental data and metabolic network model analysis.

Table 3. Material balances in fermentation

Parameter	Equation
Substrate (glucose)	$0 = q_S \cdot C_X \cdot V_L - \phi_{out} \cdot C_S + \phi_{in} \cdot C_{S,in}$
Biomass	$0 = (\mu(C_S, C_P) - K_{death}(C_P)) \cdot C_X \cdot V_L - \phi_{out} \cdot C_X$
Dead/ inactive biomass	$0 = K_{death}(C_P) \cdot C_X \cdot V_L - \phi_{out} \cdot C_{Xd}$
Product (phenol)	$0 = q_P(C_S, C_P) \cdot C_X \cdot V_L - \phi_{out} \cdot C_S - ER \cdot V_L$
Overall	$0 = \phi_{in} + \phi_{rec} + q_O \cdot C_X \cdot \frac{V_L \cdot MW_O}{\rho_w} + q_C \cdot C_X \cdot \frac{V_L \cdot MW_C}{\rho_w} - \phi_{out}$

Table 4. Additional equations for the fermentation section

Parameter	**Equation**	**Unit**
Oxygen uptake rate	$OUR = -q_o \cdot C_x$	mol.m^{-3}.h^{-1}
Oxygen transfer rate (OTR=OUR at 20% oxygen saturation)	$k_L \cdot a = \frac{-q_o \cdot C_x}{0.8 \cdot C^*_{o,L}}$ Or: $k_L \cdot a = 0.32 \cdot vG^{0.7}$	(m.s^{-1}).(m^2)
Oxygen concentration in the liquid phase at equilibrium conditions with the gas phase (P=2 atm)	$C^*_{o,L} = H_o \cdot (P \cdot x_o)$ With: $H_o = 35 \cdot \exp\left(2400 \cdot \left(\frac{1}{T + 273.15} - \frac{1}{T_0}\right)\right)$	mol.m^{-3}
Rate of heat removal in the heat exchanger system of a jacket vessel	$r_H = U \cdot \frac{A_h}{V_L} \cdot (T - T_{CW})$ With: $A_h = \pi \cdot D \cdot H$	W.m^{-3}

Appendix 1 – Supplementary data Chapter 3

Table 5. Constants used in the fermentation model

Parameter	**Symbol**	**Value**	**Unit**
Maximal growth rate	μ_{max}	0,3	h^{-1}
Glucose affinity constant	k_s	1	mol $S.m^{-3}$
Inhibition parameter 1	ε	4	mol $P.m^{-3}$
Inhibition parameter 2	δ	3	-
Maximum specific phenol production rate	q_p^{max}	0.02	mol $P.(C\text{-mol } X)^{-1}.h^{-1}$
Phenol production parameter	β	0.01	h^{-1}
Toxicity parameter	k_{tox}	5	mol $S.m^{-3}$
Maximum specific death/ inactivation rate	k_d	0.0010	h^{-1}
Death parameter	k_{cd}	5	mMol $P.m^{-3}$
Maximum yield of biomass on glucose	Y_{SX}^{max}	3	$(C\text{-mol } X).(\text{mol } S)^{-1}$
Maximum yield of phenol on glucose	Y_{SP}^{max}	0.3	$(\text{mol } P).(\text{mol } S)^{-1}$
Maintenance coefficient	$-m_s$	0.0016	$(\text{mol } S).(C\text{-mol } X)^{-1}$
Henry's constant for oxygen in water	H_o	1.2	$mol.m^{-3}.bar^{-1}$
Oxygen molar fraction present in the gas phase	x_o	0.21	-
Overall heat transfer coefficient accounting for all heat transfer resistances (280 – 850)	U	Average 565	$W.m^{-2}.K^{-1}$
Height to diameter ratio fermentor	H/D	3	$m.m^{-1}$
Gas constant	R_g	8.314	$J.g^{-1}.mol^{-1}.K^{-1}$
Specific heat capacity gas	c_{pg}	1013	$J.kg^{-1}.K^{-1}$
Temperature of the gas	T_g	30	°C
Specific heat capacity of feed substrate	c_{pS}	4186	$J.kg^{-1}.K^{-1}$
Specific heat capacity of feed nitrogen	c_{pN}	4142	$J.kg^{-1}.K^{-1}$
Specific heat capacity of feed hydrochloric acid	c_{pHCl}	2610	$J.kg^{-1}.K^{-1}$

Table 6. Equations used for fermentor sizing and utilities

Parameter	**Equation**	**Unit**
Fermentor diameter	$D = \left(\frac{4.V_{ferm}}{\frac{H}{D}.\pi}\right)^{1/3}$	m
Fermentor height	$H = \frac{H}{D}.D$	m
Fermentor gasflow power input	$P_g = F_{g,in}.R_g.T_g.\log\left(\frac{P_b}{P_t}\right)$	W
Total heat generated	$r_{ht} = r_{hm} + r_{hg} + r_{hf}$	W
Heat by metabolic activity	$r_{hm} = 460 \cdot 10^3 OUR \cdot V_{ferm}$	W
Heat by gas flowing through	$r_{hg} = c_{pg} \cdot (T_g - T_{broth}) \cdot F_{g,in} \cdot \rho_g$	W
Heat of feeding streams	$r_{hf} = r_{hS} + r_{hN} + r_{hHCl}$	W

Table 7. Equations used for the biomass separation unit

Parameter	**Equation**	**Unit**
Recycle ratio	$RR_{SL} = \frac{\phi_{rec}}{\phi_{in}}$	$(m^3.s^{-1}).(m^3.s^{-1})^{-1}$
Concentration factor	$CF = \frac{C_{x,con}}{C_x}$	$(g.L^{-1}).(g.L^{-1})^{-1}$
Volumetric medium flow rate to the fermentor	$\phi_{in} = \frac{\mu}{1 + RR_{SL} - RR_{SL} \cdot CF} \cdot V$	$m^3.s^{-1}$
Volumetric flow rate of the bleed stream after cell concentration (integrated case)	$\phi_{bleed} = \frac{\mu}{CF} \cdot V_L$	$m^3.s^{-1}$
Filtration flux	$F_{SL} = \mathrm{A_{SL}} \sqrt{\frac{2 \cdot \Delta p \cdot \omega \cdot \Delta\gamma}{\eta \cdot r \cdot C \cdot 4 \cdot \pi^2}}$ With: $A_{SL} = \pi \cdot D \cdot L$	$m^3.m^{-2}.s^{-1}$
Power input for filtration	$P_{SL} = \frac{\phi_{SL} \cdot \Delta p_{SL}}{n_{SL}}$	W

Table 8. Constants used in the biomass separation unit

Parameter	**Symbol**	**Value**	**Unit**
Recycle ratio (integrated case)	RR_{SL}	0.01	$(m^3.s^{-1}).(m^3.s^{-1})^{-1}$
Concentration factor	CF	20 (non-integr) 2 (integr)	$(g.L^{-1}). (g.L^{-1})^{-1}$
Filtrate density (water at 30°C)	ρ_f	996	$kg.m^{-3}$
Pressure drop over the membrane	Δp_{SL}	0.5	bar
Rotation speed	ω	3	rpm
Filtration angle	Δγ	2/3π	rad
Viscosity of the broth	η	0.02	$Pa.s^{-1}$
Specific cake resistance	r	$1*10^{13}$	m^{-2}
Medium resistance	C	$1*10^{10}$	m^{-1}

Table 9. Transport equations for the pertraction section

Parameter	Equation	Unit
Phenol concentration in the organic phase	$\frac{dC_p^{org}(x)}{dx} = A \cdot K^{aq} \cdot \left(C_p^{aq} - \frac{C_p^{org}(x)}{m_p^{w/org}} \right)$	
Overall mass transfer coefficient	$K^{aq} = \frac{1}{R^{total}}$ With: $R^{total} = R^{shell} + R^{memb} + R^{lumen}$	$m.s^{-1}$
Resistance in the outside of the membrane	$R^{shell} = \frac{d_o}{k_{shell} \cdot d_o}$	$(m.s^{-1})^{-1}$
Resistance in the membrane	$R^{memb} = \frac{d_o}{k_{memb} \cdot m_p^{w/org} \cdot d_{lm}}$	$(m.s^{-1})^{-1}$
Resistance in the lumen of the capillaries	$R^{lumen} = \frac{d_o}{k_{lumen} \cdot m_p^{w/org} \cdot d_i}$	$(m.s^{-1})^{-1}$
Mass transfer coefficient Shell (aqueous side)	$k_{shell} = \frac{D_w}{\Delta z}$	$m.s^{-1}$
Mass transfer coefficient membrane	$k_{memb} = \frac{D_{org} \cdot \varepsilon_m}{\tau \cdot tk}$	$m.s^{-1}$
Mass transfer coefficient lumen 1 (solvent side)	$k_{lumen1} = 1.5 \cdot \left(\frac{d_i^2 \cdot v_s}{D_{org} \cdot L} \right)^{1/3} \cdot \frac{D_{org}}{d_i}$ if: $\frac{d_i^2 \cdot v_s}{D_{org} \cdot L} > 4$	$m.s^{-1}$
Mass transfer coefficient lumen 2 (solvent side)	$k_{lumen2} = 1.62 \cdot \left(\frac{D_{org}^2 \cdot v_s}{d_i \cdot L} \right)^{1/3}$ if: $8 < k_{lumen} \cdot \frac{d_i}{D_{org}} < 40$	$m.s^{-1}$

Table 10. Additional equations pertraction

Parameter	**Equation**	
Number of membrane fibers required	$N_{fibers} = \frac{4 \cdot E}{C_p^{org} \cdot v_s \cdot \pi \cdot d_i^2 \cdot 3600}$	-
Required membrane area	$A_{memb} = N_{fibers} \cdot \pi \cdot d_{lm} \cdot L$	m^2
Specific membrane area	$a_{sp} = \frac{A_{memb}}{V_T}$	$m^2.m^{-3}$
Maximum specific membrane area	$a_{sp,\max} = \frac{\pi}{a \cdot b \cdot d_o}$ with a=2 and 1.1<b<3	$m^2.m^{-3}$
Concentration factor	$CF_P = \frac{C_p^{org,x=L}}{C_p^{aq}}$	-
External diameter of the membrane	$d_o = d_i + 2 \cdot tk$	m
Average diameter of the membrane	$d_{lm} = \frac{d_o - d_i}{\log d_o - \log d_i}$	m
Phenol diffusivity in water	$D_w = 7.4 \cdot 10^{-8} \cdot \frac{(\phi_w \cdot MW_w)^{0.5} \cdot T}{\mu_w \cdot (v_p \cdot 10^3)^{0.6}} \cdot 10^{-4}$	$m^2.s^{-1}$
Phenol diffusivity in 1-octanol	$D_{org} = 1.55 \cdot 10^{-8} \cdot T^{1.29} \cdot \frac{P_{org}^{0.5} / P_p^{0.42}}{\mu_{org}^{0.92} \cdot (v_{org} \cdot 10^3)^{0.23}} \cdot 10^{-4}$	$m^2.s^{-1}$
Solvent flux	$\phi_{tube} = \frac{E}{C_p^{org}}$	$m^3.s^{-1}$

Appendix 1 – Supplementary data Chapter 3

Table 11. Constants used in the pertraction model

Parameter	**Symbol**	**Value**	**Unit**
Solvent associated parameter water	ϕ_w	2.6	-
Solvent associated parameter 1-octanol	ϕ_{org}	1	-
Molecular weight water	MW_w	18.0	$g.mol^{-1}$
Pertraction temperature	T	30	°C
Viscosity water	μ_w	0.798	cP (at 30°C)
Visosity 1-octanol	μ_{org}	6.3	cP (at 30°C)
Density 1-octanol	ρ_{org}	824	$kg.m^{-3}$ (at 30°C)
Density water	ρ_w	996	$kg.m^{-3}$ (at 30°C)
Molecular volume phenol	ν_p	$101.6*10^{-3}$	$m^3.Kmol^{-1}$
Molecular volume 1-octanol	ν_{org}	$191.3*10^{-3}$	$m^3.Kmol^{-1}$
Partition coefficient of phenol between water and 1-octanol	$m_p^{w/org}$	28.8	-
Thickness of the diffusional layer around the membrane	Δz	10^{-5}	m
Length of the membrane	L	2.14 (I), 1.4 (NI)	m
Parachor 1-octanol	P_{org}	365.3	$cm^3.g^{1/4}.s^{-0.5}.mol^{-1}$
Parachor phenol	P_p	51	$cm^3.g^{1/4}.s^{-0.5}.mol^{-1}$
Parachor water	P_w	221.3	$cm^3.g^{1/4}.s^{-0.5}.mol^{-1}$

Table 12. Membrane characteristics (Accurel PP hydrophobic capillary membrane)

Parameter	**Symbol**	**Unit**	**Type V8/2 HF**	**Type S6/2**	**Type Q3/2**	**Type 150/330**
Pore size	d_p	mm	0.2	0.2	0.2	0.2
Internal fiber diameter	d_i	mm	5.5	1.8	0.6	0.6
Fiber wall thickness	tk	mm	1.55	0.45	0.2	0.2
Membrane tortuosity	τ	-	2.25	2.25	2.25	2.25
Membrane porosity	ε_m	-	0.8	0.8	0.8	0.8
Max. specific membrane area	a_{sp}	$m^2.m^{-3}$	61 – 166	194 – 529	524 – 1428	582 - 1587
Max. superficial solvent velocity	$v_{s,max}$ [a]	$m.s^{-1}$	0.05	0.05	0.39	-

[a] at CF>1 and ΔP<0.3 bar

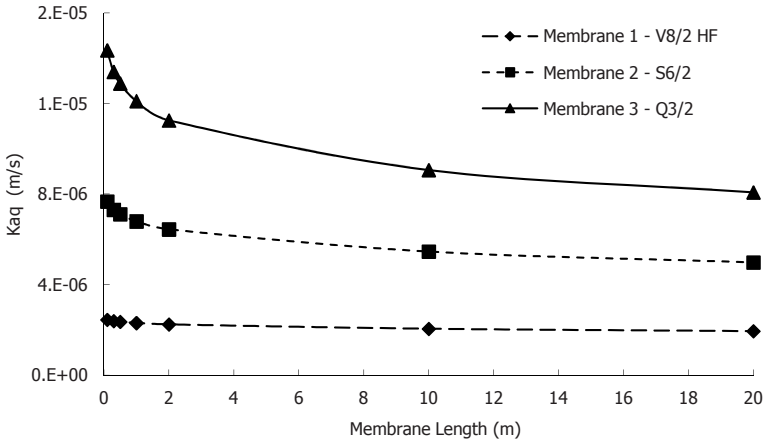

Figure 2. Analysis of the overall mass transfer coefficient (K^{aq}, $m.s^{-1}$) as a function of membrane length for three membrane types with a solvent velocity of 0.01 $m.s^{-1}$.

Table 13. Equations used for pertraction unit sizing and energy input

Parameter	**Equation**	**Unit**
Number of membrane fibers required	$N_{fibers} = \frac{4 \cdot E}{C_p^{org} \cdot v_s \cdot \pi \cdot d_i^2 \cdot 3600}$	-
Required membrane area	$A_{memb} = N_{fibers} \cdot \pi \cdot d_{lm} \cdot L$	m^2
Specific membrane area	$a_{sp} = \frac{A_{memb}}{V_T}$	$m^2.m^{-3}$
Power input for pertraction unit	$P_{ME} = \frac{P_{ME,\mathrm{mod}}}{n_{ME}} \cdot N_{\mathrm{mod}}$ With: $P_{ME,\mathrm{mod}} = \varphi_{tube} \cdot \Delta p_{ME}$	W

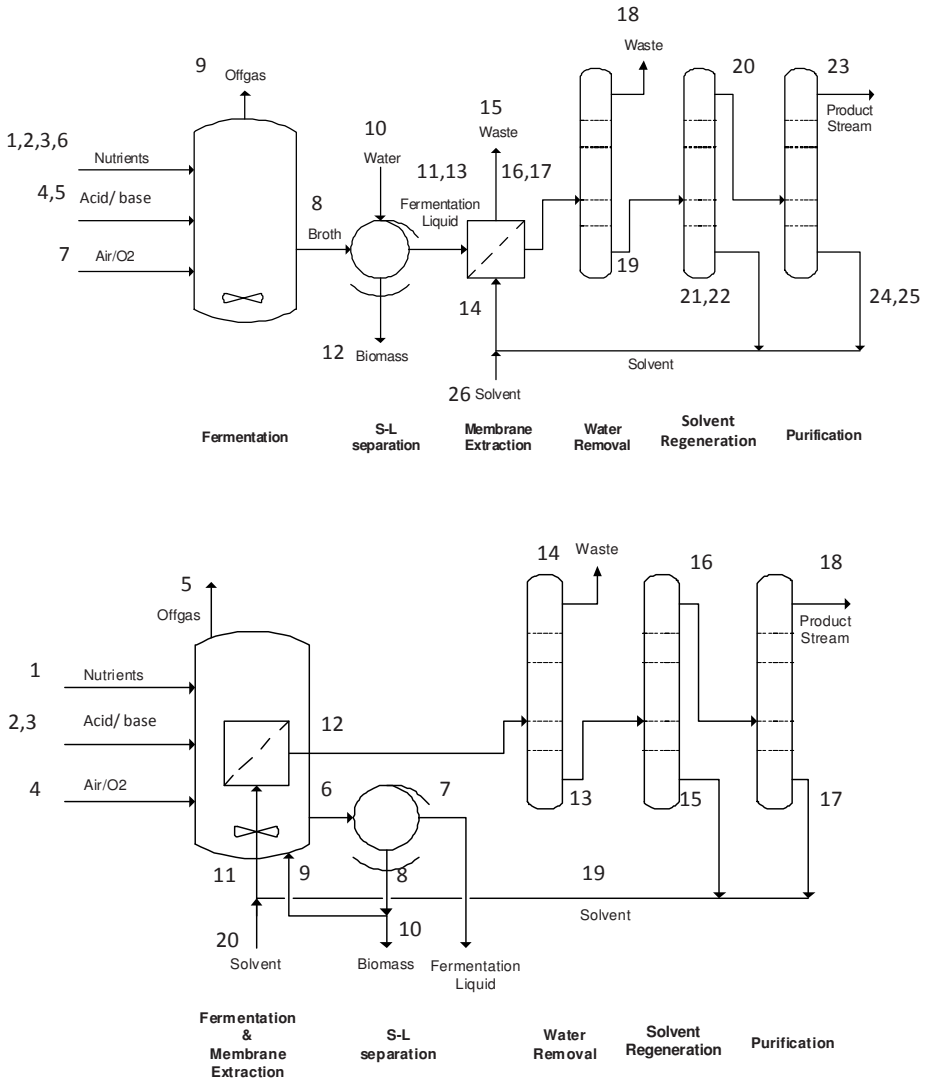

Figure 3. Illustration of the different stream numbers given in Tables 14 (top) and 15 (bottom).

Appendix 1 – Supplementary data Chapter 3

Table 14. Overall mass balances non-integrated process

Stream nr	Description	Unit#
1	Water in for glucose	F
2	Glucose in from storage	F
3	Glucose solution in	F
4	Ammonia solution in from storage	F
5	Hycrochloric acid in from storage	F
6	Inoculum and nutrients in from seeding fermentation	F
7	Gas in	F
8	Broth out	F
9	Gas out	F
10	Wash water in	SL
11	Filtrate	SL
12	Biomass cake out	SL
13	Broth out	PR & C
14	Solvent in	PR & C
15	Raffinate out to waste	PR & C
16	Solvent out	PR & C
17	Solvent out' (to Aspen)	R
18	Distillation top 1	R
19	Distillation bottom 1	R
20	Distillation top 2	R
21	Distillation bottom 2	R
22	Solvent recycle	R
23	Distillation top 3	R
24	Distillation bottom 3	R
25	Solvent recycle	R
26	Solvent make-up	R

#

F	Unit fermentation
SL	Unit cell separation
PR & C	Unit product recovery and concentration
R	Unit Regenation

Appendix 1 – Supplementary data Chapter 3

	Stream Number		1	2	3	4	5	6	7	8	9	10	11	12	13
	Temperature (ºC)		20	20	20	20	20	30	30	30	30	20	30	30	30
	Pressure (atm)		1,0	1,0	1,0	1,0	1,0	1,0	2,9	1,0	1,5	1,0	1,0	1,0	1,0
	Phase		L	S	L	L	L	S/L	G	S/L	G	L	L	S	L
	Component mass flow (Kg/h)														
1	Glucose (S)	180	0	22884	22884	0	0	29760	0	107	0	0	106	1	106
2	Ammonia (N)	17	0	0	0	577	0	1689	0	158	0	0	157	1	157
3	Viable Biomass (X)	25	0	0	0	0	0	29760	0	39993	0	0	0	0	0
4	Non viable Biomass (Xd)	25	0	0	0	0	0	0	0	5008	0	0	0	45001	0
5	Phenol (P)	94	0	0	0	0	0	0	0	1404	0	0	1392	12	1392
6	Hydrochloric acid (HCl)	36	0	0	0	0	335	0	0	335	0	0	332	3	332
7	Water (W)	18	18723	0	18723	2306	781	930794	0	976631	0	81463	1049111	8983	1049111
8	Octanol (E)	130	0	0	0	0	0	0	0	0	0	0	0	0	0
9	Oxygen (O)	16	0	0	0	0	0	0	253280	0	237351	0	0	0	0
10	Carbon dioxide (C)	44	0	0	0	0	0	0	0	0	45832	0	0	0	0
11	Nitrogen (N)	14	0	0	0	0	0	0	297373	0	297373	0	0	0	0
	Mass Flow (kg/h)		18723	22884	41607	2883	1115	992004	550653	1023635	580556	81463	1051098	54001	1051098
	Volumetric Flow (m3/h)		19		38	3	1	992	17237	1024	17261	82	1056	49	1064
	Stream Number		1	2	3	4	5	6	7	8	9	10	11	12	13
	Mass Frac														
1	Glucose (S)		0,0	100,0	55,0	0,0	0,0	3,0	0,0	0,0	0,0	0,0	0,0	0,0	0,0
2	Ammonia (N)		0,0	0,0	0,0	20,0	0,0	0,2	0,0	0,0	0,0	0,0	0,0	0,0	0,0
3	Viable Biomass (X)		0,0	0,0	0,0	0,0	0,0	3,0	0,0	3,9	0,0	0,0	0,0	0,0	0,0
4	Non viable Biomass (Xd)		0,0	0,0	0,0	0,0	0,0	0,0	0,0	0,5	0,0	0,0	0,0	83,3	0,0
5	Phenol (P)		0,0	0,0	0,0	0,0	0,0	0,0	0,0	0,1	0,0	0,0	0,1	0,0	0,1
6	Hydrochloric acid (HCl)		0,0	0,0	0,0	0,0	30,0	0,0	0,0	0,0	0,0	0,0	0,0	0,0	0,0
7	Water (W)		100,0	0,0	45,0	80,0	70,0	93,8	0,0	95,4	0,0	100,0	99,8	16,6	99,8
8	Octanol (E)		0,0	0,0	0,0	0,0	0,0	0,0	0,0	0,0	0,0	0,0	0,0	0,0	0,0
9	Oxygen (O)		0,0	0,0	0,0	0,0	0,0	0,0	46,0	0,0	40,9	0,0	0,0	0,0	0,0
10	Carbon dioxide (C)		0,0	0,0	0,0	0,0	0,0	0,0	0,0	0,0	7,9	0,0	0,0	0,0	0,0
11	Nitrogen (N)		0,0	0,0	0,0	0,0	0,0	0,0	54,0	0,0	51,2	0,0	0,0	0,0	0,0
	Total		100,0	100,0	100,0	100,0	100,0	100,0	100,0	100,0	100,0	100,0	100,0	100,0	100,0

Stream Number	14	15	16	17	18	19	20	21	22	23	24	25	26
Temperature (ºC)	30	30	30	30	79	166	122	128	128	81	128	113	20
Pressure (atm)	1.0	1.0	1.0	1.0	0.5	0.5	0.1	0.1	1.0	0.10	0.10	1.0	1.0
Phase	L	L	L	L	G/L	L	G/L	L	L	G/L	L	L	L
Component mass flow (Kg/h)													
Glucose (S)	0	0	0	0	0	0	0	0	0	0	0	0	0
Ammonia (N)	0	0	0	0	0	0	0	0	0	0	0	0	0
Viable Biomass (X)	0	0	0	0	0	0	0	0	0	0	0	0	0
Non viable Biomass (Xd)	0	0	0	0	0	0	0	0	0	0	0	0	0
Phenol (P)	0	275	1117	1276	12	1264	1264	0	6	1163	101	24	0
Hydrochloric acid (HCl)	0	0	0	0	0	0	0	0	0	0	0	0	0
Water (W)	0	1047506	1605	1571	1557	14	14	0	0	14	0	0	0
Octanol (E)	36027	367	35659	34917	183	34734	31260	3473	31554	0	31260	3358	32668
Oxygen (O)	0	0	0	0	0	0	0	0	0	0	0	0	0
Carbon dioxide (C)	0	0	0	0	0	0	0	0	0	0	0	0	0
Nitrogen (N)	0	0	0	0	0	0	0	0	0	0	0	0	0
Mass Flow (kg/h)	36027	1048149	38381	37764	1751	36013	32539	3473	31560	1178	31362	3382	32668
Volumetric Flow (m3/h)	ASPEN	1061		45	2	51	43	5	43	1	42	4	
Stream Number	14	15	16	17	18	19	20	21	22	23	24	25	27
Mass Frac													
Glucose (S)	0.0	0.0	0.0	0.0	0.0	0.0	0.0	0.0	0.0	0.0	0.0	0.0	0.0
Ammonia (N)	0.0	0.0	0.0	0.0	0.0	0.0	0.0	0.0	0.0	0.0	0.0	0.0	0.0
Viable Biomass (X)	0.0	0.0	0.0	0.0	0.0	0.0	0.0	0.0	0.0	0.0	0.0	0.0	0.0
Non viable Biomass (Xd)	0.0	0.0	0.0	0.0	0.0	0.0	0.0	0.0	0.0	0.0	0.0	0.0	0.0
Phenol (P)	0.0	0.0	2.9	3.4	0.7	3.5	3.9	0.0	0.0	98.8	0.3	0.7	0.0
Hydrochloric acid (HCl)	0.0	0.0	0.0	0.0	0.0	0.0	0.0	0.0	0.0	0.0	0.0	0.0	0.0
Water (W)	0.0	99.9	4.2	4.2	88.9	0.0	0.0	0.0	0.0	1.2	0.0	0.0	0.0
Octanol (E)	100.0	0.0	92.9	92.5	10.5	96.4	96.1	100.0	100.0	0.0	99.7	99.3	100.0
Oxygen (O)	0.0	0.0	0.0	0.0	0.0	0.0	0.0	0.0	0.0	0.0	0.0	0.0	0.0
Carbon dioxide (C)	0.0	0.0	0.0	0.0	0.0	0.0	0.0	0.0	0.0	0.0	0.0	0.0	0.0
Nitrogen (N)	0.0	0.0	0.0	0.0	0.0	0.0	0.0	0.0	0.0	0.0	0.0	0.0	0.0
Total	100.0	100.0	100.0	100.0	100.0	100.0	100.0	100.0	100.0	100.0	100.0	100.0	100.0

Appendix 1 – Supplementary data Chapter 3

Table 15. Overall mass balances integrated process

Stream nr	Description	Unit#
1	Glucose in from storage	F
2	Ammonia in from storage	F
3	Hydrochloric acid in from storage	F
4	Gas in from compressor	F
5	Gas out through condensor	F
6	Broth out	F
7	Filtrate waste	SL
8	Retentate	SL
9	Recycle biomass	SL
10	Purge	SL
11	Solvent in	PR & C
12	Solvent out	PR & C
13	Distillation bottom 1	R
14	Distillation top 1	R
15	Distillation bottom 2	R
16	Distillation top 2	R
17	Distillation bottom 3	R
18	Distillation top 3	R
19	Solvent recycle	R
20	Solvent make-up	R

#

F	Unit fermentation
SL	Unit cell separation
PR & C	Unit product recovery and concentration
R	Unit Regenation

Appendix 1 – Supplementary data Chapter 3

	Stream Number		1	2	3	4	5	6	7	8	9	10
	Temperature (ºC)		20	20	20	30	30	30	30	30	30	30
	Pressure (atm)		1,0	1,0	1,0	3,2	1,5	1,0	1,0	1,0	1,0	1,0
	Phase		L	L	L	G	G	S/L	L	S/L	S/L	S/L
	Component mass flow (Kg/h)											
1	Glucose (S)	180	12197	0	0	0	0	0	0	0	0	0
2	Ammonia (N)	17	0	132	0	0	0	6	3	3	0	3
3	Viable Biomass (X)	25	0	0	0	0	0	677	0	677	14	664
4	Non viable Biomass (Xd)	25	0	0	0	0	0	253	0	253	5	248
5	Phenol (P)	94	0	0	0	0	0	7	3	3	0	3
6	Hydrochloric acid (HCl)	36	0	0	0	0	0	0	0	0	0	0
7	Water (W)	18	9979	529	0	0	0	13928	7429	6499	130	6369
8	Octanol (E)	130	0	0	0	0	0	5	3	2	0	2
9	Oxygen (O)	16	0	0	0	28449	24233	0	0	0	0	0
10	Carbon dioxide (C)	44	0	0	0	0	12331	0	0	0	0	0
11	Nitrogen (N)	14	0	0	0	45422	45422	0	0	0	0	0
	Mass Flow (kg/h)		22176	662	0	73871	81985	14876	7438	7438	149	7289
	Mass Frac											
1	Glucose (S)		55,0	0,0	0,0	0,0	0,0	0,0	0,0	0,0	0,0	0,0
2	Ammonia (N)		0,0	20,0	0,0	0,0	0,0	0,0	0,0	0,0	0,0	0,0
3	Viable Biomass (X)		0,0	0,0	0,0	0,0	0,0	4,6	0,0	9,1	9,1	9,1
4	Non viable Biomass (Xd)		0,0	0,0	0,0	0,0	0,0	1,7	0,0	3,4	3,4	3,4
5	Phenol (P)		0,0	0,0	0,0	0,0	0,0	0,0	0,0	0,0	0,0	0,0
6	Hydrochloric acid (HCl)		0,0	0,0	30,0	0,0	0,0	0,0	0,0	0,0	0,0	0,0
7	Water (W)		45,0	80,0	70,0	0,0	0,0	93,6	99,9	87,4	87,4	87,4
8	Octanol (E)		0,0	0,0	0,0	0,0	0,0	0,0	0,0	0,0	0,0	0,0
9	Oxygen (O)		0,0	0,0	0,0	38,5	29,6	0,0	0,0	0,0	0,0	0,0
10	Carbon dioxide (C)		0,0	0,0	0,0	0,0	15,0	0,0	0,0	0,0	0,0	0,0
11	Nitrogen (N)		0,0	0,0	0,0	61,5	55,4	0,0	0,0	0,0	0,0	0,0
	Total		100,0	100,0	100,0	100,0	100,0	100,0	100,0	100,0	100,0	100,0

	Stream Number	11	12	13	14	15	16	17	18	19	20
	Temperature (ºC)	30	30	171	79	128	127	128	97	30	30
	Pressure (atm)	1,0	1,0	0,5	0,5	0,1	0,1	0,1	0,1	1,0	1,0
	Phase	L	L	L	G/L	L	G/L	L	G/L	L	L
	Component mass flow (Kg/h)										
1	Glucose (S)	0	0	0	0	0	0	0	0	0	0
2	Ammonia (N)	0	0	0	0	0	0	0	0	0	0
3	Viable Biomass (X)	0	0	0	0	0	0	0	0	0	0
4	Non viable Biomass (Xd)	0	0	0	0	0	0	0	0	0	0
5	Phenol (P)	0	1389	1376	13	0	1376	124	1252	124	124
6	Hydrochloric acid (HCl)	0	0	0	0	0	0	0	0	0	0
7	Water (W)	0	4783	5	4778	0	5	0	5	0	0
8	Octanol (E)	106290	106285	105717	568	10581	95136	95128	8	105709	5
9	Oxygen (O)	0	0	0	0	0	0	0	0	0	0
10	Carbon dioxide (C)	0	0	0	0	0	0	0	0	0	0
11	Nitrogen (N)	0	0	0	0	0	0	0	0	0	0
	Mass Flow (kg/h)	106290	112457	107098	5359	10581	96517	95252	1264	105833	129
	Mass Frac										
1	Glucose (S)	0,0	0,0	0,0	0,0	0,0	0,0	0,0	0,0	0,0	0,0
2	Ammonia (N)	0,0	0,0	0,0	0,0	0,0	0,0	0,0	0,0	0,0	0,0
3	Viable Biomass (X)	0,0	0,0	0,0	0,0	0,0	0,0	0,0	0,0	0,0	0,0
4	Non viable Biomass (Xd)	0,0	0,0	0,0	0,0	0,0	0,0	0,0	0,0	0,0	0,0
5	Phenol (P)	0,0	1,2	1,3	0,2	0,0	1,4	0,1	99,0	0,1	96,3
6	Hydrochloric acid (HCl)	0,0	0,0	0,0	0,0	0,0	0,0	0,0	0,0	0,0	0,0
7	Water (W)	0,0	4,3	0,0	89,2	0,0	0,0	0,0	0,4	0,0	0,0
8	Octanol (E)	100,0	94,5	98,7	10,6	100,0	98,6	99,9	0,6	99,9	3,7
9	Oxygen (O)	0,0	0,0	0,0	0,0	0,0	0,0	0,0	0,0	0,0	0,0
10	Carbon dioxide (C)	0,0	0,0	0,0	0,0	0,0	0,0	0,0	0,0	0,0	0,0
11	Nitrogen (N)	0,0	0,0	0,0	0,0	0,0	0,0	0,0	0,0	0,0	0,0
	Total	100,0	100,0	100,0	100,0	100,0	100,0	100,0	100,0	100,0	100,0

Table 16. Simulation results for the distillation units for the integrated and non-integrated process. The data is given for each three columns: column 1 (C1), column 2 (C2) and column 3 (C3).

Parameter	**Symbol**	**Integrated process**	**Non-integrated process**	**Unit**
Operational (bottom) temperature	T_{dest}	C1: 171 C2: 128 C3: 128	C1: 166 C2: 128 C3: 128	°C
Operational pressure	p_{dest}	C1: 0.5 C2: 0.1 C3: 0.1	C1: 0.2 C2: 0.1 C3: 0.1	atm
Number of stages	N_{stages}	C1: 15 C2: 20 C3: 40	C1: 13 C2: 30 C3: 38	-
Reflux ratio (molar) (RR for C3 is manipulated for optimization)	RR	C1: 0.5 C2: 0.5 C3: 147	C1: 0.5 C2: 0.5 C3: 31	-
Distillate to Feed ratio (D:F is manipulated for optimization)	D:F	C1: $4.8*10^{-2}$ C2: $9.0*10^{-1}$ C3: $1.3*10^{-2}$	C1: $4.6*10^{-2}$ C2: $9.0*10^{-1}$ C3: $3.6*10^{-2}$	-
Feed stage	FS	C1: 7 C2: 10 C3: 10	C1: 7 C2: 10 C3: 29	-
Packing height	H_{pack}	C1: 11 C2: 15 C3: 32	C1: 9 C2: 24 C3: 30	m
Column height	H_{column}	C1: 14 C2: 19 C3: 35	C1: 13 C2: 27 C3: 34	m
Column diameter	D_{column}	C1: 1.3 C2: 1.8 C3: 2.5	C1: 0.6 C2: 1.1 C3: 1.2	m
Energy for heating	Q_{heat}	C1: 17.5 C2: 13.9 C3: 30.8	C1: 4.9 C2: 6.5 C3: 7.0	MW
Energy for cooling	Q_{cool}	C1: 2.1 C2: 18.1 C3: 30.7	C1: 2.1 C2: 7.0 C3: 0.7	MW
Column wall thickness[A]	tw	C1: 0.12 C2: 0.034 C3: 0.039	C1: 0.22 C2: 0.058 C3: 0.078	m
Column weight	W_{column}	C1: $1.2*10^{5}$ C2: $5.2*10^{4}$ C3: $1.8*10^{5}$	C1: $2.8*10^{4}$ C2: $2.6*10^{4}$ C3: $4.1*10^{4}$	kg

[A] Calculated using http://www.engineersedge.com/calculators/shell_internal_long_pop.htm assuming a maximum stress value of 1 bar (14.5 psi).

Table 17. Overdesign factors (ODF) assumed for the process unit operations

Unit operation	**Overdesign factor**
Fermentor	-
SL separation	0.1
Pertraction unit	1.2
Condensors, reboilers, heaters, coolers	0.1
Storage tanks, decanters, reflux drums	0.1

Table 18. Assumed costs for waste treatment and utilities

Parameter	**Value**	**Unit**	**Source**
Organic waste (e.g. biomass) treatment	0.16	€.kg-1	Straathof 2006
Waste water treatment	1.0	€.kg-1	Assumption based on Seader p.573*
Electricity	0.05	€.kWh-1	DACE, Prijzenboek
Low-medium pressure steam (3-10 bar, 190-220 °C)	0.01	€.kg-1	DACE, Prijzenboek
Cooling water (3 bar, Tin=20°C, Tout=40°C)	0.08	€.m-3	DACE, Prijzenboek
Chilled water (3 bar, Tin=5°C, Tout=20°C)	0.32	€.m-3	DACE, Prijzenboek
Pressurized air	0.01	€.m-3	DACE, Prijzenboek

*Seader, J. D.; Henley, E. J., Separation Process Principles. John Wiley & Sons, Inc.: 1998

Table 19. Assumed costs for major raw materials

Parameter	Value	Unit	Source
Glucose (C-source)	0.16	€.kg^{-1}	Straathof 2007
Ammonia (N-source)	0.24	€.kg^{-1}	Straathof 2007
Hydrochloric acid (pH controlling agent)	0.13	€.kg^{-1}	Straathof 2007
1-octanol (solvent)	0.63	€.kg^{-1}	ICIS

Table 20. Assumptions for economic calculations

Parameter	Value	Unit
Interest rate	10	%
Tax rate	30	%
Internal rate of return	20	%
Conversion factor Euro-Dollar	1.43	(Sep-2009)

List of symbols

Symbol	Explanation	Units
Fermentor		
C_S	Substrate concentration	mol.L^{-1}, mol.m^{-3}, kg.m^{-3}
C_P	Product concentration	mol.L^{-1}, mol.m^{-3}, kg.m^{-3}
C_X	Biomass concentration	g.L^{-1}
C_{Xd}	Death biomass concentration	g.L^{-1}
$C_{p,org,x=L}$	Product concentration in the solvent phase at x=L	mol.L^{-1}, mol.m^{-3}, kg.m^{-3}
□	Biomass specific growth rate	h^{-1}
□^{max}	Maximum biomass specific growth rate	h^{-1}
k_s	Glucose affinity constant	mol S.m^{-3}
ε	Inhibition parameter 1	mol P.m^{-3}
δ	Inhibition parameter 2	-
q_p^{max}	Maximum specific phenol production rate	mol P.(C-mol X)$^{-1}$.h^{-1}
β	Phenol production parameter	h^{-1}
k_{tox}	Toxicity parameter	mol S.m^{-3}
k_d	Maximum specific death/ inactivation rate	h^{-1}
k_{cd}	Death parameter	mMol P.m^{-3}
Y_{SX}^{max}	Maximum yield of biomass on glucose	(C-mol X).(mol S)$^{-1}$

Y_{SP}^{max}	Maximum yield of phenol on glucose	(mol P).(mol S)$^{-1}$
$-m_s$	Maintenance coefficient	(mol S).(C-mol X)$^{-1}$
H_o	Henry's constant for oxygen in water	mol.m^{-3}.bar^{-1}
x_o	Oxygen molar fraction present in the gas phase	-
U	Overall heat transfer coefficient accounting for all heat transfer resistances (280 – 850)	W.m^{-2}.K^{-1}
H	Fermentor height	m
D	Fermentor diameter	m
H/D	Height to diameter ratio fermentor	m.m^{-1}
R_g	Gas constant	J.g^{-1}.mol^{-1}.K^{-1}
c_{pg}	Specific heat capacity gas	J.kg^{-1}.K^{-1}
T_g	Temperature of the gas	°C
c_{pS}	Specific heat capacity of feed substrate	J.kg^{-1}.K^{-1}
c_{pN}	Specific heat capacity of feed nitrogen	J.kg^{-1}.K^{-1}
c_{pHCl}	Specific heat capacity of feed hydrochloric acid	J.kg^{-1}.K^{-1}
K, k	Mass transfer coefficient	m.s^{-1}
V_L	Liquid fermentation volume	m^3
V_{ferm}	Fermentor total volume	m^3
MW	Molecular weight	g.mol^{-1}
$\square_{in}$	volumetric medium/feed flow rate	m^3.s^{-1}
$\square_{out}$	Volumetric flow rate of the fermentation unit outlet	m^3.s^{-1}
$\square_{rec}$	Volumetric flow rate of the fermentation unit cell recycle	m^3.s^{-1}
ρ	Density	kg.m^{-3}
vG	Superficial gas velocity	m.s^{-1}
OUR	Oxygen uptake rate	mol.m^{-3}.h^{-1}
Kl.a	Oxygen transfer rate	(m.s^{-1}).(m^2)
P	Total pressure	atm
r_H	Rate on heat removal in the heat exchanger system of a jacket vessel	W
A_h	Heat transfer area	m^2
T	Temperature of the fermentation broth	K
T_{CW}	Temperature of cooling water	K
P_b	Pressure at the bottom of the fermentor	atm
P_t	Pressure at the top of the fermentor	atm
F_{ch}	Flow of chilled (cooling) water fermentor	kg.h^{-1}
q_S	Glucose specific consumption rate	mol.mol^{-1}.h^{-1}
q_P	Phenol specific production rate	mol.mol^{-1}.h^{-1}
q_o	Oxygen specific consumption rate	mol.mol^{-1}.h^{-1}
$C_{o,L}^*$	Oxygen concentration in the liquid phase at equilibrium conditions with the gas phase	mol.m^{-3}
P_g	Fermentor gas flow power input	W
F_g	Fermentor gas (in)flow rate	m^3.s^{-1}
r_{ht}	Total heat generated	W
r_{hm}	Heat by metabolic activity	W
r_{hg}	Heat by gas flowing through	W
r_{hs}	Heat generated by the stirrer	W
r_{hv}	Heat loss by vaporization	W

r_{hw}	Heat loss through fermentor walls	W
r_{hh}	Heat generated by other sources	W
r_{hf}	Heat of feeding streams	W
Solid-liquid separation unit		
F_{SL}	Filtration flux	$L.m^{-2}.s^{-1}$, $m^3.m^{-2}.s^{-1}$
P_{SL}	Power input for filtration	W
A_{SL}	Solid-liquid filtration area	m^2
RR_{SL}	Recycle ratio (integrated case)	$(m^3.s^{-1}).(m^3.s^{-1})^{-1}$
ρ_f	Filtrate density (water at 30°C)	$kg.m^{-3}$
Δp_{SL}	Pressure drop over the membrane	bar
ω	Rotation speed	rpm
$\Delta\gamma$	Filtration angle	rad
η	Viscosity of the broth	$Pa.s^{-1}$
r	Specific cake resistance	m^{-2}
C	Medium resistance	m^{-1}
CF	Concentration factor, ratio between biomass concentration in the recycle to biomass concentration in effluent	$(g.L^{-1}).(g.L^{-1})^{-1}$
$C_{X,con}$	Biomass concentration after concentration	$g.L^{-1}$
Pertraction		
E	Required phenol removal rate	$mol.h^{-1}$
L	Length of the membrane	m
ER	Phenol volumetric extraction rate	$mol.m^{-3}.s^{-1}$, $kg.m^{-3}.h^{-1}$
N_P	Phenol transport flux	$kg.m^{-2}.s^{-1}$
x	Spatial coordinate	m
J_P	Phenol phase transfer flux	$kg.m^{-2}.s^{-1}$
v_s	Average linear solvent velocity in the tubes	$m.s^{-1}$
K^{aq}	Overall mass transfer coefficient	$m.s^{-1}$
R^{shell}	Resistance in the outside of the membrane	$(m.s^{-1})^{-1}$
R^{memb}	Resistance in the membrane	$(m.s^{-1})^{-1}$
R^{lumen}	Resistance in the lumen of the capillaries	$(m.s^{-1})^{-1}$
k_{shell}	Mass transfer coefficient Shell (aqueous side)	$m.s^{-1}$
k_{memb}	Mass transfer coefficient membrane	$m.s^{-1}$
k_{lumen1}	Mass transfer coefficient lumen 1 (solvent side)	$m.s^{-1}$
k_{lumen2}	Mass transfer coefficient lumen 2 (solvent side)	$m.s^{-1}$
N_{fibers}	Number of membrane fibers required	-
A_{memb}	Required membrane area pertraction	m^2
a_{sp}	Specific membrane area pertraction	$m^2.m^{-3}$
$a_{sp,max}$	Maximum specific membrane area pertraction	$m^2.m^{-3}$
CF_P	Concentration factor pertraction	-
d_o	External diameter of the membrane	m
d_{lm}	Average diameter of the membrane	m
D_w	Phenol diffusivity in water	$m^2.s^{-1}$
D_{org}	Phenol diffusivity in 1-octanol	$m^2.s^{-1}$
Φ_{tube}	Solvent flux	$m^3.s^{-1}$

ϕ_w	Solvent associated parameter water	-
ϕ_{org}	Solvent associated parameter 1-octanol	-
MW_w	Molecular weight water	$g.mol^{-1}$
T	Pertraction temperature	°C
μ_w	Viscosity water	cP (at 30°C)
μ_{org}	Visosity 1-octanol	cP (at 30°C)
ρ_{org}	Density 1-octanol	$kg.m^{-3}$ (at 30°C)
ρ_w	Density water	$kg.m^{-3}$ (at 30°C)
v_p	Molecular volume phenol	$m^3.Kmol^{-1}$
v_{org}	Molecular volume 1-octanol	$m^3.Kmol^{-1}$
$m_p^{w/org}$	Partition coefficient of phenol between water and 1-octanol	-
Δz	Thickness of the diffusional layer around the membrane	m
L	Length of the membrane	m
P_{org}	Parachor 1-octanol	$cm^3.g^{1/4}.s^{-0.5}.mol^{-1}$
P_p	Parachor phenol	$cm^3.g^{1/4}.s^{-0.5}.mol^{-1}$
P_w	Parachor water	$cm^3.g^{1/4}.s^{-0.5}.mol^{-1}$
d_p	Pore size	mm
d_i	Internal fiber diameter	mm
tk	Fiber wall thickness	mm
τ	Membrane tortuosity	-
ε_m	Membrane porosity	-
$v_{s,max}^{a}$	Max. superficial solvent velocity	$m.s^{-1}$
P_{ME}	Power input for pertraction unit	W
$P_{ME,mod}$	Power input for pertraction unit per module	W
Distillation		
T_{dest}	Operational (bottom) temperature	°C
p_{dest}	Operational pressure	atm
N_{stages}	Number of stages	-
RR	Reflux ratio (molar) (RR for C3 is manipulated for optimization)	-
D:F	Distillate to Feed ratio (D:F is manipulated for optimization)	-
FS	Feed stage	-
H_{pack}	Packing height	m
H_{column}	Column height	m
D_{column}	Column diameter	m
Q_{heat}	Energy for heating	MW
Q_{cool}	Energy for cooling	MW
t_w	Column wall thicknessA	m
W_{column}	Column weight	kg
Superscripts and substripts		
O	Oxygen (electron acceptor)	-
C	Carbon dioxide	-
S	Glucose (substrate, C-source)	-
N	Ammonia (N-source)	-

HCl	Hydrochloric acid (pH controlling agent)	-
P	Phenol (product)	-
X	Active/viable biomass	-
Xd	Inactive/dead biomass	-
W	Water	-
Org	Solvent (1-octanol)	-
Process economics		
PEC	Purchased equipment costs	kEUR
TCI	Total capital investment	kEUR
DPC	Direct plant costs	kEUR
IPC	Indirect plant costs	kEUR
FCI	Fixed capital investment	kEUR
VC	Variable costs	$kEUR.yr^{-1}$
TMC	Total manufacturing cost	$kEUR.yr^{-1}$
TPC	(annual) total production costs	$kEUR.yr^{-1}$
OL	Operating labour	$kEUR.yr^{-1}$
GE	General expenses	$kEUR.yr^{-1}$
ROI	Return on investment	%
t	Tax rate	%
S	Annual sales revenues	$kEUR.yr^{-1}$
PCP	Minimum product cost price	$EUR.kg^{-1}$
D	Depreciation	%